VNiVERSiDAD D SALAMANCA

CAMPUS DE EXCELENCIA INTERNACIONAL

ESCVELA POLITÉCNICA SVPERIOR DE ÁVILA.
DEPARTAMENTO DE INGENIERÍA CARTOGRÁFICA Y DEL TERRENO

TESIS DOCTORAL

Desarrollo de metodologías y herramientas software y hardware de bajo coste para la integración de sensores en Geomática

José Alberto Torres Martínez

Ávila, 2017

Universidad de Salamanca
Escuela Politécnica Superior de Ávila
Departamento de Ingeniería Cartográfica y del Terreno

AUTOR:

José Alberto Torres Martínez

DIRECTORES:

Dr. David Hernández López

Dr. Diego González Aguilera

2017

Desarrollo de metodologías y herramientas software y hardware de bajo coste para la integración de sensores en Geomática

Tesis Doctoral presentada por José Alberto Torres Martínez

Informe de los Directores de Tesis

La Tesis Doctoral "*Desarrollo de metodologías y herramientas software y hardware de bajo coste para la integración de sensores en Geomática*", presentada por José Alberto Torres Martínez, se inserta en la línea de investigación de documentación del patrimonio arqueológico por medio de la fusión de técnicas fotogramétricas y de láser escáner terrestre.

Se trata de una línea muy activa y relevante en la comunidad científica internacional, con múltiples propuestas de mejora que se estimulan unas a otras, gracias a lo cual estamos viviendo un periodo de progreso de las Geotecnologías en el ámbito arqueológico. El trabajo desarrollado se sitúa de forma significativa y eficaz en el contexto de dichas aportaciones y logros con un alto grado de sintonía y de contribución al avance del conocimiento científico y tecnológico.

Se trata asimismo de una línea de investigación promovida y desarrollada por el Grupo de Investigación reconocido TIDOP (http://tidop.usal.es) de la Universidad de Salamanca y que vienen desarrollando propuestas en el seno de proyectos de investigación competitivos y en colaboración con otros grupos punteros a nivel nacional, como el Instituto de Desarrollo Regional (IDR) de la Universidad de Castilla-La Mancha, con quienes se ha colaborado durante el desarrollo de esta Tesis Doctoral.

La Geomática y en particular las geotecnologías láser y fotogramétricas vienen experimentando una serie de innovaciones de gran alcance que han transformado profundamente su contexto de aplicación frente a las aplicaciones más clásicas (Cartografía y Topografía) en las que se venía

trabajando años atrás. Estas innovaciones se articulan fundamentalmente en torno a la capacidad de captura masiva de información, la hibridación de sensores, el empleo de técnicas de bajo coste y la automatización de determinados procesos para generar productos de calidad con propiedades métricas.

Además, en los últimos diez años, las geotecnologías láser y fotogramétricas han demostrado ser técnicas complementarias, lo que las ha situado en un horizonte muy prometedor y competitivo en todos los contextos y más concretamente en el ámbito arqueológico.

La Tesis Doctoral aborda un adecuado estado del arte de manera que permite identificar claramente la oportunidad estratégica de la aportación que se realiza como lo demuestra el hecho de que la Tesis se articula en torno a la modalidad de compendio de artículos publicados en revistas científicas y tecnológicas con impacto reconocido. Dos de ellas pertenecientes al primer cuartil-Q1 y alto factor de impacto (Journal of Archaeological Science; Remote Sensing) y otra perteneciente al tercer cuartil-Q3 (Digital Applications in Archaeology and Cultural Heritage).

Estos artículos han verificado los correspondientes procesos de evaluación crítica y revisión por parte de expertos internacionales de trayectoria reconocida. Estas contribuciones se centran en:

- La generación de productos geomáticos de alta precisión (modelos densos 3D y ortofotografías verdaderas) mediante la hibridación de información fotogramétrica, procedente de diversas plataformas aéreas y terrestres, y de láser escáner.
- El desarrollo de una plataforma giroestabilizadora para la captura de información fotogramétrica aérea desde paramotor.
- La integración de diversas fuentes de información y la difusión vía Web de los productos geomáticos mediante el empleo de Sistemas

de Información Geográfica 3D Web (Web 3DGIS) haciendo para ello uso de procedimientos de optimización en la generación de modelos 3D.

- La comparación de los procesos de clasificación no supervisada en el ámbito del análisis de pinturas rupestres y la mejora de los mismos mediante el uso combinado de información geométrica y radiométrica.

La Tesis Doctoral concluye con el correspondiente apartado de Conclusiones en el que de forma precisa y concreta se especifican las principales aportaciones realizadas de tal manera que puedan ser objeto de crítica y de proyección hacia el desarrollo de futuros trabajos integrados en línea de investigación.

En Ávila, a 24 de Abril de 2017,

David Hernández López Diego González Aguilera

La presente Tesis Doctoral corresponde a un compendio de tres artículos científicos previamente publicados en revistas internacionales de impacto y que se especifican a continuación:

1. **A hybrid measurement approach for archaeological site modelling and monitoring: the case study of Mas D'Is, Penàguila.**

   Jose Alberto Torres[a], David Hernandez-Lopez[b], Diego Gonzalez-Aguilera[a], Miguel Angel Moreno Hidalgo[c]

   [a] Department of Cartographic and Land Engineering, Avila, University of Salamanca, Spain.
   [b] Institute for Regional Development (IDR), Albacete, University of Castilla La Mancha, Spain.
   [c] Centro Regional de Estudios del Agua (CREA), Albacete, University of Castilla La Mancha, Spain.

   DOI: 10.1016/j.jas.2014.08.012

2. **A Multi-Data Source and Multi-Sensor Approach for the 3D Reconstruction and Web Visualization of a Complex Archaelogical Site: The Case Study of "Tolmo De Minateda".**

   Jose Alberto Torres-Martínez[1], Marcello Seddaiu[2], Pablo Rodríguez-Gonzálvez[1], David Hernández-López[3] and Diego González-Aguilera[1]

[1] Department of Cartographic and Land Engineering, Avila, University of Salamanca, Spain.
[2] Dipartimento di Storia, Scienze dell' Uomo e della Formazione, Sassari, Università degli Studi di Sassari, Italy.
[3] Institute for Regional Development (IDR), Albacete, University of Castilla La Mancha, Spain.

DOI:10.3390/rs8070550

3. Combining geometrical and radiometrical features in the evaluation of rock art paintings.

Jose Alberto Torres-Martínez[a], Luis Javier Sánchez-Aparicio[a], David Hernández-López[b], Diego González-Aguilera[a]

[a] Department of Cartographic and Land Engineering, Avila, University of Salamanca, Spain.
[b] Institute for Regional Development (IDR), Albacete, University of Castilla La Mancha, Spain.

DOI: 10.1016/j.daach.2017.04.001

AGRADECIMIENTOS

La finalización de esta Tesis Doctoral cierra una emocionante etapa marcada por el aprendizaje y el descubrimiento, pero también por el trabajo, el esfuerzo y la dedicación. Es seguro que sin la inestimable ayuda de numerosas personas no hubiera sido posible llevarla a cabo con éxito. A ellos quiero agradecerles y dedicarles este trabajo.

En primer lugar quiero dar las gracias a los directores de esta Tesis Doctoral, quienes siempre han sido para mí un referente en calidad profesional y humana.

Gracias a David, director de esta Tesis Doctoral, por animarme, darme la oportunidad y confiar en mí para llevarla a cabo. Sin su constante e incalculable ayuda desde el primer día, no hubiese sido capaz de llegar hasta aquí.

Gracias a Diego por su dedicación, paciencia y ánimo, y por haber ejercido sobremanera sus funciones como director de esta Tesis Doctoral, estando siempre disponible y brindando todo su apoyo y conocimientos.

Gracias a los Doctores Pablo Rodríguez Gonzálvez y Luis Javier Sánchez Aparicio, por permitirme compartir objetivos y horas de trabajo y quienes me han ayudado y brindado desinteresadamente su conocimiento.

Gracias también a mi pareja, Elena, por apoyarme en todo momento, en este y en cada uno de los proyectos que he decidido acometer.

Por último, gracias a mis padres, para los que no tengo suficientes palabras de agradecimiento, por ser siempre soporte, referente y guía en cada uno de los pasos que he dado en la vida.

A todos, gracias.

RESUMEN

La descripción geométrica ha estado siempre presente entre las labores a realizar en el análisis de un yacimiento arqueológico. Sin embargo, la conservación de los elementos que componen el yacimiento exige de técnicas no invasivas que permitan el mismo o mayor grado de precisión alcanzable mediante las técnicas topográficas y de delineación tradicionales. En este marco, las técnicas de modelización tridimensional mediante fotogrametría y láser escáner aparecen como una solución ideal.

Avanzando más en esta idea, en esta Tesis Doctoral se ha demostrado como la integración de las diferentes técnicas disponibles (fotogrametría terrestre y aérea, y láser escáner terrestre) mejoran el resultado obtenido por cada una de ellas independientemente, siendo, por tanto, herramientas complementarias. Se comprueba que es posible obtener productos geomáticos de alta precisión minimizando a la vez los costes asociados y cómo es posible realizar la divulgación de estos productos para una gran variedad de público, permitiendo la interacción con los mismos desde incluso dispositivos portátiles como smartphones. Igualmente, se ha mostrado como mediante el empleo de sistemas de información geográficos tridimensionales (GIS3D), la información obtenida por técnicas tradicionales, como pueden ser los croquis del yacimiento, es integrable con los productos geomáticos generados, y cómo esta integración aumenta la capacidad de análisis, por ejemplo mediante el análisis multi-temporal.

Finalmente, se muestra también como los productos geomáticos de alta precisión obtenidos constituyen una fuente de información adecuada para el análisis de elementos de mayor detalle, presentes en yacimientos

arqueológicos, como pinturas o grabados en roca. De esta manera, se analiza, cualitativa y cuantitativamente, como la realización de un análisis combinado de información geométrica y radiométrica supone una ventaja frente al habitual empleo de información únicamente radiométrica. Se ha podido comprobar la versatilidad que supone esta combinación de información en el análisis de abrigos rupestres tanto a nivel global, el propio yacimiento, como a nivel local, las pinturas.

Las metodologías derivadas de las líneas de investigación abordadas en esta Tesis Doctoral se han validado en una variedad de yacimientos que presentan una diversidad tanto geográfica como temporal, abarcando periodos desde la prehistoria hasta la Edad Media.

ABSTRACT

The geometrical description has always been one of the mandatory labors for the analysis of an archaeological site. However, the preservation of the elements presented in the site demands non-invasive techniques that allow the same or greater degree of precision reachable through traditional techniques such as delineation or topography. In this frame, tridimensional modelling techniques like photogrammetry and laser scanner emerge as an ideal solution.

Moving forward on this idea, in this Doctoral Dissertation has been demonstrated how the integration of different available techniques (terrestrial and aerial photogrammetry, and terrestrial laser scanner) improves the results obtained by using them independently, being, therefore, complementary. It has been proven that is possible to obtain high precision geomatic products minimizing, at the same time, the costs associated and how it is possible to divulgate these products to a wide variety of public, allowing the interaction even through portable devices such as smartphones. Likewise, it has been shown how by means of three-dimensional geographical information systems (GIS3D), the information obtained by traditional techniques, such as sketches, may be integrated with the geomatic products generated and how this integration increases the analytical capacity, for example, through multi-temporal analysis.

Finally, it is also shown how the accurate geomatic products obtained constitute a suitable information source for the analysis of more detailed elements, existing in archaeological sites, such as paintings or rock engravings. In this manner, it is qualitatively and quantitatively tested how a

combined radiometric and geometric analysis means an advantage against the usual employment of only radiometric information. It has been possible to verify the versatility of this combination of information in the analysis of rock shelters both at a global level, the site, and at a local level, the paintings.

The derived methodologies of the lines of research approached in this Doctoral Dissertation have been validated in a variety of archaeological sites that present both geographical and temporal variety, including periods from prehistoric times to middle ages.

ÍNDICE

1. INTRODUCCIÓN

El complejo proceso de documentación arqueológica de un yacimiento requiere, para ser completo, de una descripción geométrica precisa del mismo. Por este motivo, han sido numerosas las metodologías empleadas a lo largo del tiempo, como los croquis a mano alzada, las fotografías o los levantamientos topográficos. Con el avance de la tecnología y de técnicas como la visión computacional, disciplinas como la fotogrametría aérea o terrestre y técnicas como el láser escáner terrestre son cada día más empleadas para realizar estas tareas.

Respecto al empleo de *fotogrametría aérea*, su aplicación en arqueología comienza con la realización de fotografías oblicuas empleadas para fotointerpretación y monitorización. El primer ejemplo de aplicación de esta metodología en arqueología se encuentra en Persépolis en el año 1879 por el alemán Friedrich Stoltze (Ceraudo, 2013). Las primeras plataformas aéreas empleadas consistieron en globos aerostáticos (Whittlesey, 1971, Aguilera et al., 2006, Mozas-Calvache, 2012) y cometas (Aber et al., 1999, Anderson, 2001, Thomas, 2016). Estas plataformas, que aún siguen siendo objeto de estudio hoy en día, se ven muy limitadas por la intensidad de viento y por la baja maniobrabilidad. Por ello, posteriormente, se extendió el empleo de aviones ligeros para la captura de fotografías aéreas de yacimientos arqueológicos (Oltean, et al., 2007, Verhoeven, 2010). No obstante, debido al elevado coste que supone la realización de los vuelos, en numerosas ocasiones se ha recurrido al empleo de fotografías aéreas históricas, derivadas en su mayoría de reconocimientos del terreno realizados por vuelos militares (Block 1988, Doneus et al., 2015). Sin

embargo, el empleo de fotografías históricas puede presentar una serie de inconvenientes a la hora de realizar la integración con otras fuentes de datos, ya que no siempre poseen suficiente calidad métrica y no suelen estar disponibles los parámetros de calibración de la cámara, necesarios para el proceso fotogramétrico (Cowley et al., 2012).

Actualmente, el principal factor que ha permitido disminuir los costes operativos de esta metodología ha sido la proliferación de los vehículos aéreos no tripulados (UAVs). Gracias a la versatilidad de los UAVs es posible obtener productos de alta resolución geométrica y temporal, ya que la repetitividad de la operación no está condicionada a los complejos y costosos medios anteriormente empleados como aviones o helicópteros. Además, la capacidad de los UAV de permanecer estáticos en un punto de toma permite la obtención de fotografías tanto verticales como oblicuas, las cuales son de gran interés en zonas de difícil acceso o en yacimientos con geometrías complejas. Estos aspectos junto a la elevada precisión alcanzable, gracias a la posibilidad de adquirir imágenes a muy corta distancia, y los bajos costes de operación asociados, han propiciado que se extienda ampliamente la aplicación de la fotogrametría aérea (tanto vertical como oblicua) desde UAV en el ámbito arqueológico y de conservación del patrimonio (Roosvelt, 2014, Themistocleous et al., 2015, Achille et al., 2015).

En comparación con el resto de técnicas geomáticas, la *fotogrametría terrestre o de objeto cercano* es, sin duda, la solución más económica y fácilmente implementable. La primera aplicación de esta técnica en el campo de la arqueología parece haber sido realizada en el año 1885 y consistió en el levantamiento de las ruinas de Persépolis (Fussel, 1982). Para la toma de datos en campo únicamente es necesario el empleo de una cámara fotográfica calibrada de alta resolución. Por este motivo, y

debido a la facilidad de captura de datos, es común el empleo de esta técnica en arqueología (Lerma et al., 2010, Lai et al., 2015). Además, puesto que la información recabada en campo se compone principalmente de imágenes fotográficas, la captura de datos fotogramétrica sirve también como documentación gráfica del yacimiento, aportando tanto información cuantitativa como cualitativa. Recientemente, el empleo de esta técnica, así como de su homóloga aérea, se ha visto impulsada gracias al avance en técnicas de visión computacional como el Structure from Motion (SfM), implementado en herramientas software de bajo coste e incluso gratuitas, lo que ha permitido automatizar en mayor grado las operaciones facilitando el post-proceso de cara al usuario no experto en técnicas fotogramétricas. Este aumento de automatismo, no obstante, deteriora el grado de control sobre el proceso (soluciones "caja negra") y por ende el análisis de la calidad del producto obtenido, siendo necesario un balance entre la calidad requerida y el grado de automatismo deseado (Remondino, 2012).

Por su parte, el *láser escáner terrestre* (Terrestrial Laser Scanner-TLS) se caracteriza por la precisión, rapidez y elevada captura de información, pudiendo alcanzar centenares de miles de puntos en segundos. El empleo del TLS permite una determinación geométrica de precisión milimétrica, siempre que sea usado en el rango óptimo. El empleo de esta técnica comienza a ser habitual desde principios de la década del 2000, siendo aplicado en diferentes campos como arquitectura, topografía, conservación del patrimonio o arqueología (Mills et al., 2011). A diferencia de las técnicas fotogramétricas, su uso es idóneo en yacimientos o partes de los mismos cuyas geometrías sean irregulares (González-Aguilera et al., 2011a,b), esto es, superficies con formas difícilmente parametrizables, proporcionando propiedades métricas en el momento de la captura. La diversidad de tipos y formatos de láser escáner existentes permite un amplio

uso de esta técnica, desde la representación tridimensional de pequeños elementos como piezas o esculturas (Tucci et al., 2011, Kuznetsova et al., 2015), cuevas (Lindgren et al., 2013, Cosso et al., 2014), o yacimientos arqueológicos (Hakonen et al., 2015), hasta el análisis de parámetros intangibles como la calidad de los materiales de un monumento (Casula et al., 2009). Además, la elevada precisión y resolución geométrica alcanzable convierte a los modelos tridimensionales obtenidos mediante esta técnica en una herramienta adecuada para la evaluación de otras metodologías, pudiéndose establecer como verdad terreno aquellos productos derivados del empleo del TLS (Rodríguez-Gonzálvez et al., 2017).

Como se ha mostrado, la aplicación de estas tecnologías es adecuada en el campo arqueológico. No obstante, son también diversos los inconvenientes que presentan, por lo que no resulta óptimo el empleo de las mismas por separado. Así pues en el **Artículo 1** de esta Tesis Doctoral son evaluadas las técnicas por separado y conjuntamente, presentándose como solución idónea la integración de las tres técnicas, de modo que se puedan aprovechar las ventajas que cada metodología presenta y se descarten los inconvenientes de cada una.

Entre los diversos inconvenientes que se encuentran, el empleo de fotogrametría aérea clásica demuestra no ser adecuada cuando se quiere documentar un escenario con planos predominantemente verticales, habituales en un yacimiento arqueológico. En estos casos, el empleo de fotogrametría aérea conlleva mayor problemática y costes asociados que el empleo de fotogrametría terrestre o TLS. Por otra parte, se ha comentado la proliferación del empleo de fotogrametría con cámaras embarcadas en UAV en la documentación de yacimientos arqueológicos, lo cual podría, en ciertas ocasiones, solventar el problema de las superficies verticales debido a la posibilidad de permanencia en el punto de captura y la realización de

fotografías oblicuas. Sin embargo, la limitada capacidad de carga de estas plataformas aéreas, junto con su reducida autonomía, hace necesaria la búsqueda de alternativas más adecuadas para la documentación de aquellos yacimientos con grandes extensiones. De este modo, en el **Artículo 2** de esta Tesis Doctoral se ha evaluado también el empleo del paramotor como plataforma aérea tripulada de bajo coste. El empleo del paramotor en la documentación de grandes extensiones ha sido estudiado por diversos autores (Ortega-Terol et al., 2014) y particularmente en el ámbito arqueológico (Hailey, 2005). A diferencia de los UAVs, esta plataforma permite la incorporación de múltiples sensores al mismo tiempo (cámaras fotográficas, multiespectrales, térmicas, sensores de posicionamiento y navegación, etc.), así como una mayor autonomía (Herrero-Huerta et al., 2014). La principal problemática de esta metodología es la imposibilidad de captura estática de imágenes, lo que en ciertas condiciones de iluminación, y para ciertos tipos de cámaras, puede dar lugar a que las condiciones de exposición deriven en pérdidas de nitidez, siendo también más complicado garantizar la verticalidad de las tomas y el registro correcto de los diferentes sensores. Para minimizar estos efectos ha sido necesaria la construcción de una plataforma giroestabilizadora que ha sido utilizada en el **Artículo 2** de la presente Tesis Doctoral. Esta plataforma se compone de dos servomotores, una unidad IMU (Inertial Measurement Unit) y una placa Arduino. Igualmente, ha sido necesario desarrollar el software correspondiente en la placa Arduino de modo que ésta procese las señales detectadas por los tres acelerómetros y tres giróscopos que componen la unidad IMU, para que calcule las variaciones en la posición de la cámara y envíe las correspondientes señales a los servomotores para su corrección.

En el caso del empleo independiente de fotogrametría terrestre, su uso se ve limitado por la propia altura del punto de toma, no siendo posible su aplicación en zonas muy elevadas respecto al punto de toma o inaccesibles por el operador de la cámara, pudiendo minimizarse este problema con el empleo de soportes telescópicos. Por otra parte, cuando se demandan resultados de calidad se hace necesaria la utilización de cámaras calibradas en laboratorio o, en su defecto, el empleo de metodologías de auto-calibración avanzadas durante el ajuste fotogramétrico, siendo necesario tener un conocimiento de los procesos fotogramétricos. Ambas técnicas fotogramétricas, tanto terrestre como aérea, presentan el inconveniente propio de los sensores pasivos, es decir, requieren de una fuente de iluminación natural o artificial homogénea donde no se presenten zonas sub-expuestas ni sobre-expuestas, lo cual suele ser complicado en yacimientos a cielo abierto, siendo la mejor solución la planificación del instante óptimo para la captura de datos en campo.

El empleo del TLS conlleva inconvenientes comunes a los presentados para la fotogrametría terrestre. Estos inconvenientes son derivados de la limitación en la posición de los puntos de captura de datos o estacionamientos, generándose problemas de oclusiones, zonas inaccesibles, etc. A ello se añade el elevado coste del material y la compleja movilidad de la mayoría de estos sistemas, sin olvidar también el conocimiento avanzado que hay que tener para el procesado de los datos. El principal inconveniente del TLS frente a la fotogrametría de rango cercano es que, o bien no se co-registra imagen, o bien no presenta la calidad geométrica y radiométrica de la obtenida por las técnicas fotogramétricas, debido a las diferentes especificaciones de las cámaras empleadas. No obstante, la captura de imágenes con las cámaras incluidas en los TLS, o aquellas obtenidas mediante el empleo de cámaras montadas en rótulas co-registradas con el

TLS, permite generar documentos a modo de visita virtual métrica, muy útiles para explotar el propio producto métrico derivado del TLS.

A la vista de la problemática presentada por cada una de las metodologías independientemente, en el desarrollo de esta Tesis Doctoral se ha elaborado un procedimiento de trabajo que permita la integración de la información proveniente de cada una, aprovechando al máximo los puntos fuertes que presentan. La integración de múltiples geotecnologías en el ámbito arqueológico resulta de interés para la generación de productos geomáticos de calidad como Modelos Digitales del Terreno (DTM) y ortofotografías verdaderas del yacimiento (Eisenbeiss et al., 2007, Lambers et al., 2007, Remondino et al., 2009). Por ello, y debido a las condiciones técnicas y posibilidades de cada metodología, ha sido necesaria la realización de un procedimiento integrador cuyo pilar básico es el sistema de referencia coordenado. Con la finalidad de evitar los problemas derivados del empleo de coordenadas de elevada magnitud presentes en los sistemas de referencia absolutos, en los trabajos realizados en esta Tesis Doctoral se ha optado por el empleo de un *sistema de referencia geodésico local*. Esta opción es adecuada en yacimientos arqueológicos debido a la, relativamente, escasa extensión que abarcan. Sin embargo, la necesidad de difusión de los productos geomáticos derivados y de interacción con otras fuentes de información como los Sistemas de Información Geográficos (GIS), Google Earth, etc., requieren del empleo final de un sistema cartográfico absoluto. Para resolver esta dualidad, los puntos de apoyo o dianas empleados en cada metodología son medidos en un sistema de referencia absoluto (ETRS89 y proyección UTM, junto al sistema de altitudes ortométricas con origen en Alicante) y en un sistema local, mediante diverso instrumental topográfico. La principal ventaja del empleo de un sistema local comparado a un sistema absoluto, desde el punto de

vista geodésico, es que operaciones tales como el paso del terreno al elipsoide y la proyección de las medidas del elipsoide en el plano UTM pueden ser evitadas, aplicando un proceso de cálculo que no precisa realizar aproximaciones en el proceso de reducción, proyección y cálculo de desniveles, lo que se traduce en evitar pérdida de precisión por la comisión de errores sistemáticos de modelización. Además, si el producto final requiere ser representado mediante un sistema cartográfico absoluto, es posible realizar la transformación con un algoritmo que garantice la precisión necesaria.

La rigurosa determinación del sistema de referencia comentado, no solo permite la integración de las tres metodologías empleadas en esta Tesis Doctoral, sino que también es clave para poder llevar a cabo labores de monitorización y comparación cuantitativa y cualitativa de la variación del estado del yacimiento en diferentes instantes, así como para la integración con información procedente de diversas fuentes, esto es, croquis, archivos vectoriales, ortofotografías, etc. En este aspecto, los sistemas de información geográfica 3D (GIS3D) son la herramienta ideal para el análisis conjunto de la información.

El empleo del GIS3D permite realizar la integración de información de múltiples fuentes y tipologías. De esta forma es posible inferir conclusiones que de un análisis individualizado no sería posible. Un ejemplo de este tipo de aplicación es la aparición o desaparición de cualquier elemento representado en un croquis del yacimiento frente al modelo 3D. Por otra parte, también resulta de utilidad la inclusión de cualquier elemento reconstruido virtualmente, de modo que la representación del yacimiento pueda llevarse a un estado anterior al actual (Wüst et al., 2004, Landeschi et al., 2016).

Sin embargo, el potencial de los GIS3D gracias a esta capacidad de integración multi-dato está generalmente limitado al empleo de software específico, lo que conlleva una serie de inconvenientes como el coste del software, la especialización del usuario o la limitación de funcionalidades. Por tanto, con la finalidad de poder hacer más accesible la información, así como la interactuación con los productos geomáticos, resulta de interés la difusión mediante visores Web apoyados en plataformas de código abierto.

Son numerosas las ventajas que presenta el empleo de visores Web para la difusión de los productos geomáticos. Entre otras, es posible acercar de forma interactiva tanto información 2D como 3D al usuario no experto, permitiendo a este la interactuación de manera sencilla e intuitiva. Este mayor alcance de difusión de la información se ve incrementado debido al hecho de que la información es almacenada de forma centralizada por el servidor, eliminando la necesidad de almacenamiento y de descarga completa por parte del receptor. Además, el acceso mediante web permite el empleo de dispositivos móviles como smartphones y tablets, abriendo de este modo la posibilidad de consulta, análisis y edición de la información directamente en campo.

Actualmente, existen diversas soluciones para la difusión de información 3D en visores Web. Uno de los más empleados consiste en el lenguaje VRML (Virtual Reality Modeling Language), un ejemplo se puede encontrar en (Le, 2010), donde los autores crearon su propio GIS3D empleando este lenguaje. Sin embargo, el empleo de este formato se ve condicionado por la necesidad de la instalación de complementos (plug-ins) en los visores a utilizar por parte del usuario. Por otra parte, este lenguaje no permite la optimización del uso de los recursos mediante el empleo del procesador de gráficos GPU (Graphic Processor Unit), algo crucial a la hora de manejar modelos 3D texturizados de alta resolución. Otras soluciones

hacen uso de la librería Unity, como en Schwerin et al., (2013), donde los autores optan por el empleo de esta librería para la visualización de los modelos 3D en un sistema GIS3D desarrollado mediante PostgreSQL y PostGIS, denominado QuaeryArch3D y aplicado en el yacimiento arqueológico "Maya de Copan", en Honduras, Patrimonio de la Humanidad por la UNESCO. De este modo eliminan los problemas asociados a VRML, presentando el inconveniente de que se trata de una librería cuyo propósito principal es la creación de videojuegos, donde los escenarios presentan geometrías más simplificadas que en escenarios reales, por lo que no posee un sistema de visualización jerárquica que permita la carga de la información según la resolución demandada (e.g. imágenes piramidales). Por ello, el empleo de esta librería encuentra problemas para el manejo de grandes modelos 3D, como los obtenidos mediante nubes de puntos TLS o fotogrametría. Con la finalidad de solventar la problemática asociada tanto a VRML como a Unity, en el **Artículo 2** de esta Tesis Doctoral se presenta como solución óptima el uso del estándar WebGL, empleando para ello la librería Open Source Cesium, desarrollada en 2011 por la empresa Analytical Graphics, Inc. (AGI, Greenbelt, MD, USA).

La gran cantidad de información presente en los modelos 3D de alta resolución hace que, al margen del método de difusión empleado, sea necesario buscar métodos de simplificación que permitan eliminar parte de la información, sin por ello mermar la precisión geométrica del modelo, especialmente si se pretende hacer accesible mediante el empleo de dispositivos móviles como tablets o smartphones. En este sentido, los métodos de simplificación tradicionalmente se adaptan a una resolución definida por el usuario mediante la eliminación de puntos y/o triángulos hasta alcanzar un umbral determinado, centrándose únicamente en el aspecto geométrico y no en el aspecto visual del modelo simplificado. Por

este motivo, en esta Tesis Doctoral se ha testeado como método de simplificación la técnica denominada "smooth looking" presentada en Rodríguez-Gonzálvez et al., (2015), la cual tiene en cuenta el aspecto visual durante el proceso de simplificación, a la vez que también mantiene la geometría según los parámetros definidos por el usuario. Esta técnica consiste en la generación directa del mallado de la nube de puntos mediante la aplicación del algoritmo de triangulación de Poisson (Kazhdan et al., 2006), cuya resolución se determina en función del nivel de octree seleccionado, siendo este escogido acorde a la resolución espacial deseada, seguida de un proceso de optimización mediante la eliminación de información redundante.

Se ha mostrado el valor que aporta una determinación geométrica precisa en el ámbito arqueológico. Sin embargo, en ocasiones el elemento de estudio precisa además de otras fuentes de información no geométrica como por ejemplo la respuesta espectral en diferentes longitudes onda. Este es el caso del análisis de pinturas rupestres, donde el estudio de los motivos requiere la determinación de características como el color, el material, la forma o las dimensiones entre otras. Tradicionalmente, la captura de esta información ha sido realizada mediante calcos directos en la roca o dibujos a mano alzada intentando recrear lo más fielmente posible los motivos. Sin embargo, estas técnicas poseen diversos inconvenientes como la invasividad, en el primer caso, propiciando el deterioro de las pinturas debido al contacto, o la subjetividad del dibujante, en el segundo. Recientemente, las técnicas geomáticas han permitido solventar tales inconvenientes, mostrando ser herramientas idóneas para el estudio de pinturas y grabados (Defrasne, 2014, Seidl, et al., 2015; Zeppelzauer et al., 2015). Mediante técnicas fotogramétricas o TLS es posible realizar la captura y análisis de información tanto radiométrica como geométrica,

permitiendo así mismo la documentación de áreas inaccesibles o el análisis de la influencia de la topografía en las pinturas o grabados (Lejeune, 1985, López-Montalvo and Sanz, 2005, Robert, 2016, Sauvet et al., 1998). Así, el uso de TLS permite, además de una determinación geométrica, el registro de los valores de intensidad reflejados por el objeto en relación a la longitud de onda empleada. Por su parte, las técnicas fotogramétricas permiten el empleo de imágenes de diferentes sensores, como cámaras RGB o multiespectrales, permitiendo realizar un análisis en una amplia variedad de longitudes de onda.

Las técnicas empleadas habitualmente para la evaluación de pinturas a partir de imágenes hacen uso de estrategias de decorrelación (Decorrelation Strech o Análisis de Componentes Principales), las cuales únicamente tienen en cuenta la respuesta radiométrica capturada por los sensores. Estas técnicas han demostrado obtener resultados satisfactorios en algunas aplicaciones (Le Quellec et al., 2015, Rogerio-Candelera, 2015). Sin embargo, presentan el inconveniente de ser incapaces de discriminar diferentes elementos cuando su respuesta espectral es muy similar, por ejemplo, un motivo de color negro y una sombra generada por un hueco en la roca. Por esta razón, en el **Artículo 3** de esta Tesis Doctoral, se presenta una solución a esta problemática mediante el análisis combinado de información geométrica y radiométrica. De esta manera, se muestra como a partir de la generación de un modelo 3D de alta precisión y el co-registro de la información radiométrica (RGB, Infrarrojo cercano, etc.) es posible mejorar los resultados obtenidos por algoritmos de clasificación no supervisada. Finalmente, en ese mismo artículo, se muestra también como este acercamiento combinado es beneficioso para el estudio de pinturas rupestres, no solo por la mejora en los resultados de clasificación, sino también para el análisis de la relación de las pinturas en su entorno.

2. HIPÓTESIS DE TRABAJO Y OBJETIVOS

2.1 HIPÓTESIS

Para la consecución de los objetivos de la presente Tesis Doctoral, se establecen, a priori, las siguientes hipótesis de trabajo:

- Las técnicas fotogramétricas de rango cercano, aérea y terrestre, así como el escaneo mediante láser escáner terrestre, son métodos óptimos, no invasivos, para la modelización geométrica de yacimientos arqueológicos.

- La hibridación de geo-tecnologías como la fotogrametría y el láser escáner terrestre mejora los resultados obtenidos por las mismas de forma individual.

- El empleo de vehículos aéreos no tripulados (UAVs) y sistemas tripulados de bajo coste del tipo paramotor, junto con técnicas de visión computacional como Structure from Motion, permiten una documentación y modelización eficiente de yacimientos arqueológicos.

- La aplicación conjunta de análisis radiométrico y geométrico mejora los resultados y aumenta el automatismo en los métodos de clasificación no supervisados de imágenes multiespectrales.

- La difusión y análisis de productos geomáticos puede hacerse más accesible mediante el empleo de Sistemas de Información Geográfica 3D (GIS3D) y visores Web-GIS.

2.2 OBJETIVOS

El propósito de esta Tesis Doctoral consiste en el cumplimiento del objetivo general y los objetivos específicos que a continuación se detallan.

2.2.1 Objetivo general

Integrar múltiples sensores con el fin de aplicar técnicas laser, fotogramétricas y de teledetección de rango cercano para la obtención de productos geomáticos de alta resolución que permitan mejorar la calidad y eficiencia en la modelización, el análisis y la monitorización de yacimientos arqueológicos.

2.2.2 Objetivos específicos

i. Analizar las técnicas y procedimientos para la selección y utilización de sistemas de referencia óptimos para la integración de la información procedente de diversos sensores geomáticos.

ii. Incorporar los algoritmos de última generación de fotogrametría (e.g. extracción de características y matching denso), tanto aérea como terrestre.

iii. Desarrollo de una plataforma giroestabilizadora para su aplicación en cámaras fotográficas a bordo de paramotor.

iv. Realizar el registro de imágenes procedentes de distintos sensores (e.g. cámaras RGB, multiespectrales, etc.) mediante algoritmos basados en intensidad, para su empleo conjunto como imágenes multi-capa.

v. Generación de modelos tridimensionales optimizados para su visualización web en plataformas móviles (e.g. tablet y smartphone).

vi. Empleo de GIS3D en yacimientos arqueológicos para el análisis multi-dato, a partir de información procedente de diferentes fuentes, y el análisis multi-temporal, mediante la obtención de información en diferentes instantes (e.g. análisis de variaciones, cubicaciones, etc.).

vii. Generación de ortofotografías verdaderas y modelos tridimensionales foto-realísticos, así como de imágenes en diferentes bandas del Infrarrojo cercano derivadas de imágenes adquiridas con sensores multiespectrales.

viii. Análisis y optimización de técnicas de realce y clasificación no supervisada de imágenes multiespectrales mediante la combinación de información geométrica y radiométrica.

3. ARTÍCULOS PUBLICADOS

Se presentan en esta sección los tres artículos que han sido publicados en revistas especializadas de impacto internacional. Se incluye un resumen previo a cada artículo donde se señala la labor investigadora acometida.

3.1 Un acercamiento a la medición híbrida para la modelización y monitorización de yacimientos arqueológicos: El caso de estudio de Mas D'Is, Penàguila.

En el presente artículo se evalúa la idoneidad de tres técnicas geomáticas de amplia utilización en la documentación geométrica de yacimientos arqueológicos: el láser escáner terrestre, la fotogrametría aérea desde vehículos no tripulados (UAVs) y la fotogrametría terrestre. Se han valorado las tres metodologías tanto por separado como conjuntamente, concluyéndose que la solución combinada es la idónea al permitir aprovechar los puntos fuertes de cada una de las mismas y descartar sus deficiencias. De este modo, se ha aprovechado la altura dominante y la precisión que otorga la fotogrametría aérea desde UAV en la determinación de los planos horizontales de una superficie; la elevada resolución y velocidad proporcionada por el láser escáner terrestre permitiendo su empleo en superficies de geometría irregular; y la versatilidad y calidad radiométrica que aporta la fotogrametría terrestre en la determinación de geometrías con orientación predominantemente vertical.

Se demuestra como la hibridación de técnicas geomáticas es una realidad aplicable en la documentación de yacimientos arqueológicos, mejorando los resultados respecto al enfoque de la aplicación individual de cada una de las metodologías.

Para la consecución de la integración se presenta un flujo de trabajo donde prima la rigurosa selección y determinación del marco de referencia cartográfico, garantizando así la precisión y homogeneidad, permitiendo además evitar los problemas derivados de proyecciones cartográficas, así como del manejo de coordenadas de elevadas dimensiones en modelos tridimensionales, sin perder por ello la capacidad de visualización e integración con información geoespacial mediante visores GIS o Google Earth.

Como resultado de la metodología híbrida empleada se han obtenido productos geomáticos de precisión, como son el modelo tridimensional del yacimiento y la ortofotografía verdadera de alta resolución.

Además, se ha mostrado el valor añadido que presenta el empleo de UAV frente a las plataformas tradicionales de fotogrametría aérea (e.g. avionetas fotogramétricas) mostrando la facilidad en la captura de datos y permitiendo la repetitividad (resolución temporal) de la operación con un menor coste asociado. La metodología propuesta en este artículo ha sido aplicada con éxito en dos instantes temporales diferentes en el yacimiento arqueológico Mas D'is, en Penàguila (Alicante, España). Gracias a la documentación en diferentes intervalos temporales se ha realizado la monitorización de las excavaciones.

De las investigaciones llevadas a cabo en este artículo se ha concluido que las metodologías empleadas son idóneas para su aplicación en yacimientos arqueológicos al no ser invasivas y permitir la obtención de

productos geomáticos de alta precisión. Además, se ha demostrado como la mejor solución pasa por un empleo combinado de las técnicas de modo que se aprovechen las ventajas de cada una y se eliminen los inconvenientes. Para ello, se ha mostrado la importancia de la correcta selección y utilización de los sistemas de referencia, lo que permite, no sólo la integración de metodologías, sino también la monitorización en diferentes instantes.

Journal of Archaeological Science 50 (2014) 475–483

Contents lists available at ScienceDirect

Journal of Archaeological Science

journal homepage: http://www.elsevier.com/locate/jas

A hybrid measurement approach for archaeological site modelling and monitoring: the case study of Mas D'Is, Penàguila

Jose Alberto Torres [a], David Hernandez-Lopez [b], Diego Gonzalez-Aguilera [a, *], Miguel Angel Moreno Hidalgo [c]

[a] Department of Cartographic and Land Engineering, Avila, University of Salamanca, Spain
[b] Institute for Regional Development (IDR), Albacete, University of Castilla La Mancha, Spain
[c] Centro Regional de Estudios del Agua (CREA), Albacete, University of Castilla La Mancha, Spain

ARTICLE INFO

Article history:
Received 23 February 2014
Received in revised form
29 July 2014
Accepted 11 August 2014
Available online 19 August 2014

Keywords:
Archaeological settlement
Geo-technologies
Hybrid approaches
Unmanned aerial vehicle
Terrestrial laser scanner
Terrestrial photogrammetry
Surveying methods
Coordinate reference system
Geo-referencing
True-orthophoto

ABSTRACT

There are several methodologies for obtaining and processing geospatial data with the aim of generating 3D models that represent reality. Thus, it is necessary to analyse the performance and capabilities of each methodology and its integration into archaeological heritage documentation. This paper analyses and compares the generation of 3D archaeological site models through the integration of aerial photogrammetry from an unmanned aerial vehicle, terrestrial photogrammetry and laser scanning. This process is carried out for two different excavation campaigns to monitor the sites based on dimensional analysis. Finally, a hybrid 3D model is generated by merging the three methodologies into a true orthophoto of the archaeological site for each campaign. One of the most relevant aspects of the model is the integration of multiple geo-technologies, which requires establishing a rigorous methodology for geo-referencing different data and equipment that is supported by the use of a dual geodesic coordinate system. The results obtained confirm that the geo-technologies proposed for integration are perfectly complementary, providing high quality and thorough models of archaeological sites.

1. Introduction

Knowledge of the topographic features of an archaeological site is essential for its full documentation. Methodologies such as terrestrial laser scanning (TLS) and terrestrial and aerial photogrammetry, the latter from unmanned aerial vehicles (UAVs), have been used to document archaeological sites, each showing great potential separately. Terrestrial photogrammetry offers a low-cost, highly flexible alternative by allowing automated methods, and it opens procedures to all users for performing dimensional analyses and even reconstructing simplified models from images taken with any type of camera (Tokmakidis and Skarlatos, 2002). In addition, the recent emergence of UAV technology has allowed these principles to be extrapolated to aerial photogrammetric imagery with spatial and temporal resolution impossible to achieve with standard satellite procedures (Gomez-Lahoz and Gonzalez-Aguilera, 2009). At an archaeological site, because it is a great advantage to have vertical and oblique bird's eye view images without any obstacles and from a unique perspective, UAV photogrammetry has emerged as a technology of great interest to the scientific archaeological community. However, one of the biggest drawbacks of both terrestrial and UAV photogrammetry lies in the difficulty of modelling and treating complex non-parametric geometries. Lately, laser scanning technology is being applied to the recording and 3D modelling of highly complex archaeological sites, for example, archaeological sites and/or underground caves where the complexity of the shapes and object sizes necessitates non-destructive techniques for documentation and reconstruction (González-Aguilera et al., 2011a,b). However, one of the major drawbacks in its lone application resides in the lack of semantic information in the resulting point clouds, which is vital in the process of archaeological interpretation.

Therefore, various authors have chosen to integrate different geo-technologies in order to make use of hybrid synergy and obtain more complete and competitive products. Eisenbeiss et al. (2007),

* Corresponding author. Department of Cartographic and Land Engineering, University of Salamanca, Hornos Caleros, 50, 05003 Avila, Spain. Tel.: +34 920353500; fax: +34 920353505.
E-mail addresses: josealberto@usal.es (J.A. Torres), david.hernandez@uclm.es (D. Hernandez-Lopez), daguilera@usal.es (D. Gonzalez-Aguilera), miguelangel.moreno@uclm.es (M.A. Moreno Hidalgo).

http://dx.doi.org/10.1016/j.jas.2014.08.012
0305-4403/

Lambers et al. (2007) and Remondino et al. (2009) use aerial photogrammetry taken by UAV, terrestrial photogrammetry and TLS to obtain digital terrain models (DTMs) of archaeological settlements. They combine information from different sensors and methodologies to obtain a DTM that overcomes the deficiencies of the individual methodologies.

In an attempt to merge satellite data, Patias et al. (2009) use a UAV-helicopter, TLS and QuickBird satellite images to carry out the documentation of archaeological sites. In this case, the satellite images provide added value because they allow geolocation and a general representation of the whole environment.

Although all of the cited works have integrated geotechnologies, none of them have developed a thorough georeferencing methodology capable of guaranteeing high precision and enabling automation in the registration process of all the data and sensors. This aspect is crucial in archaeological campaigns where numerous sensors are used and the data obtained correspond to different methods. A proper georeferencing system would allow adaptive hybridization of the models so that redundant information is removed in common areas and extra information is provided in shadow areas. Furthermore, the registration of images from UAV and terrestrial photogrammetry incorporates breaklines through stereoscopic restitution processes, providing higher quality and authenticity to the final model, two key aspects in the generation of a true-orthophoto.

This paper describes how three capture techniques: aerial photogrammetry from UAVs, laser scanning and terrestrial photogrammetry, can be integrated to generate hybrid archaeological products: a three-dimensional model and a true orthophoto, allowing archaeological site monitoring to quantify the degree of progress at a site. The development of a rigorous geo-referencing method will be of great utility for future archaeological works, making it possible to obtain better results while establishing a basis for automated sensor registration.

The modelling methodology used here allows the generation of a three-dimensional hybrid model with its corresponding true orthophoto. To demonstrate the added value of hybridization methods in 3D modelling, a series of comparisons (quantitative and qualitative) are made in order to evaluate and quantify the advantages and disadvantages of each methodology separately and together. Finally, the variable of time is incorporated to monitor the degree of evolution of the site. More specifically, we propose to perform a dimensional analysis to assess the excavation volume and identify areas most affected in two different campaigns.

2. Materials

2.1. Site description

Placed in the municipality of Penàguila (Alicante, Spain), the archaeological site of Mas D'Is is set in the location known as “Les Puntes”, close to the Penàguila River. The site proves to be in flat terrain in an agricultural area. This is why the terracing under the crop fields is hidden. This site holds great interest for the archaeological scientific community, offering a new image of the Neolithic communities in the Mediterranean area of the Iberian Peninsula. In contrast to the traditional view, which considered some continuity between habitat sites of Mesolithic and Neolithic groups with a preferential use of caves, recent data suggests the development of sedentary villages in the locational strategies of the early farming groups (Bernabeu Aubán et al., 2003) (see Fig. 1).

Several geometrical shapes and various irregular reliefs can be found in the settlement of Mas D'Is. The former are related to human presence, whereas the latter correspond to the morphology of the terrain. These characteristics provide the site great complexity,

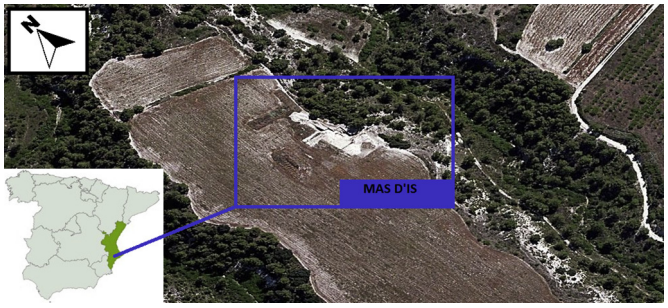

Fig. 1. Aerial image of the archaeological settlement.

so it is important for them to be recorded and reconstructed by hybrid approaches and models. On the other hand, factors such as vegetation and the depth of excavations create added drawbacks in terms of shadows and matching errors, seriously affecting the final product if they are not carefully filtered.

2.2. Instruments for reference system definition

The instruments used for establishing a reference frame (Fig. 2) include a total station, Topcon Imaging Station, a high-accuracy GPS type RTK GNSS Leica System 1200 and several artificial targets for geo-referencing the dataset acquired from each sensor. A complete description of each instrument is detailed below.

2.2.1. Total station

To obtain the coordinates of the points that enclose the common framework of the work equipment is used that ensures precise topographic observations (Fig. 2). Total Station Imaging Station 2 allows the measurement of points without a prism reflector from a distance of 250 m to 2000 m. Moreover, with the use of a prism the range can be extended up to 3000 m. Prism measurements can be performed by a single operator using the robotic tracking receiver RC-3. The range precision for that instrument is ±2 mm + 2 ppm for distances with prism measurements and ±3 mm for reflectorless measurements. It also has dual axis compensator ±6 ' accuracy. The minimum angular reading is 1 mgon and since the maximum working distance is approximately 40 m, all this translates into accuracy in determining the position of better than 0.01 m.

2.2.2. High accuracy GPS

The linkage of this work to a cartographic reference system is performed by GPS sensors (Fig. 2). Leica System 1200 receptors works with the L1 and L2 frequencies emitted by the constellation satellites GPS and GLONASS. This allows measurement in real time kinematic (RTK) mode while static observations are recorded in the base receiver. In the subsequent post-processing step, the coordinates of the measured points are obtained in a global system with centimetre accuracy. To minimise the possibility of recording false coordinates, this equipment updates its position with a frequency of 20 Hz (0.05 s). Absolute positioning, when points were surveyed in static mode, provided accuracy of 5 mm + 0.5 ppm in horizontal and 10 mm + 0.5 ppm in vertical, and 10 mm + 1 ppm in horizontal and 20 mm + 1 ppm in vertical when points were surveyed in cinematic mode.

2.2.3. Targets for geo-referencing the obtained models

The need to integrate all the data captured by each of the sensors under the same coordinate reference system requires that targets be of different types depending on their use. Stakes with a nail in the centre were used for installing the base of the GPS,

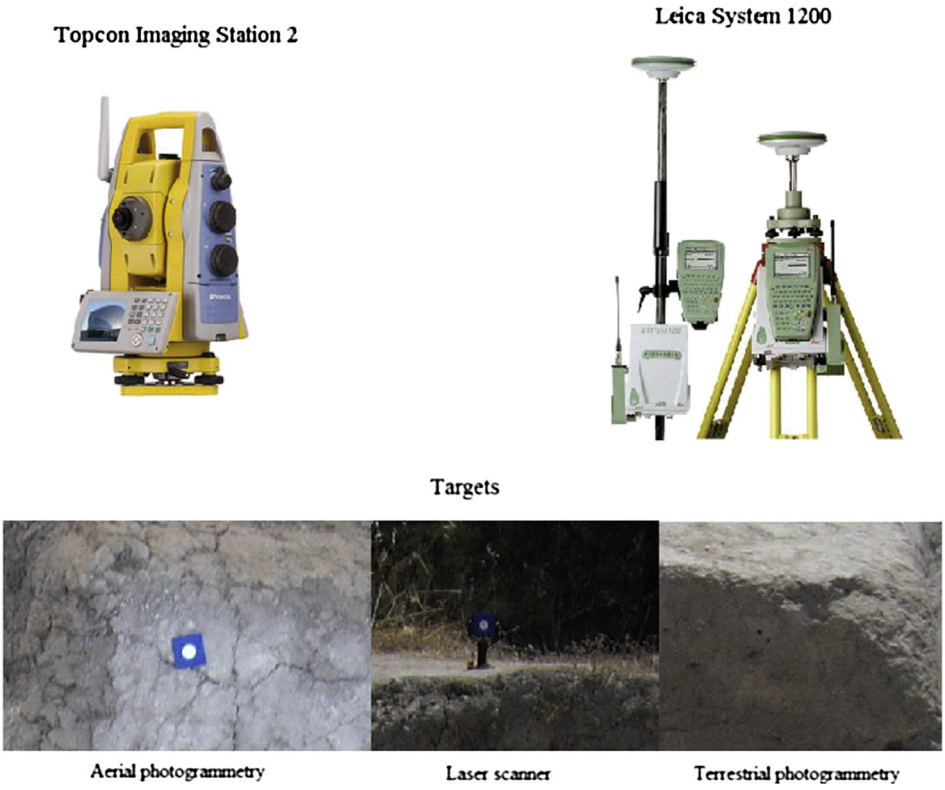

Fig. 2. Topographic equipment used in this work (Above). The different types of targets used in the archaeological survey (Below).

targets with blue background and a 3-cm diameter white circle were used for aerial photogrammetry and laser scanning, and targets made of black acetate with a 1.5-cm diameter circumference were used for terrestrial photogrammetry (Fig. 2). The choice of this latter type of target for use in terrestrial photogrammetry is based on the shorter distance to the object, so that the spatial resolution is increased. Therefore, with these targets the visual impact on the texturing of 3D models obtained by terrestrial photogrammetry can be minimised. In addition, these targets were surveyed from a single station in order to minimise error propagation, guaranteeing a relative precision of 0.005 m.

2.3. Instruments for image acquisition

The instruments for image acquisition include an UAV of the quadracopter (Microdrones, md4-200) type, a Pentax Optio A40 compact digital camera and a Leica ScanStation 2 laser scanner (Fig. 3). The equipment meets the needs for carrying out this work. A complete description of each instrument is provided.

2.3.1. Unmanned aerial vehicle

Different types of model aircraft have different capabilities, with advantages or disadvantages depending on purpose (Hunt et al., 2005). Compromises must be made between ease of flying, stability in wind, handling flight failures, distance covered, and take-off/landing requirements. In this study, a Microdrone md-400 (Microdrones, Inc., Kreuztal/Germany) was utilised. It is a vertical take-off and landing (VTOL) quadracopter aircraft (Fig. 3). The acronym VTOL denotes the capability of a flight vehicle to take off and land in the vertical direction without the need of a runway. It employs four rotors or propellers on vertical shafts mounted on one level of the bodywork. The advantage of this concept is the movement of the UAV body can be controlled in three directions by a simple variation in thrust (and therefore torque) of each of the four propellers, if the direction of rotation for each of them has been appropriately selected. Each 24-pole motor has a gross weight of 40 g and a diameter of 48 mm. A brushless external rotor motor has 18 slots and 24 magnets and has fully synchronised commutation. Each of the motors is supplemented with three Hall–sensors, which relay the momentary position and turning speed of the magnets to the control electronics. Integrated control of the motors is mediated via a Controller–Area–Network (CAN–bus) with each motor having a unique address. The joint operation of all components creates a closed control loop at a dynamic fast enough to

Fig. 3. Sensors used in this work.

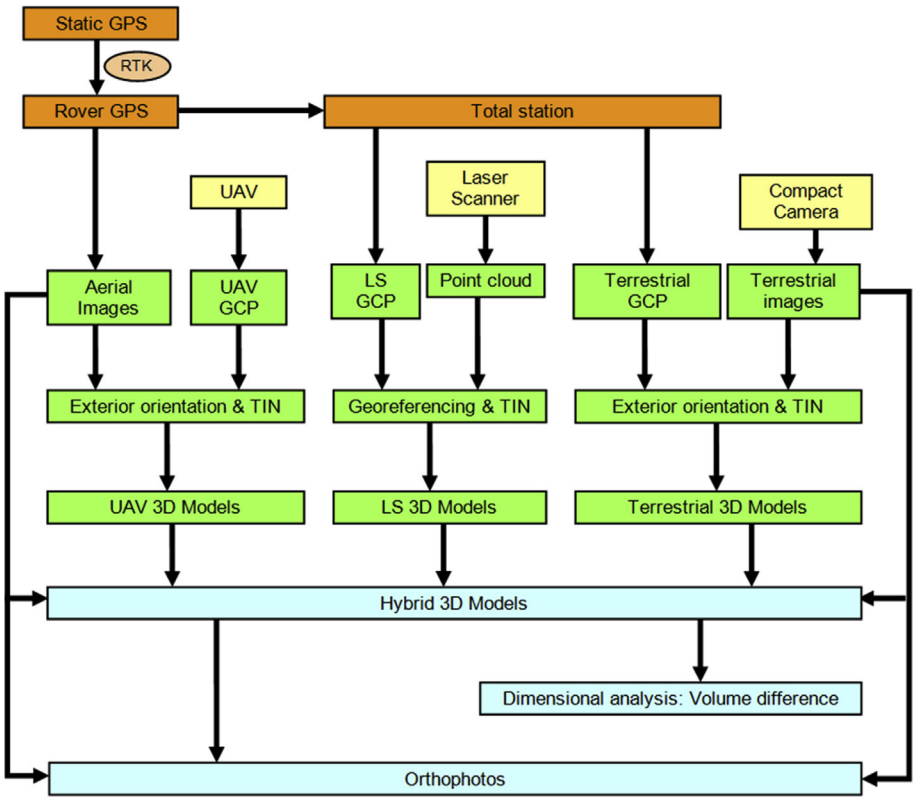

Fig. 4. Scheme of the workflow performed in the hybridization of geo-technologies for modelling and monitoring the Mas D'Is Penàguila archaeological site.

enable accurate and rapid control of each motor's momentum and thereby stabilise the aircraft.

The core component of the electronics is the IMU (Inertial Measurement Unit) module, which includes a bearing fixture and barometric altitude stabilization. This device comprises a set of mutual communicating sensors that are combined in a Kalman filter. A 32-bit embedded controller calculates the requested control vectors in millisecond intervals. This type of generic control allows for basic stabilization of the drone's position and bearing during flight and facilitates the manual control tasks of the pilot.

Heading retrieval, an accelerometer and a baroaltimeter for heading and altitude control are also installed in the IMU-module. The flight controller (FC) permits user interpretation of the radio controlled (RC) commands including a mixer, safety features and motor management, among others. A Global Positioning System (GPS) U-Blox 6 is also installed for reporting and controlling the location of the aircraft.

2.3.2. *Terrestrial laser scanner*

To perform laser scanning surveying, Leica ScanStation 2 equipment was used based on the time of flight (ToF) principle with a scanning speed up to 50,000 points per second. This laser scanner has a 360° × 270° – Horizontal × Vertical-field of view, with an angular resolution of 0.0023° in horizontal/vertical and a precision in angular measurement of 0.0034°. The laser beam diameter is 6 mm for 50 m and works in the visible green electromagnetic spectrum with a wavelength of 532 nm. The measurement distance ranges from 30 cm to 300 m, and the precision of a simple measurement goes from 4 mm to 50 mm. Although in this work the images obtained with the Pentax camera have been used for the mapping texture process, the Leica ScanStation 2 incorporates an integrated 1 megapixel camera. The intensity values are registered with 12 bit radiometric resolution. It also includes a dual-axis compensator with a precision of 0.00015°. The spatial resolution used was 5 mm at 20 m distance.

2.3.3. *Conventional RGB compact digital camera*

A Pentax Optio A40 digital camera (PENTAXTM, Golden, Colorado, USA) was utilised to obtain images in the visible spectrum. The main characteristics of the camera for this study are:

- Sensor: 1/1.7" type CCD, 12.0 million effective pixels and pixel size of 0.0018 mm.
- Image size: 4000 x 3000 (columns × rows).
- Lens: 37–111 mm (35 mm), 3x optical zoom, Focal of 2.8–5.4.
- Focal length: 7.9 mm
- Pixel size: 0.0018 mm
- ISO sensitivity: ISO 50–ISO 1600.
- Internal memory (21 Mb) and SD memory card.

3. Methods

The method developed can be observed in Fig. 4. Due to the role of the different sensors used, the first step establishes a common reference frame based on the use of different artificial targets that perform as ground control points. The high precision of the surveying equipment together with the rigour of the reference system definition guarantees that data based on aerial images (UAV), point clouds (TLS) and terrestrial images (digital camera) can be integrated. After data have been acquired with each technology, the information is processed in order to generate hybrid geomatic products. Finally, the assessment of the results obtained and their monitoring over time allow us to derive conclusions about the evolution of the archaeological settlement.

3.1. Reference system definition

The definition of the reference system with the geo-referencing methodology is a key factor enabling the results of different methodologies to be merged and compared. To do this, a reference system together with its common and proper coordinates must be chosen, establishing a homogenous network of control and check points that allow us to geo-reference the different datasets acquired by different sensors. The targets aimed at in aerial photogrammetry are located in horizontal planes, while those for terrestrial photogrammetry and laser scanning are placed in vertical planes. Then, the GPS base is placed and the coordinates are surveyed in static mode. This process is intended to bind all the measurements in the correct places after processing the observations. At the same time, all the station bases and the control points for aerial photogrammetry are surveyed by GPS in real time kinematic (RTK) mode. Two bifrequency GPS units were used in order to establish rigour in the surveying of control points, and a relative precision of 0.02 m was obtained. Then, the targets for terrestrial photogrammetry and laser scanning are surveyed by the total station.

One of the most relevant aspects proposed in this paper involves the choice of an appropriate reference and coordinate system. According to ISO 191111, a coordinate reference system (CRS) can be geodesic or local. Ideally, for archaeological work, a local CRS would be desirable because the work area is small and all coordinates in metres are small in magnitude, avoiding problems related to the generation of certain model formats (e.g., VRML, OBJ, PLY) when cartographic CRS coordinates are used such as UTM.

However, the requirement for correct geo-referencing in geomatics products is strong due to the convenience of having overlapping information from different sources and to the need to publish the products into globalised systems like Google Earth. In this sense, the methodology proposed in this paper aims to take advantage of both CRS types, taking the easy way in the management of local CRSs and addressing the possibility of geo-referencing geodetic CRSs. The geodetic reference system used in this work is the ETRS89 (European Terrestrial Reference System 1989), an official reference system in Spain since 2007. The local system used, LGCSPA (Local Geodetic Coordinate System for Anchor Point), is the local geodetic system linked to the anchor point, which is supported by the GPS base and whose position is determined with high accuracy after post processing with two Spanish global navigation satellite system (GNSS) stations. This coordinate system is realised as: origin: point itself; *Z* axis: according to the geodesic vertical in the anchor point; *Y* axis: according to the direction of geodetic north and an *X* axis completing a right-handed triplet. To avoid negative coordinates in planimetry, the origin has been moved 100 m in each coordinate axis. In order for heights to be orthometric a translation in the *Z* axis is considered, HPA (height of anchor point), obtained as the coordinates of the anchor point: (100, 100, HPA).

To ensure that all work is referenced to LGCSPA the following methodology is defined:

1. Get the coordinates of the points measured by GPS-RTK. This includes the total station bases and the targets that are the control points for UAV photogrammetry.
2. Calculate the points surveyed by the total station in this LGCSPA system. This group of points includes the targets that are control points for the terrestrial photogrammetry and laser scanning.

The main advantage of working with this LGCSPS system compared to the UTM coordinate system, from a geodetic point of view, is that operations such as passing from terrain to ellipsoid and projecting the ellipse's measurements onto the UTM plane can be avoided, resulting in better quality archaeological site data. However, if the final products, DTM and the true orthophoto, require a cartographic projection, it is possible to get these models into the UTM coordinate system by applying a simple rotation and scaling translation.

3.2. Data acquisition

In this section the data acquisition process is described, which consists of 1) aerial image acquisition, 2) laser scanner data acquisition and finally 3) ground image acquisition.

3.2.1. Aerial imagery

Before executing a flight, flight planning should be performed in such a manner that permits implementing the photogrammetric algorithms, mainly with respect to overlap, verticality and image scale. To do so, the authors developed the MFlip software (Hernandez-Lopez et al., 2013) (Fig. 5), which was awarded the ASPRS (American Society of Photogrammetry and Remote Sensing) John I. Davidson President's Award. On the first day of data acquisition, the planned flight height was approximately 60 m, which resulted in a GSD of approximately 0.014 m. In this case, two

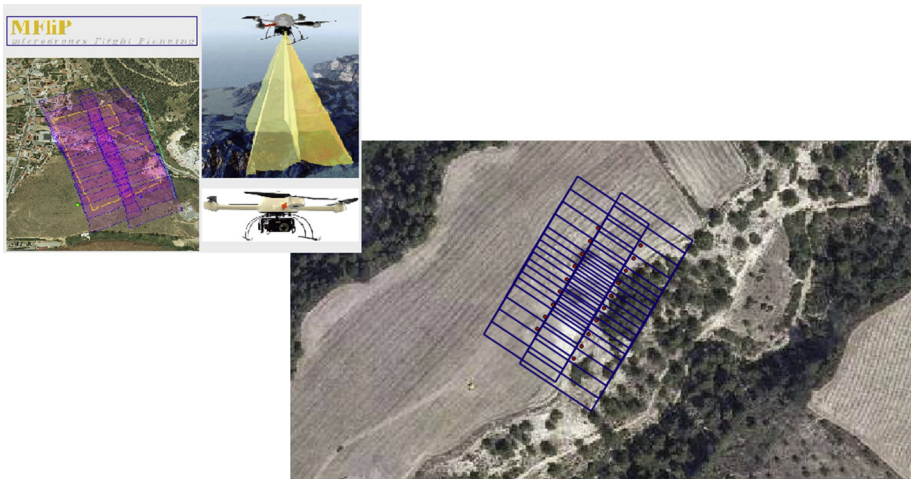

Fig. 5. Flight planning software used for the UAV survey of the archaeological settlement.

parallel flights were necessary. On the second day the flight plan consisted of performing three parallel flights at a height of approximately 40 m, resulting in a GSD of approximately 9 mm. For both flights the forward overlap between images was 60% while the side overlap was 30%. The flight parameters defined for the UAV were the following: 1) a horizontal speed of 4 m/s, 2) vertical speed of 2 m/s, 3) landing speed of 2 m/s. Two shots of the camera were programmed for each image acquisition point to ensure sharpness (the best image was selected during the processing work). In particular, the images were taken with a short fixed focal length using a diaphragm aperture of f/2.8, exposure time 1/1000 s and ISO 100. The parameters defined for each flight plan were written in an ascii file that was saved in a SD card incorporated into the UAV, which permitted the flight to be performed automatically (only take-off and landing were manual).

3.2.2. Laser scanner data

After flying the UAV, laser scanner data acquisition was performed. It was necessary to perform three scans from different locations on each of the days to acquire data from the entire site. The above-described targets were located across the site to align the point clouds generated at each base. The spatial resolution was established for the worst case at 5 mm, considering that the maximum scan distance would be less than 20 m. Thus, for closer objects, the spatial resolution was even higher than 5 mm.

3.2.3. Terrestrial imagery

Terrestrial image acquisition was performed with a camera that was mounted in the UAV with the objective of improving the texture of the vertical planes. Several images were obtained, which allowed the whole archaeological site to be covered. The images were captured according to a photogrammetric procedure (Hanke and Grussenmeyer, 2002). The distance to the object was approximately 6 m. Thus, the images were captured within a distance of 2 m, maintaining a base/distance to the object ratio of 1/3, which is adequate for photogrammetric purposes. The whole site was covered with a GSD of 3 mm by 36 images. In addition, the terrestrial images were taken with a short fixed focal length with a diaphragm aperture of f/8, exposure time 1/500 s and ISO 100.

3.3. Data processing

The information processing was carried out in two steps. Firstly, data were processed from each of the separate methodologies (aerial imagery, terrestrial imagery and laser scanning). Thus, three DTMs in TIN format (triangular irregular network) were obtained. After evaluating and analysing all the models for discrepancies, errors were detected, classified and evaluated. As a result, a single DTM was developed that considers for each area the model that best represents that portion of space. The DTM is textured with the highest quality images, using the aerial images for the horizontal planes and terrestrial images for vertical planes. Thus, a hybrid 3D model that best represents the archaeological site was obtained. In order to accurately process all this information, it is necessary to calibrate the camera and the laser scanner. If the images are oriented and the laser point clouds are aligned, a DTM can be developed. In a further step, the hybrid model and the true orthophoto are generated.

3.3.1. Calibration

Using the camera as a measurement instrument requires previous modelling of the physical and geometric parameters that define the behaviour of the optical components. In this case laboratory calibration was performed with *Image Master Calib* software. Taking images of a known pattern from different positions and orientations, it is possible to determine the focal length (f), optical centre coordinates (x_{ppa}, y_{ppa}), radial distortion according to the Gaussian model (k_1, k_2) (Brown, 1971) and tangential distortion (p_1, p_2). Because the same camera is used for all photogrammetric processes, only one calibration is required.

Likewise, and although not as standardised, the use of a laser scanning system requires, in the interest of higher quality results, to have its internal parameters calibrated and its systematic errors modelled. To do this, we have made use of an existing calibration field placed in the Higher Polytechnic School of Ávila (Spain) that has allows us to work with a total of 21 internal orientation parameters divided into: 9 parameters for measuring distance (ρ), 7 parameters for the horizontal angle (Θ) and 5 parameters for the elevation angle (α). Some of these parameters refer to classic systematic errors of topographic equipment, while many others were obtained through tests and empirical evidence (González-Aguilera et al., 2011a,b).

3.3.2. Orientation

The coordinates of the control points and the calibration parameters of the camera are the inputs that allow the orientation of the terrestrial and aerial images. This process comprises two phases. The first involves extraction and an automatic feature-matching algorithm that is performed by ASIFT (Affine Scale Invariant Feature Transform) developed by Morel and Yu (2009). The reason for using ASIFT lies in its robust performance with images that show marked differences in scale and rotation. In the second step, the points found by ASIFT are matched with the manually measured ground control points to compute the absolute positioning and orientation of the images based on bundle adjustment. This adjustment consists of an iterative least square process with collinearity equations (Kraus, 1993). The calculation and adjustment of the absolute orientation of the images is carried out with the Image Master® Pro software, taking as input the automatic correspondence of interest points extracted by ASIFT. The method employed, known as blunder adjustment, is the least squares resolution of a redundant system generated from the collinearity equations. In this system, the input data are the image coordinates of the control and matching points, the calibrated focal length, the coordinates of the optical centre and the geometrical distortion parameters. Furthermore, the unknowns are the position (X_L, Y_L, Z_L) and orientation (ω, φ, χ) of the camera at the instant of the image's acquisition and the ground coordinates of the matching points (X, Y, Z).

3.3.3. Alignment

In order to completely register the archaeological site and due to its geometry and dimensions, scans were performed from different locations. From each scan a point cloud was obtained, which was aligned, geo-referenced and debugged. Alignment and geo-referencing processes were performed with Leica Cyclone® software. To do so, four of the above-described targets were located around the site. The targets were scanned from each of the basements of the scans and the coordinates of the targets were calculated by topographic methods.

3.3.4. Integration

Placed on rock, the study site presents complex geometry, so the best representation of the surface is generated by the combination of TLS and photogrammetry; thus the regular surfaces are described by a three-dimensional model generated by photogrammetry. This model is obtained from point clouds by automatic correlation with a spatial resolution of 2 cm, and it has the great advantage of incorporating digitalised breaklines from stereoscopic restitution of the aerial and terrestrial images. Moreover, the point

cloud obtained by TLS is used for irregular areas with non-parametric surfaces, where breaklines are not required, obtaining a resolution of 3 mm. The complementarity of these two models is evident, the shadowed areas generated by TLS are supplemented by photogrammetry.

The meshing strategy employed is Delaunay triangulation based on the incremental method (Bourke, 1989) and enhanced with the addition of breaklines as geometric constraints. More specifically, significant features related to edges and slope changes of the field lines (essentially vertical walls) are restored from the oriented UAV images, using for this the combination of the collinearity conditions with the internal and external orientations of the images.

Finally, the generation of the hybrid 3D model resulting from the integration of independent 3D models consists of three basic operations: (1) the identification and marking of informationless areas due to occlusions and/or shadows corresponding to each model, (2) superposition of the 3D models, and (3) the removal of redundant and overlapping areas.

After obtaining the 3D hybrid model resulting from the integration of the three geo-technologies, we will be able to generate a true orthopohoto. Removing shadows and occlusions in hybrid DTM allows us to implement a process of adaptive true orthorectification that incorporates two novel steps compared with the classical process of generating orthophotos (Kraus, 1993): (1) the integration process of orthoprojection using the different images taken by the UAV (2) determining the visible and occluded parts of each image.

4. Results

The results were obtained based on two field campaigns performed on 27th May 2010 and 2nd July 2010. The goal of using two different campaigns was two-fold: on one hand, the different technologies and approaches can be compared, and on the other hand, the archaeological settlement can be monitored in terms of the material extracted through a dimensional analysis of volumes. Although each technique allows us to obtain a detailed description of the settlement, none is able to provide an integral reconstruction of the site in terms of completeness. Through the method presented in this paper each technology is reinforced by the integration of others, and thus the results guarantee the best quality in terms of precision, reliability and completeness, minimizing economic and temporal costs.

4.1. Comparison of geo-technologies

The utilised geo-technologies were compared to ascertain the precision of each technique (Fig. 6) and to deeply analyse the strengths and weaknesses of each method from data acquisition to final model development (Table 1). Because the positioning was performed with a mixed methodology (total station and GPS), the absolute precision in the position of each model is 1.6 cm in planimetry and 2.3 cm in height. A sketch with the positions of the sensor stations and control points is shown (Fig. 7).

The different DTMs obtained were compared from a quantitative point of view. The areas affected by gross errors are discarded, only taking into account the overlap areas. In these areas a dimensional analysis based on discrepancies along the vertical (Z) direction is performed. The different resolutions obtained by the different geotechnologies together with their georeferencering systems provide discrepancies between MDTs of around several centimetres. The larger discrepancies are obtained in those areas that are especially unfavourable (i.e., horizontal planes obtained for terrestrial photogrammetry or vertical planes modelled from aerial images). The results are show in Table 1.

Table 1
Comparison of geo-technologies: differences between DSM (in metres) obtained along vertical direction (Z).

DSM comparison	Minimum	Maximum	Average
Laser scanner vs. terrestrial photogrammetry	0.001	0.021	0.006
Laser scanner vs. aerial photogrammetry	0.002	0.032	0.008
Terrestrial photogrammetry vs. aerial photogrammetry	0.001	0.020	0.004

From a qualitative point of view (Table 2), an initial visual analysis of the models allows us to confirm that there is no single geo-technology that provides a complete model of the site. Occlusions and shadows in the case of laser scanning, viewpoint limitations in photogrammetry and low quality of the vertical walls inside the model in the case of UAV photogrammetry all lead to a lack of information for a specific area. It should be noted that the correct representation of the deeper areas inside the site does not appear in the DTM made by terrestrial photogrammetry. This area does not appear in the DTM made by TLS due to problems related to the shadow areas and the obliquity of the scan angles.

The model obtained by UAV photogrammetry covers the whole archaeological site, highlighting the speed and simplicity of this method. However, this method implies lower geometric resolution, with a point each 5 cm. On the other hand, the models obtained by terrestrial photogrammetry and TLS show the best resolution values, with 2 cm and 5 mm, respectively, which is significant in defining the breaklines. In addition, there are difficulties related to the representation of vertical planes, obtaining overly sharp triangles, as well as shadow zones. These vertical areas represent a complicated matching process that generates ambiguities and therefore an erroneous representation of the surface.

By contrast, in the terrestrial photogrammetry the error associated with the representation of vertical planes disappears, giving rise to the same error, in this case, expressed in horizontal planes. The complementarity of the two methodologies is apparent. On the other hand, the disadvantage resulting from shadow generation in the photographs remains, as well as dealing with complex non-parametric geometries. That is why those shadow areas are represented by TLS. However, TLS also carries a number of associated errors such as lack of information in hidden areas, excess of information outside the study area and lower quality due to the obliquity of the scan and the increment of beam divergence.

4.2. Hybrid products: DTM and true orthophoto

The hybrid products obtained (DTMs and true orthophotos) correspond to two different excavation campaigns and have

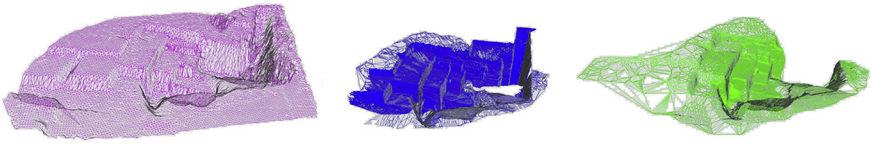

Fig. 6. DTMs obtained via: (left) aerial photogrammetry, (centre) ground photogrammetry, and (right) laser scanning.

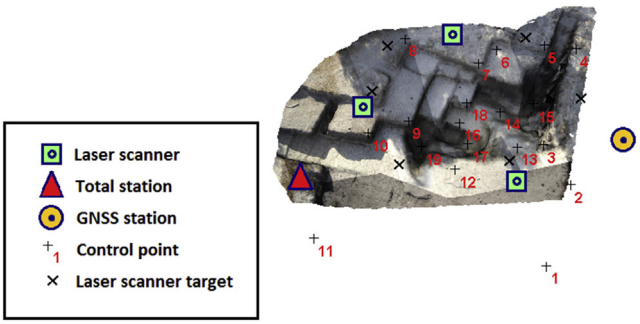

Fig. 7. Sketch showing the positions of sensor stations and control points.

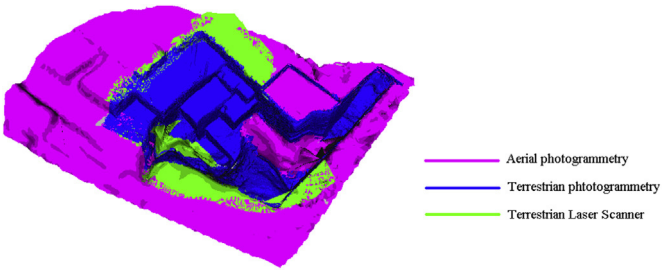

Fig. 8. The hybrid DTM corresponding to the second excavation campaign.

different characteristics. More specifically, for the creation of the first DTM, aerial photogrammetry and laser scanning were used, obtaining a DTM with 520,705 points and 24 breaklines, of which 206,116 points correspond to TLS, whereas the rest were found from the UAV photogrammetry by using automatic image matching. A similar DTM was generated for the second excavation campaign, with the exception of the addition of terrestrial photogrammetry (Fig. 8). In this case there were 30 breaklines and 889,450 points, of which 138,047 points were obtained by TLS and 751,403 points by automatic matching using aerial and terrestrial photographs.

Due to the fact that hybrid and integral DTM are available for the whole archaeological settlement of both excavation campaigns, another hybrid product can be created, the true orthophoto. The images taken by the UAV are used to generate both orthophotos, and since both were taken during a low-altitude flight, it is possible to generate a high-resolution orthophoto with a GSD of 2 cm (Fig. 9). The output size was 1020 × 1560 pixels and the GeoTIFF format was chosen in order to preserve the geo-referencing, enabling its geographical information system (GIS) integration.

4.3. Monitoring: dimensional analysis

During the excavation work in an archaeological site, there are amounts of dug material that would be interesting to analyse dimensionally, sometimes to consider and study associated expenses, to foresee future excavation ratios or for other reasons.

Throughout, between the two existing volumes subtracted from the corresponding DTMs obtained at different stages of the excavation, a variation of 11.5 m^3 was observed. This was to be expected considering that only extraction works were carried out and there was no ground-fill involved. In Table 3, the excavation depth values can be observed.

Fig. 9. The true-orthophoto for the second excavation campaign: GSD 2 cm.

Table 2
Qualitative summary comparison for the three proposed geo-technologies.

		Laser scanning	UAV photogrammetry	Terrestrial photogrammetry
Cost	Data acquisition	8–16 h/man Two person working simultaneously	1–2 h/man Two person working simultaneously	0–1 h/man
	Point cloud	Nothing	Average (min-h), depend on the number of photos and CPU processor used.	Average (min-h), depend on the number of photos and CPU processor used
	Technology	(10,000–130,000 Euros)	(3000–30,000 Euros)	(100–500 Euros)
Automation level		Manual intervention in the filtering and cleaning process.	Manual intervention in the definition of control points.	Manual intervention in the definition of control points.
Space requirement		1–2 Gb point cloud per campaign	1–100 Mb point cloud per campaign. Images of 0.1–1 Gb per campaign	1–100 Mb point cloud per campaign. Images of 0.1–1 Gb per campaign
Accuracy/Resolution		Very high/5 mm	High/5 cm	High/2 cm
Photo alignment with the point cloud model		Manual	Automatic	Automatic
Need for training to operate		Yes	No	No

Table 3
Monitoring: dimensional analysis resulting from both campaigns (in metres).

Monitoring	Minimum depth	Maximum depth	Average depth
Fist excavation campaign	0.000	5.121	0.733
Second excavation campaign	0.000	6.325	1.864
Difference	0.000	−1.204	−1.131

5. Conclusions and future work

The integrated geo-technologies proposed in this paper offer an accurate and rapid assessment of the as-built status of an archaeological site, providing the opportunity to easily and quickly understand, analyse and identify discrepancies in the current state of the settlement. Considering the current status of the various geo-technologies, it is clear that no single geo-technology solves all the needs of archaeological surveying such as reconstructing as-built models and monitoring the advance of a settlement. In this sense, photogrammetric and laser scanning technologies are complementary when used in combination, providing added value through hybrid products: MDT and true orthophotos. Last but not least, the generation of hybrid products requires correct and rigorous geo-referencing, and thus the geo-referencing method proposed in this paper contributes to this aim. The accuracy attained by this method proves to be of paramount value to the employment of this kind of model for the study and measurement of excavation sites. In this case, differences of mere centimetres have been found; this is only possible thanks to the precise methods of geo-referencing.

With regard to future perspectives some avenues to future work remain open, for instance the automatic incorporation of breaklines into DTMs based on vectorization processes and the automatic registration of sensors based on the proposed geo-referencing method.

Acknowledgements

This work is financed by the Spanish Government (2008–2011 National Research Plan) and the European Union (FEDER Funds) by means of the grants ref. BIA2010-15145 and INNPACTO IPT-120000-2010-039.

References

Bernabeu Aubán, J., Orozco Köhler, T., Díez Castillo, A., Gómez Puche, M.Y., Molina Hernández, F.J., 2003. Mas d'Is (Penàguila, Alicante): aldeas y recintos monumentales del Neolítico inicial en el valle del Serpis. Trab. Prehist. 60 (2), 39–59. CSIC.

Bourke, P., 1989. An algorithm for interpolating irregularly-spaced data with applications in terrain modelling. In: Pan Pacific Computer Conference, Beijing, China, 6 pages.

Brown, D.C., 1971. Close range camera calibration. Photogramm. Eng. 37 (8), 855–866.

Eisenbeiss, H., Lambers, K., Sauerbier, M., 2007. Photogrammetric recording of the archaeological site of Pinchango Alto (Peru) using a mini helicopter. In: Figueiredo, A., Velho, G.L. (Eds.), The World is in Your Eyes – Proceedings of the 33rd CAA Conference, Tomar, Portugal, Trabalhos de Arqueologia. Instituto Português de Arqueologia, Lisbon.

Gomez-Lahoz, J., Gonzalez-Aguilera, D., 2009. Recovering traditions in the digital era: the use of blimps for modelling the archaeological cultural heritage. J. Archaeol. Sci. 36 (1), 100–109.

González-Aguilera, D., Muñoz-Nieto, A., Rodriguez-Gonzalvez, P., Menéndez, M., 2011a. New tools for rock art modelling: automated sensor integration in Pindal Cave. J. Archaeol. Sci. 38 (1), 120–128.

González-Aguilera, D., Rodríguez-Gonzálvez, P., Armesto, J., Arias, P., 2011b. Trimble GX200 and Riegl LMS-Z390i sensor self-calibration. Opt. Express 19 (3), 2676–2693.

Hanke, K., Grussenmeyer, P., 2002. Architectural Photogrammetry: Basic Theory, Procedures, Tools. ISPRS Commission, Corfu, 5 tutorial.

Hernandez-Lopez, D., Felipe-Garcia, B., Gonzales-Aguilera, D., Arias-Perez, B., 2013. An automatic approach to UAV flight planning and control for photogrammetric applications: a test case in the Asturias Region (Spain). Photogramm. Eng. Remote Sens. 79 (1), 87–98.

Hunt, E.R., Cavigelli, M., Daughtry, C.S.T., McMurtrey, J.E., Walthall, C.L., 2005. Evaluation of digital photography from model aircraft for remote sensing of crop biomass and nitrogen status. Precis. Agric. 6, 359–378.

Kraus, K., 1993. Photogrammetry Fundamentals and Standard Processes, vol. I. Dummlers Verlag, Bonn, Germany, ISBN 3-427-78684-6.

Lambers, K., Eisenbeiss, H., Sauerbier, M., Kupferschmidt, D., Gaisecker, T., Sotoodeh, S., Hanusch, T., 2007. Combining photogrammetry and laser scanning for the recording and modelling of the late intermediate period site of Pinchango Alto, Palpa, Peru. J. Archaeol. Sci. 34 (10), 1702–1710.

Morel, J.M., Yu, G., 2009. ASIFT: a new framework for fully affine invariant image comparison. SIAM J. Imaging Sci. 2 (2), 438–469.

Patias, P., Olga, G., Charalampos, G., Anastasios, G., Tassopoulou, M., 2009. Photogrammetric documentation and digital representation of excavations at Keros island in the Cyclades. In: ISPRS Archives Vol. XXXVIII-3/W8, XXII CIPA Symposium, Kyoto, Japan.

Remondino, F., Gruen, A., von Schwerin, J., Eisenbeiss, H., Rizzi, A., Sauerbier, M., Richards-Rissetto, H., 2009. Multi-sensors 3D documentation of the Maya site of Copan. In: Proceedings of 22nd CIPA Symposium, Kyoto, Japan.

Tokmakidis, K., Skarlatos, D., 2002. Mapping excavations and archaeological sites using close range photos. In: Proceedings of the ISPRS Commission V Symposium, WG V/4, Corfu, September, Greece.

3.2 Un acercamiento multi-sensor y multi-fuente de datos para la reconstrucción 3D y visualización Web de un yacimiento arqueológico complejo: El caso de estudio de "El Tolmo de Minateda".

En este artículo se continúa con la investigación en el acercamiento híbrido para la modelización tridimensional de yacimientos arqueológicos. Para la captura de las imágenes aéreas empleadas en el proceso fotogramétrico se emplean dos plataformas diferentes: UAV y paramotor. Para el segundo caso, se ha construido una plataforma giroestabilizadora que permite obtener imágenes de calidad y permitir la captura nadiral de las tomas fotográficas. Se ha demostrado la idoneidad del empleo de ambas aeronaves, al permitir ajustar la toma de datos al área de trabajo, de modo que las grandes extensiones son recopiladas de manera más rápida y ágil con el empleo del paramotor, y las zonas de mayor detalle y más difícil acceso son documentadas mediante UAV. Por su parte, los detalles arquitectónicos que componen las murallas del yacimiento han requerido de un levantamiento de mayor resolución empleando para ello el láser escáner terrestre. Adicionalmente, se han empleado técnicas de fotogrametría terrestre con la finalidad de obtener texturizados de calidad que complementen la información geométrica obtenida de la nube de puntos láser.

Con este acercamiento multi-sensor y multi-dato se ha demostrado la eficacia de la metodología propuesta en la documentación de yacimientos arqueológicos complejos y, frente al elevado coste computacional que requieren las técnicas de reconstrucción fotogramétricas, se ha mostrado que

mediante el empleo de algoritmos robustos y eficientes es posible obtener de forma rápida productos geomáticos de alta calidad (e.g. modelo 3D y ortofotografía verdadera).

Además, se ha evaluado el valor añadido que presenta el análisis tridimensional de yacimientos arqueológicos en conjunción con otras fuentes de información como croquis realizados a mano alzada por arqueólogos expertos, realizando la integración de toda la información en un GIS3D.

Finalmente, se han aplicado y evaluado técnicas de simplificación y optimización de los modelos 3D que permiten la divulgación de los productos geomáticos mediante visores Web accesibles incluso desde plataformas móviles como smartphones, acercando de esta forma al usuario la realidad del yacimiento arqueológico de un modo interactivo.

De las investigaciones llevadas a cabo en este artículo se ha concluido que la metodología empleada puede resultar de gran interés a:

- ✓ Investigadores: Para la interpretación, análisis temporal y espacial del yacimiento, gracias a la capacidad de integración y portabilidad del sistema.
- ✓ Gestores: Para la monitorización de las variaciones del yacimiento, divulgación de información, videos, etc.
- ✓ Estudiantes: Pudiendo explotar las posibilidades didácticas de la inspección de modelos 3D, así como la posibilidad de interactuar y de superponer de información.

- ✓ Público en general: Permitiendo un acceso más fácil y cómodo al yacimiento arqueológico que complementa y añade valor a la visita al propio yacimiento.

remote sensing

MDPI

Technical Note

A Multi-Data Source and Multi-Sensor Approach for the 3D Reconstruction and Web Visualization of a Complex Archaelogical Site: The Case Study of "Tolmo De Minateda"

Jose Alberto Torres-Martínez [1,*], Marcello Seddaiu [2], Pablo Rodríguez-Gonzálvez [1], David Hernández-López [3] and Diego González-Aguilera [1]

1 Department of Cartographic and Land Engineering, High School of Ávila, University of Salamanca, 37008 Salamanca, Spain; pablorgsf@usal.es (P.R.-G.); daguilera@usal.es (D.G.-A.)
2 Dipartimento di Storia, Scienze dell' Uomo e della Formazione, Università degli Studi di Sassari, 07100 Sassari, Italy; marcelloseddaiu@gmail.com
3 Regional Development Institute-IDR, University of Castilla-La Mancha, Albacete 02071, Spain; david.hernandez@uclm.es
* Correspondence: josealberto@usal.es; Tel.: +34-61-060-5608

Academic Editors: Fabio Remondino, Soe Myint and Prasad S. Thenkabail
Received: 9 May 2016; Accepted: 24 June 2016; Published: 29 June 2016

Abstract: The complexity of archaeological sites hinders creation of an integral model using the current Geomatic techniques (i.e., aerial, close-range photogrammetry and terrestrial laser scanner) individually. A multi-sensor approach is therefore proposed as the optimal solution to provide a 3D reconstruction and visualization of these complex sites. Sensor registration represents a riveting milestone when automation is required and when aerial and terrestrial datasets must be integrated. To this end, several problems must be solved: coordinate system definition, geo-referencing, co-registration of point clouds, geometric and radiometric homogeneity, etc. The proposed multi-data source and multi-sensor approach is applied to the study case of the "Tolmo de Minateda" archaeological site. A total extension of 9 ha is reconstructed, with an adapted level of detail, by an ultralight aerial platform (paratrike), an unmanned aerial vehicle, a terrestrial laser scanner and terrestrial photogrammetry. Finally, a mobile device (e.g., tablet or smartphone) has been used to integrate, optimize and visualize all this information, providing added value to archaeologists and heritage managers who want to use an efficient tool for their works at the site, and even for non-expert users who just want to know more about the archaeological settlement.

Keywords: 3D reconstruction; web visualization; multi-sensor; multi-data; aerial photogrammetry; laser scanning; computer vision; archaeology

1. Introduction

Several techniques have been applied thus far for the 3D reconstruction and visualization of archaeological settlements based on the use of close-range photogrammetry [1,2], terrestrial laser scanner (TLS) [3,4] or unmanned aerial vehicles (UAV) [5]. However, due to the inherent complexity of these sites, several problems arise when 3D reconstruction of these sites is mandatory and just one type of geotechnology is applied. For instance, aerial photogrammetry exhibits problems reconstructing vertical planes, common in archaeological sites, whereas terrestrial laser scanners or terrestrial photogrammetry could provide good results. However, these terrestrial techniques are subject to problems with horizontal surfaces or elevated areas. Other authors have explored multi-data and multi-sensor approaches to record and reconstruct complex archaeological sites. Recently in [6], the

potential of this type of hybrid approach is shown for the analysis and interpretation of 3D/4D information applied to archaeological settlements. In order to guarantee geometric and radiometric quality, a combination of TLS and terrestrial photogrammetry is used and applied, enabling the monitoring of the settlement based on a volume analysis. However, this approach has problems related to the recording of more elevated areas. In order to solve this limitation, in [7], the authors use an aerial multi-sensor approach for the 3D reconstruction and visualization of archaeological settlements which provides a very good coverage of those elevated areas. The quality and precision of the TLS and UAV registration has been outlined in [8] where authors reconstruct the interior and exterior of the Church of Santa Barbara (Italy) after the earthquake it suffered in 2012. Trying to overcome the main UAV limitations, payload and autonomy, other authors have proved that low-cost manned platforms such as the paratrike can be an efficient solution for the recording of large sites [9], including archaeological sites [10], and allowing to put on board multiple sensors such as thermographic or multispectral cameras [11]. In those cases where the archeological site is complex and subterranean, other hybrid, dynamic and terrestrial approaches could be interesting. Unfortunately, there are not many mobile laser scanners, photogrammetric or hybrid systems for subterranean sites available in the market [12,13], even less specific for the field of archaeological recording. Some authors such as Canter et al. [14] have developed indoor mapping systems for the generation of indoor cartography from accurate geospatial information. The main advantage of these systems is that they integrate high-precision GNSS with advanced inertial technology (accelerometers and gyroscopes) for the geo-referencing of the site using measures from its exterior, apart from an Applanix POS system for positioning and orientation that provides uninterrupted measurements of the true position, roll, pitch and yaw of the vehicle moving indoors. Other authors have advanced more sophisticated systems based on a wheeled mobile robot and a multi-sensor global registration approach [15]. In particular, a geometric model to derive depth information is proposed based on a registration of heterogeneous 3D data arising from eight ultrasonic sonars, one TLS and three visual sensors.

It thus becomes clear that with the advances in multi-sensor and multi-data from different sources, data integration has become as a valuable tool in archaeological applications. The main objective of multi-sensor data integration is to register sensor data from different sources—with different characteristics, resolution, and quality in order to provide more reliable, accurate, and useful information required for diverse archaeological applications. In addition, this multi-data and multi-sensor integration can be improved through 3D geographical information systems (3DGIS) together with the final presentation of the products based on 3D Web.

The goal of this study is to propose a multi-data source and multi-sensor workflow in order to obtain high quality archaeological products, contributing to the robust interpretation of the observed objects/scenes and providing the basis of effective planning and decision making, essential in archaeology. To this end, terrestrial scans and images will be registered with aerial images acquired from a paratrike and an unmanned aerial vehicle (UAV). The methodology employed for data processing has been extensively tested by several authors. In [16], the authors employed computer vision algorithms for image-based modelling from aerial imagery and point cloud generation in urban environments, which are similar to those used in this work.

To carry out studies of characterization, measurement and analysis of the surface and the elements presented in the site, the geometrical information (acquired with geomatic sensors) is combined with other available thematic data such as photographs, sketches, restoration reports, schedules, etc. in a 3DGIS, Geoweb3D® [17]. In this way, a description of the site through time is possible. Also, the availability of the three-dimensional information of the settlement through the Web using mobile devices provides added value for archaeologists and heritage managers, simplifying the data acquisition, as well as its analysis in the field. Moreover, the centralization of the information and its external storage means it becomes available to different experts and organizations. Last but not least, the knowledge of the settlement is open to the general public based on an easy-to-use interface which integrates different 2D and 3D resources.

In this study, a specific simplification and optimization procedure was implemented to visualize the different 3D products through the Web using mobile devices and the Open Source library Cesium [18], developed by the company Analytical Graphics, Inc. (AGI, Greenbelt, MD, USA) [19]. Other authors [20] have developed similar works using their own system, *SGIS3D*, which uses VRML (Virtual Reality Modeling Language) format. However, one of the main limitations of this language is the mandatory use of plugins, as well as its lack of optimization through the graphical processing unit (GPU), crucial in those steps related to texture mapping. Another similar approach in the archaeological field is developed by [21], who implements a spatial data infrastructure known as *QuaeryArch3D* and applied it to the archaeological settlement of "Maya de Copan" in Honduras, a UNESCO World Heritage Site. In this case, they use the Open Source PostgreSQL and PostGIS for the integration and management of information in the database, whereas the 3D visualization is performed with Unity. However, one of the main limitations of Unity is dealing with huge 3D models coming from the point clouds. To overcome this problem, WebGL seems to provide an appropriate solution using similar developments to those presented in [22] or developing a new approach as the one presented in this paper. Furthermore, advancing a 3DGIS Web solution requires using different simplification and optimization processes, as well as different hierarchical (i.e., pyramidal) strategies for visualization which are not compatible with the Unity engine.

This paper is organized as follows: after this introduction, in Section 2, the different sensors employed and their characteristics are detailed. In Section 3, the proposed multi-data source and multi-sensor approach is described, as well as the simplification and optimization process. Experimental results are shown and discussed in Section 4. Conclusions and future directions are given in Section 5. Finally, two appendices are included; the first corresponding to the abbreviations used in the paper, whereas the second encompasses the explanation of the methodology employed for 3D Web visualization.

2. Materials

2.1. Paratrike

The main aerial platform employed to the documentation of the archaeological site was a paratrike (Figure 1a). It is a low-cost aircraft with more flexibility than conventional aircrafts, and more autonomy and payload capacity than the UAVs. This last characteristic allows the possibility of boarding better sensors than the UAVs, or even multiple sensors in a stabilized gimbal (MUSAS-MUltiSpectral Airborne Sensors). In particular, a tandem trike AIRGES (Table 1) was used to map the whole archaeological site following a vertical flight and using a full-frame reflex camera.

Table 1. Technical specifications of the paratrike.

Motor	**Rotax 503 Two-Stroke Motor**
Trike	Tandem Trike AIRGES
Tandem paraglide	MAC PARA Pasha 4 Trike 39 ó 42
Emergency system	Ballistic parachutes GRS 350
Weight	110 kg
Weight capability	165–250 Kg
Air velocity range	30–60 km/h

The use of the gyro-stabilized camera platform, MUSAS (Figure 1b), guarantees the accurate orientation of the camera according to the flight planning by two servomotors arranged on the x and y axes, controlled by an Arduino board, which incorporates an IMU with 6 degrees of freedom: three accelerometers, a double-shaft gyroscope (for pitch and roll) and an additional gyroscope for yaw.

For the paratrike, a full-frame reflex camera, Canon 5D MkII, with a fixed focal length to achieve a GSD of 3 cm, was used. This camera was also used for the terrestrial photogrammetry and photorealistic texture mapping due to its better image quality.

In contrast to the UAV platform which encloses an integrated navigation system (GPS, IMU and barometric altimeter), the paratrike requires an external set of sensors in order to provide navigation capabilities and thus fulfill photogrammetric constraints for data acquisition. In particular, the planimetric position is provided by a GPS antenna (Trimble Bullet III), installed in the camera platform close to the optical centre of the camera, connected to a mono-frequency receiver Ublox EVK-6T-0. This system yields an absolute precision of ± 9 m on the horizontal axis for 95% of the time [23]. During data acquisition the pilot follows the planned photogrammetric mission in a rugged table connected to the GPS system, where the real-time track is contrasted with the planned flight. The final component in the navigation system, the altimetry, which affects the GSD, is controlled by an altimetric barometer (DigiFly VL100) with an absolute precision of ± 8 m. This solution is chosen instead of GPS receiver, since the absolute altimetric GPS precision is just ± 15 m.

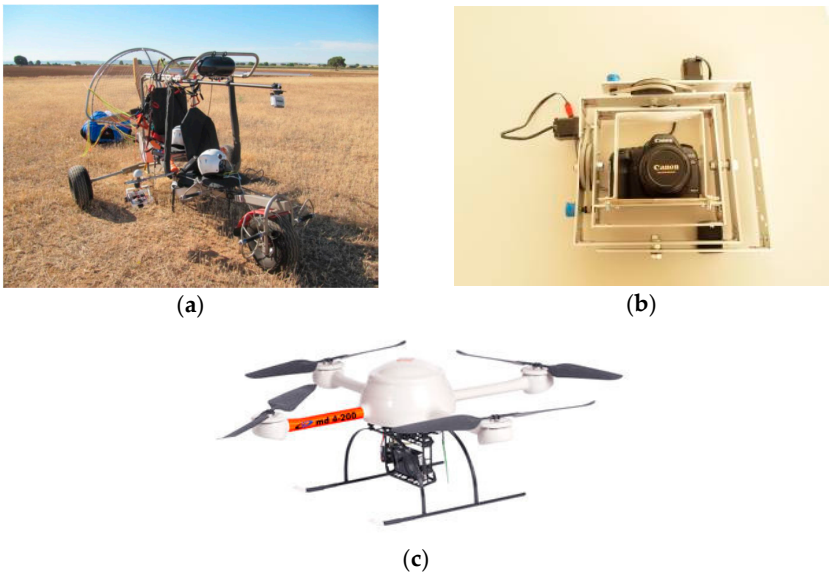

(**a**) (**b**) (**c**)

Figure 1. Paratrike employed (**a**); detail of the stabilization platform "MUSAS" (**b**) and UAV used in complex areas (**c**).

2.2. Unmanned Aerial Vehicle

For the aerial photogrammetric acquisition in the "El Reguerón" site, the paratrike platform was rejected due to the morphological characteristics of the terrain and the height of flight required to reach the high spatial resolution (GSD of 1 cm). The main drawback was the need to vary the flying height to keep the same scale, due to the presence of high reliefs along the strips. As an additional disadvantage, the walled constructions were occluded between walls of natural rock. Therefore, in order to complete the archaeological site documentation, a UAV was employed. Specifically, a Microdrone md4-200 (Table 2) was used (Figure 1c) to map the most challenging area following vertical and oblique flights through use of a compact camera.

In spite of the manoeuvrability provided by this UAV, it has a limited payload required to employ a compact camera for the photogrammetric flight.

For the UAV, an ultra-compact camera, Canon IXUS 115 HS, was chosen allowing a GSD of 1 cm.

Basically, the multi-data obtained by UAV and paratrike is geometrical, i.e., two point clouds with metric properties and texture information (RGB) which are homogenized under a common reference system based on a network of control and check points.

Table 2. Technical specifications of the Microdrone md4-200 platform.

UAV Weight	900 g
Payload	up to 200 g
Size	54 cm between rotors
Flight time	10 to 20 min
Operating temperature	−10 to 50 °C
Max. height flight	500 m
Max. wind	5 m/s

2.3. Terrestrial Laser Scanner

In those complex zones, a phase shift terrestrial laser scanner, Faro Focus 3D, was employed (Table 3).

Table 3. Technical specifications of the terrestrial laser scanner (TLS), Faro Focus 3D.

Model	Faro Focus 3D
Principle	Phase Shift
Wavelength	905 nm (Near infrared)
Field of view	360° H × 320° V
Range std. deviation	2 mm at 25 m
Measurement range	0.19 mrad
Beam divergence	8 mm at 50 m
Scanning speed	976,000 points/s

According to the archaeological settlement characteristics and the TLS technical specifications, laser stations were established in a network that guaranteed an average spatial resolution of 5 mm for the whole scenario. The mean distance acquisition was 15 m.

2.4. Geo-Referencing System

The establishment of the mapping frame in the study area is performed with two GNSS bi-frequency (L1, L2) receivers, Topcon manufacturer. The GNSS observation method was real-time kinematic (RTK) getting a relative and absolute precision of 1 cm and 3 cm, respectively.

The coordinate reference system was comprised of the official coordinate system established by Spanish law, a Compound Coordinate Reference System (CCRS) integrated by horizontal CRS referred to ETRS89 geodetic reference system and UTM Zone 30 mapping projection (EPSG: 25830), and vertical CRS with geoid´s origin defined in Alicante (Spain) (EPSG: 5782). This mapping frame was materialized by a GNSS surveyal using natural features for "El Reguerón" area, which could be clearly identified on aerial images (e.g., corners of well-defined objects, small features with excellent contrast, etc.). In this way, we avoid artificial targets appearing in those more emblematic parts of the archaeological settlement. On the contrary and due to the large extension area, artificial targets were used for the full recording of the archaeological settlement (with the paratrike) in order to establish a network of control and checkpoints.

3. Methodology

Given the complexity of the archaeological site and the archaeological documentation requirements, the aerial and terrestrial data acquisition was planned in order to provide an integral and integrated recording of the site.

All the data from the different sensors and plataforms were processed according to the workflow outlined in Figure 2 and explained in the following subsections.

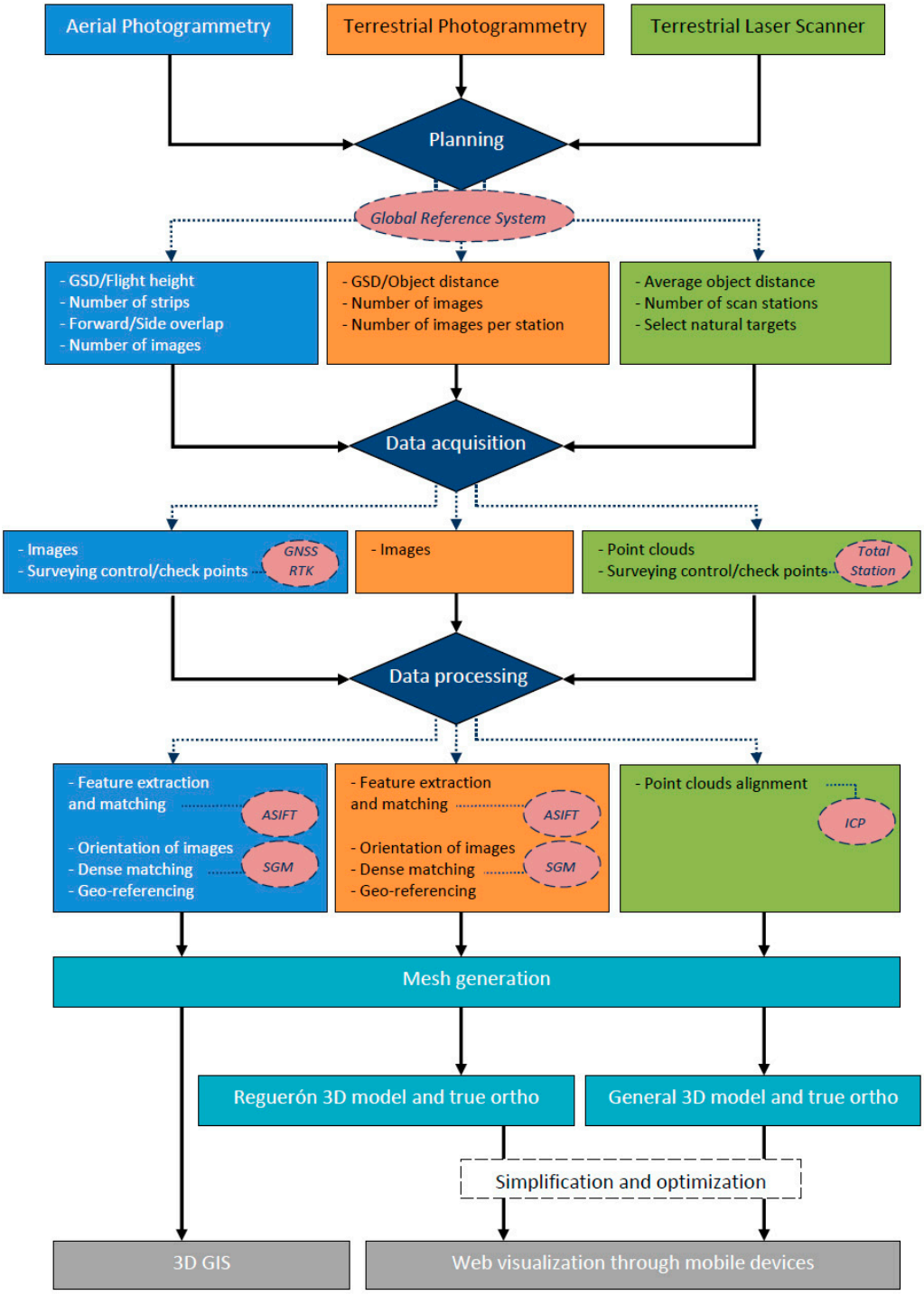

Figure 2. Multi-sensor and multi-data source workflow for the 3D reconstruction of complex archaeological sites.

3.1. Data Acquisition

Each technique (i.e., photogrammetry, laser scanning) requires different procedures and protocols for data acquisition.

In the case of aerial data acquisition, image projection centers and camera attitude must be previously defined according to the classical photogrammetric parameters. The flight planning was done using the in-house software, MFlip and PFlip, for the UAV and paratrike flights, respectively [24].

The main difference between both flights was the type of flight planning: for the paratrike, a standard stereoscopic photogrammetric flight was undertaken (Figure 3a), whereas for the case of UAV, oblique and vertical images were also considered. Therefore, data acquisition was completely planned in order to get better results. In particular, for the UAV, a script was prepared for an automatic photogrammetric flight; whereas for the paratrike, the flight axis and flight height were planned and followed by the pilot. Both flights were planned with higher overlaps in order to get better results in the dense matching process and both flights were planned considering the relief variation using a public digital terrain model (DTM) [24].

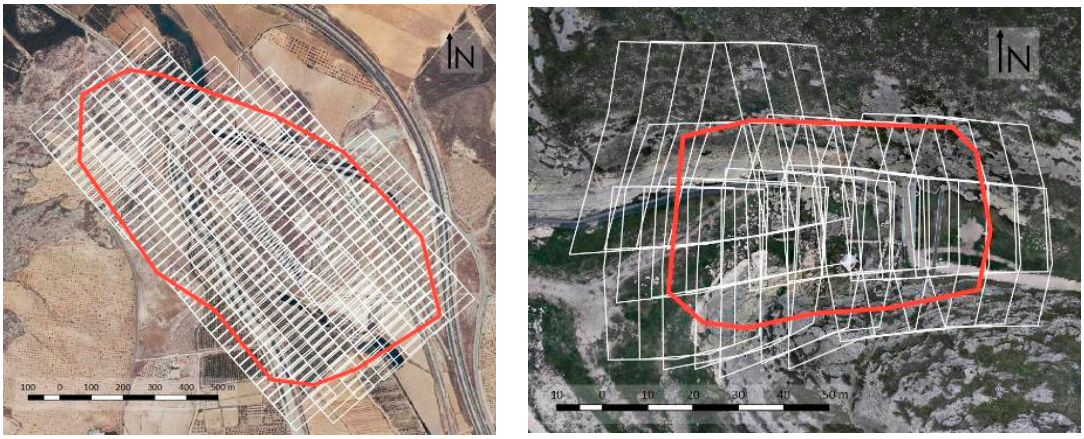

(**a**) (**b**)

Figure 3. Example of image footprints projected over terrain (**white** line) and the different workspaces (**red** line). (**a**) Paratrike flight planned over the whole area and (**b**) UAV flight planned over "El Reguerón" area.

The result shown in Figure 3b corresponds to the UAV flight planning, which was complemented with oblique aerial images acquired manually. As can be seen through the image footprints, the relief effects make it difficult to maintain a constant GSD, so the data acquisition is complemented with terrestrial images. For its part, the paratrike was used for the whole recording of the settlement due to the autonomy and sensors limitations of the UAV.

For the "El Reguerón" area a more detailed flight with the UAV was designed using the ultra-compact camera.

An important issue for the aerial data acquisition was the image sharpness, which affects the final photogrammetric reconstruction. This issue is affected by the camera parameters (i.e., aperture, shutter time and sensibility), the platform performance (i.e., flight speed and efficiency of the stabilized gimbal to absorb the paratrike vibrations) and the scenario illumination conditions. The flight was executed on a cloudy day to avoid shadows being projected, and the camera sensibility and shutter time were set up for these conditions. The aperture and the focal length were fixed constant to avoid variations in the internal camera parameters.

As commented previously, the high vertical reliefs of the site and the level of detail required in some areas (e.g., those constructive elements that integrate the defensive system of the entrance, details of the walls, etc.) entailed that aerial images were not suitable; terrestrial images were thus acquired with the full-frame reflex camera. In addition, terrestrial laser scans were used in those complex areas where photogrammetry could entail problems requiring a lot of images to enclose the whole geometry or due to the presence of textureless objects or materials. A network of 13 TLS stations (Figure 4) was designed for an average distance of 15 m with an average spatial resolution of 5 mm.

From Figure 4, it can be observed that two laser scanning campaigns were planned for two different areas. The first campaign (orange colour) was designed for recording the existing

constructions using six stations. The second campaign (blue colour) was designed for recording the walls of "El Reguerón" and the adjacent environment using seven stations.

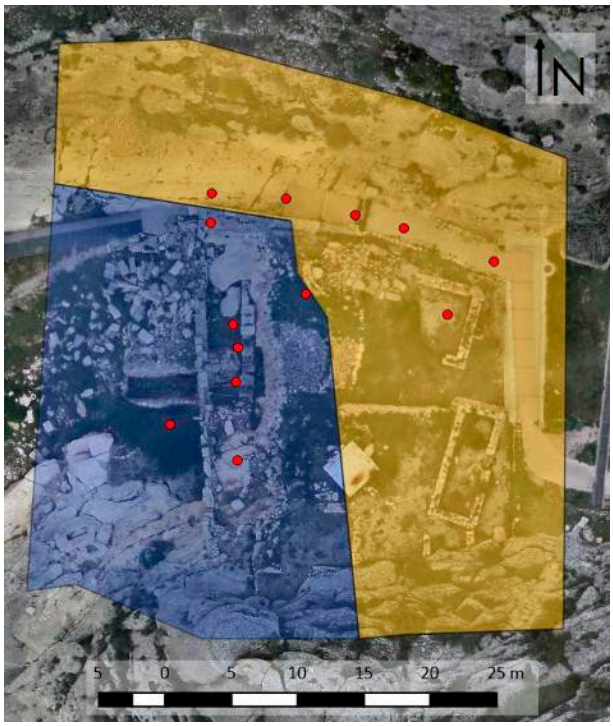

Figure 4. TLS stations distribution (**red** circles), including the area surveyed with TLS during the different campaigns performed (first campaign in **orange** colour and second campaign in **blue** colour).

3.2. Data Processing

Handling multiple sensors requires multi-data processing approaches that take the point cloud as the basic unit. However, since all data must be integrated to generate a single model, it is necessary to homogenize the information, establishing filtering, simplification and optimization algorithms. Thus, the result obtained by each method is the corresponding point cloud that will be registered, triangulated and textured for generating a single 3D model with metric and radiometric capabilities.

3.2.1. TLS Filtering and Alignment

Data acquired with TLS were processed with commercial software FARO SCENE 5.4 [25]. The raw TLS scans were filtered removing noise and undesired information which could affect the alignment process. Automatic filtering has been applied in those more conflictive areas. Firstly, each scan was filtered according to a distance threshold (20 m) in order to remove distant points. Afterwards, two specific filters (intense-based filter and outlier filter) were applied. The former applies a reflectance threshold to remove those points with the lowest intensity, whereas the latter analyses the point and its environment (3×3) using distances. For instance, if there is a distance variation of 1 cm between the point and its neighbourhood for more than the 50% of the neighbourhood, the point will be removed. These thresholds should be tested adaptively by the user depending on the type and geometry of the area. Finally, the more delicate areas (i.e., walls or vegetation) have been filtered manually. For instance, vegetation between the blocks of the wall was identified and removed manually.

Since artificial targets were not used, scan alignment was done by a solid rigid transformation of an iterative closest point (ICP) technique [26]. This iterative process was applied in pairwise stations, so the final a priori error was computed on the basis of the number of stations and the technical

specifications of the TLS (Table 4) reaching 1.3 cm for the assumption of two consecutive overlapping point clouds. The reference system of the aligned TLS point cloud is defined through a local Cartesian system corresponding to the first scan station with coordinates (300,000, 4,000,000, 1000).

Table 4. Simplification and optimization results for "El Reguerón" area.

	Simplified	**Simplified and Optimized**
Number of points	11,267,122	2,816,853
Number of triangles	22,532,754	5,635,313
Spatial resolution * (Min, Avg, Max)	(60.5, 64.3, 69.1) mm	(69.2, 81.1, 98.9) mm

* Confidence Interval = 1σ.

3.2.2. Photogrammetric Processing

The generation of the dense point cloud, from both aerial and terrestrial images, was automatized through the Photogrammetry Workbench (PW) in-house software [27], following a three step workflow: 1. Image registration; 2. Camera orientation and 3. Dense matching.

The aerial images, coming from the paratrike and UAV, were processed to generate a hybrid model, with a total of 293 images and two different cameras. The dataset was checked to assure the sharpness of the images, which could be decreased by the motion blur.

1. The feature extraction has been carried out by the ASIFT (Affine Scale-Invariant Feature Transform) algorithm [28]. As its most remarkable improvement, ASIFT includes the consideration of two additional parameters that control the presence of images with different scales and rotations. In this manner, the ASIFT algorithm can cope with images displaying a high scale and rotation difference, common in oblique images. The result is an invariant algorithm that considers the scale, rotation, and movement between images. The main contribution in the adaptation of the ASIFT algorithm is its integration with robust strategies that allow us to avoid erroneous correspondences. These strategies are the Euclidean distance [29] and the Moisan-Stival ORSA (Optimized Random Sampling Algorithm) [30]. This algorithm is a variant of Random Sample Consensus (RANSAC) [31] with an adaptive criterion to filter erroneous correspondences by the employment of the epipolar geometry constraints. Once the feature points have been extracted and described, the final matching points are assessed based on their spatial distribution on the CCD. An asymmetric distribution (radial and angular) of matching points regarding the principal point will affect the correct determination of internal camera parameters and also the image orientation. Therefore, if the matching points do not cover an area more than two-thirds of the CCD format, the user will be alerted in order to modify the detector (ASIFT) and descriptor (SIFT) parameters. Through this quality control we try to minimize problems associated with the weakness and common deficiencies in the photogrammetric network geometry of both aerial flights (UAV and paratrike).

This result provides the next expression:

$$\mathbf{A}_F = \begin{bmatrix} a & b \\ c & d \end{bmatrix} = H_\lambda R_1(\kappa) T_1 R_2(\varpi) = \lambda \begin{bmatrix} \cos\kappa & -\sin\kappa \\ \sin\kappa & \cos\kappa \end{bmatrix} \cdot \begin{bmatrix} t & 0 \\ 0 & 1 \end{bmatrix} \cdot \begin{bmatrix} \cos\varpi & -\sin\varpi \\ \sin\varpi & \cos\varpi \end{bmatrix} \quad (1)$$

where $\mathbf{A_F}$ is the affinity transformation that contains scale, λ, rotation, κ, around the optical axis (swing) and the perspective parameters that correspond to the inclination of the camera optical axis, φ (tilt) or the vertical angle between optical axis and the normal to the image plane; and ϖ (axis), the horizontal angle between the optical axis and the fixed vertical plan.

In order to accelerate the process, the overlapped aerial images were identified by their approximate camera orientations provided by the navigation system. In the case of terrestrial images,

an all-to-all comparison was applied. This sub-step is a time-consuming process which increases exponentially with the number of images [32].

2. The multi-image protocol acquisition will require robust orientation procedures. For this purpose, a combination between computer vision and photogrammetric strategies was used. This combination is fed by the resulting keypoints extracted previously. In a first step, an approximation of the external orientation of the cameras was calculated following a fundamental matrix approach [33]. Later, these spatial (*X,Y,Z*) and angular (*ω-omega, φ-phi, and χ-kappa*) positions are refined by a bundle adjustment complemented with the collinearity condition [34]. In this field, several open source tools have been developed such as Bundler [35] and Apero [36]. For the present case study, both were combined and integrated. In particular, a specific converter has been developed for reading Bundler orientation files (*.out) and computing the three rotation angles and three translation coordinates of the camera in Apero. In addition, a coordinate system transformation has been implemented for passing from the Bundler to the Apero coordinate system. It is remarkable that at the same time, thanks to the reliability of the photogrammetric procedures used, it is possible to integrate as unknowns several internal camera parameters (focal length, principal point, and radial distortions). This possibility allows the use of non-calibrated cameras and guarantees acceptable results. For the present case study, a self-calibration strategy supported by a basic calibration model which encloses five internal parameters (focal length, principal point, and two radial distortion parameters) was used [37,38]. In order to provide metric capabilities to the model, manual identification of ground control points (GCPs) in the images were accomplished. Including these as an input in the bundle adjustment, the model is oriented according to the global coordinate system.

$$\begin{aligned}(x - x_0) + \Delta x &= -f\frac{r_{11}(X-S_X)+r_{21}(Y-S_Y)+r_{31}(Z-S_Z)}{r_{13}(X-S_X)+r_{23}(Y-S_Y)+r_{33}(Z-S_Z)}\\ (y - y_0) + \Delta y &= -f\frac{r_{12}(X-S_X)+r_{22}(Y-S_Y)+r_{32}(Z-S_Z)}{r_{13}(X-S_X)+r_{23}(Y-S_Y)+r_{33}(Z-S_Z)}\end{aligned} \quad (2)$$

where x and y are the known image coordinates, X_i, Y_i and Z_i are the corresponding known GCPs, r_{ij} are the unknown 3 × 3 rotation matrix elements, S_X, S_Y and S_Z represent the unknown camera position, f is the principal distance, x_0 and y_0 are the principal point coordinates and Δx and Δy are the lens distortion parameters. These internal camera parameters may be known or unknown by the user and thus are introduced as equations or unknowns (self-calibration), respectively.

3. One of the greatest breakthroughs in recent photogrammetry has been exploiting, from a geometric point of view, the image spatial resolution (size in pixels). This has made it possible to obtain a 3D object point of each of the image pixels. Different strategies have emerged in recent years, such as the Semi-Global Matching (SGM) approach [39] that allows the 3D reconstruction of the scene, in which an object point corresponds with a pixel in the image. These strategies, fed by the external and internal orientations and complemented by the epipolar geometry, are focused on the minimization of an energy function [39]. However, besides the classical SGM algorithm based on a stereo-matching strategy, multi-view approaches are incorporated in order to increase the reliability of the 3D results and to better cope with the case of complex archaeological sites (where the images are captured with different sensors). Considering the two types of flights performed (UAV and paratrike), two different multi-view algorithms were used. For the vertical flight (paratrike), the multi-view MicMac algorithm [40] was used. Meanwhile, for the oblique flight (UAV), the multi-view SURE algorithm [41] was used, which allows a complete reconstruction of the scene. Both strategies consist of minimizing an energy function throughout the eight basic directions that a pixel can take (each 45°). This function is composed of a function of cost, **M** (the pixel correspondence cost), that reflects the degree of the similarity of the pixels between two images, x and x', together with the incorporation of two restrictions, P_1 and P_2, to show the possible presence of gross errors in the process of SGM. In addition, a third constraint has been added to the process of SGM; it consists of the epipolar geometry derived from the

photogrammetry, and it can enclose the search space of each pixel in order to reduce the enormous computational cost. In that case, it will generate a dense model with multiple images, obtaining more optimal processing times.

$$E(D) = \sum_{x} \left(M(x, D_x) + \sum_{x' \in N_x} P_1 T[|D_x - D_{x'}| = 1] + \sum_{x' \in N_x} P_2 T[|D_x - D_{x'}| > 1] \right) \quad (3)$$

where $E(D)$ is an energy function that must be minimized on the basis of the disparity (difference of correspondence) through the counterpart characteristics, the function M (the pixel correspondence cost) evaluates the levels of similarity between the pixel x and its counterpart x' through its disparity Dx, while the terms P_1 and P_2 correspond with two restrictions that allow for avoiding gross errors in the dense matching process for the disparity of 1 pixel or a larger number of them, respectively.

3.2.3. Data Fusion

Data fusion has been performed homogenizing the data provided for each sensor and generating a common product, a point cloud, with metric properties' multi-resolution and photorealistic texture. Concretely, in order to fuse data, both flights (UAV and paratrike) were solved under a combined photogrammetric bundle adjustment using common control points and two different cameras. Through this combined bundle adjustment, a better and more homogeneous aerial photogrammetric point cloud is obtained, avoiding errors that would be obtained and propagated using a solid rigid transformation. In particular, the combined bundle adjustment (UAV-*uav* and paratrike-*pt*) is solved through a least square adjustment based on collinearity condition Equation (2), as follows:

$$x = x\left(\bar{c}_{pt},\ \bar{c}_{uav}, \overline{eo}_{pt\ i},\ \overline{eo}_{uav\ j},\ \overline{X}_k\right) y = y\left(\bar{c}_{pt},\ \bar{c}_{uav}, \overline{eo}_{pt\ i},\ \overline{eo}_{uav\ j},\ \overline{X}_k\right) \quad (4)$$

where:

- $\bar{c}_{pt}$ *and* $\bar{c}_{uav}$ are the camera vectors used for paratrike and UAV, respectively, and which include the internal camera parameters (principal point and focal length) and lens distortion coefficients (radial-*K*, decentering-*P* and affinity parameters-*b*). A total of ten unknowns were used for each camera vector, $\bar{c} = (x_0,\ y_0, f,\ K_1,\ K_2,\ K_3, P_1,\ P_2, b_1,\ b_2)$.
- $\overline{eo}_{pt\ i}$ *and* $\overline{eo}_{uav\ j}$ correspond with the six unknowns of the external orientation for paratrike and UAV images, respectively. Being the external orientation vector, $\overline{eo} = \left(S_x,\ S_y,\ S_z,\ \omega,\ \varphi,\ \chi\right)$.
- $\overline{X}_k$ represents the spatial coordinates vector (*X*,*Y*,*Z*) of the unknown object points.

Therefore, the equation system is defined as follows:

$$\mathbf{A}x - \mathbf{K} = V \quad (5)$$

where **A** corresponds with the design matrix based on collinearity equations and linearized through a first-order Taylor series, **K** is the observations matrix, V is the residual vector and x is the unknown's vector solved through a least squares adjustment as follows:

$$x = \left(A^T PA\right)^{-1} A^T PK \quad (6)$$

P is the weight matrix which corresponds with the inverse cofactor matrix of the observations. The equation system is solved through a twofold step: first by computing the exterior orientation parameters, $\overline{eo}$, and then computing the object points, $\overline{X}_k$, that represent the point cloud.

Next, the remaining step is the registration of the aerial point clouds derived from the different sensors under a global coordinate system. To this end, a GNSS campaign of 3 h based on three permanent ERGNSS stations was performed in order to provide precise coordinates to the GNSS base station used in the archaeological settlement. GNSS observations were processed guaranteeing an

absolute error of 3 cm. The RTK surveying of the GCPs allowed us to obtain the aerial point cloud (i.e., coming from UAV and paratrike) under a global coordinate system (EPSG: 25830 and height EPSG: 5782), reaching a final relative precision of 1 cm.

Finally, regarding terrestrial laser scanner (TLS), the different scans were aligned and then co-registered with the photogrammetric point cloud coming from UAV and paratrike, using matching points defined manually as initial approximations. This was carried out using each dataset of coordinates in its coordinate system, that is, the local system in the case of the aligned TLS point cloud and the absolute system for the photogrammetric point cloud, and then applying a variation of the ICP technique, Least Squares Matching (LSM). A figure (Figure 5) to visually illustrate how this fusion has been done is included. A is the function that represents the point cloud coming from the aerial photogrammetry (UAV and paratrike) and B is the function that represents the aligned TLS point cloud, the registration of both point clouds will be obtained as follows:

$$A_i\,(x,y,z) - \ e_i\,(x,y,z) = B_j\,(x,y,z)\ \ i,j = 1,\ldots,n\ , i \neq j \tag{7}$$

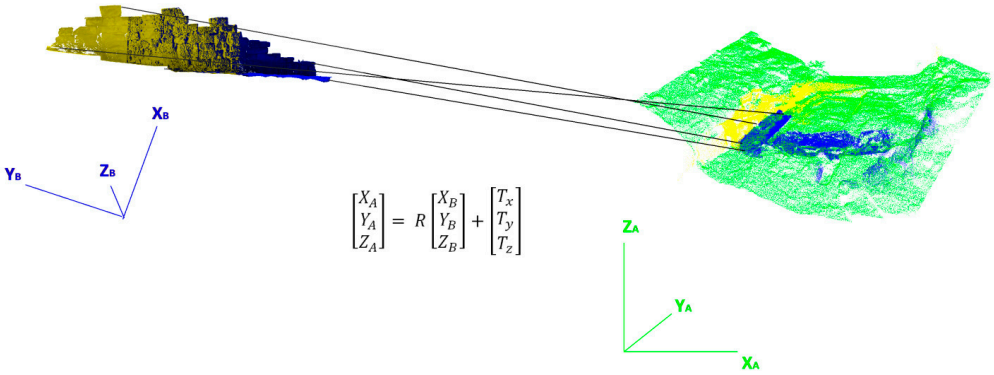

Figure 5. An example of data fusion using Least Squares Matching (LSM) between the laser (**Left**) and photogrammetric (**Right**) point clouds.

The equation that relates both models is a solid rigid transformation with seven parameters:

$$\begin{bmatrix} X_A \\ Y_A \\ Z_A \end{bmatrix} = R \begin{bmatrix} X_B \\ Y_B \\ Z_B \end{bmatrix} + \begin{bmatrix} T_x \\ T_y \\ T_z \end{bmatrix} \tag{8}$$

where **R** represents the rotation matrix and T the translation vector. The correspondence between both point clouds is obtained through a minimisation, based on least squares adjustment, of the Euclidean distances between both point clouds. Since the rotation matrix is composed of non-linear functions, first-order Taylor series were used for the linearization of the Equation (8) as follows:

$$\begin{aligned} -e_i\,(x,y,z) = B_j^0\ (x,y,z) + \frac{B_j^0(x,y,z)}{\partial x_j}dx_j + \frac{B_j^0(x,y,z)}{\partial y_j}dy_j + \frac{B_j^0(x,y,z)}{\partial z_j}dz_j - \ A_i^0\ (x,y,z) \\ -\frac{A_i^0(x,y,z)}{\partial x_i}dx_i - \frac{A_i^0(x,y,z)}{\partial y_i}dy_i - \frac{A_i^0(x,y,z)}{\partial z_i}dz_i \end{aligned} \tag{9}$$

where:

$$\begin{aligned} dx &= dt_x + a_{10}dm + a_{11}d\omega + a_{12}d\varphi + a_{13}d\kappa \\ dy &= dt_y + a_{20}dm + a_{21}d\omega + a_{22}d\varphi + a_{23}d\kappa \\ dz &= dt_z + a_{30}dm + a_{31}d\omega + a_{32}d\varphi + a_{33}d\kappa \end{aligned} \tag{10}$$

Through an iterative process, the linear system $-e = Ax - l$ is solved, x being the unknown's vector encompassing the transformation parameters ($dt_x, dt_y, dt_z,\ dm,\ d\omega,\ d\varphi,\ d\kappa$), whereas l is the

observation vector enveloping the discrepancies of Euclidean distances between both point clouds, and e is the residual vector.

Figure 5 graphically outlines the process followed for data fusion. An example of the aligned TLS point clouds for two scans of the wall (yellow and blue point clouds) in a local coordinate system is outlined to the left side of the image. Subsequently, the aligned TLS point clouds are fused with the photogrammetric point cloud in a global coordinate system (green point cloud) by means of LSM.

3.2.4. Post-Processing

Once a metric and geo-referenced point cloud was generated, a mesh strategy was applied to generate the digital surface model (DSM). In this case, the incremental Delaunay triangulation algorithm was applied [42].

To improve the model quality, break lines were incorporated as geometric constraints. Break lines were manually restituted by the operator. Its use is relevant for the accurate representation of significant slope changes, as well as for correctly defining the defensive walls of the site.

In those cases where images come from different methodologies or acquisition time, a radiometric adjustment was necessary to improve the final model visualization and avoid abrupt radiometric changes in the texture.

Once the DSM was obtained, it was possible to generate a true orthoimage from the oriented images. Since the multi-data source and multi-sensor approach provide different DSM resolutions, it was possible to generate true orthoimages with different spatial resolutions. For instance, a true orthoimage that depicts the complete archaeological site was generated with a resolution of 10 cm; whereas a 2 cm spatial resolution was employed for the settlement entrance area in order to appreciate the construction features.

3.2.5. Simplification and Optimization

Different simplification and optimization strategies were applied to the different geomatics products (DSM and orthoimages) in order to access and analyse 2D and 3D information through a Web service using mobile devices such as tablets or smartphones. In particular, a pyramidal structure was generated for the Web visualization of the 2D orthoimages and 3D models, including "El Reguerón" as the area with the most resolution. The methodology used for simplifying the 3D models is based on the strategy "smooth looking" [43] which consists in a straightforward mesh generation procedure applying the Poisson algorithm [44] to the hybrid point cloud. The mesh resolution is determined by the octree level, chosen according to the user-defined spatial resolution. Unlike a direct mesh generation process, which usually requires mesh editing operations such as filtering and refinement [45,46], Poisson algorithm directly encloses a smoothing step and provides a continuous geometry. This process could be controlled by some computation parameters as the minimum number of sample points that should fall within a node of the resulting octree. This parameter controls the loss of detail by the smoothing process. Although a high number of sample points implies a decrease of the number of mesh vertices, its geometry could be affected, being the final mesh mildly shrunk. For this reason, and as the noise level of the hybrid point cloud is low, the threshold value was kept low in order to avoid redundant smoothing processes. Then, a mesh optimization strategy, based on reducing the final number of triangles through the "collapse" of non-relevant areas without losing significant level of detail, is performed. For this purpose, an iterative process is proposed where the mesh derived from the previous procedure (smooth-looking) is "collapsed" by 5% of the total number of triangles using the quadratic edge collapse algorithm [47]. The algorithm essentially removes edges by merging and regrouping nearby vertices. With the aim of minimising the distortion of the surface geometry, it is necessary to establish a precision threshold to stop the iterative process. So that, if the resulted mesh error against the original input point cloud remains unchanged (with respect to the previous iteration), the collapse process continues. An iterative procedure is required since the quadratic edge collapse algorithm implementation does not allow decimation at fixed spatial resolution.

Although our approach is based on an edge-collapse algorithm for the mesh optimisation, others approaches could be applied, such as the remeshing with recursive resampling as shown in [48] based on the Marching Cubes algorithm [49]. However, this remeshing approach exhibits higher deviations from the original model, up to 20 times higher than the quadratic edge collapse algorithm [48], and is therefore inadequate for our final archaeological products.

Finally, a texture mapping of the simplified and optimised mesh was performed using the commercial software Agisoft Photoscan®.

4. Experimental Results

4.1. Area of Study

The city of "Tolmo de Minateda" (Figure 6) was a strategic settlement of great importance for several centuries, largely because of its peculiar topography and geographical location. It is placed on a plateau hill of about 50 m of height, located at the junction of the route from Complutum to Carthago Nova, one of the principal Roman routes connecting the interior of the plateau with the southeast coast, and a road connecting Castulo with Saetabis.

Figure 6. Aerial view of the study area "Tolmo de Minateda" (from [50]).

The archaeological research from the last 30 years has highlighted the importance of this site, revealing a history from the Middle Bronze Age, through the Iberian era, the Roman period, and the Middle Ages to the twentieth century. The Middle Age period provided most of the information by an important Visigoth settlement located in the upper part of the "El Tolmo", where an important Christian basilica was found between houses and cemeteries.

One of the most interesting areas of the archaeological site is "El Reguerón" (Figure 6), an area of natural drainage 12 m in width, with a main entrance at the top of the hill where the city was located. In the settlement, an important fortification system consisting of three walls of different chronology and architectural typologies has been documented [51]. The oldest fortification is represented by the so-called "embanked" wall and was built during the final phase of the Iberian period (4th−2nd century B.C.). Currently, only the remains of a wall 6 m high and 10 m wide at the top, embanked in the external front and built in irregular masonry work, was preserved in the soil. During the archaeological excavation of this ancient wall, an earlier phase, which dates back to the Middle Bronze Age, was discovered. The Iberian wall was successively used as a retaining wall for a new fortification building during Roman times when the "Tolmo de Minateda" probably received the title of municipality.

The last fortification found in "El Reguerón" comes from the period of peninsula occupation by the Visigoths (5th–6th century A.D.). This wall is presented as a solid, L-shaped bulwark that encloses the valley and flanks the main road access to the city. It is here at this point that a monumental gate,

probably formed by two solid towers of blocks, was once located. Only partial remains have been preserved. The wall is formed by a line of blocks with inscriptions and architectural elements from older constructions (among which are examples from the Roman period).

The relevant archaeological stratification of this area with different structures and building types requires of a multi-data source and multi-sensor approach that allows us to properly record and classify archaeological surfaces, thereby establishing an integration of topographic data with documents of archaeological excavations.

In order to fulfill the archaeological documentation requirements, the aerial data gathering was performed with a paratrike which allows us to enclose the whole extension of the archaeological site using a full-frame reflex camera, assisted by a specific gyrostabilized platform (MUSAS-MUltiSpectral Airborne Sensors) with a ground sample distance (GSD) of 3 cm. According to the GSD desired for the whole archaeological site and considering the camera specifications, a maximum flight height of 224 m was established. As a result, a total of 268 images along seven strips (NW-SE direction) were required for guaranteeing a side overlap of >30% and a forward overlap of >70%.

To record with higher spatial resolution the area of interest of the "El Regueron" site (Figure 7), an UAV with an ultra-compact camera (Table 5) acquired the fortified walls with a GSD of 1 cm. Finally, 25 images and a flight height of 32 m guaranteed the desired spatial resolution. The overlap parameters were the same.

Figure 7. Location of the defensive area "El Reguerón".

Table 5. Geo-referencing errors.

Check Points			Discrepancies with 3D Model Coordinates			
X (m)	*Y (m)*	*H (m)*	*ΔX (m)*	*ΔY (m)*	*ΔXY (m)*	*ΔH (m)*
621,321.452	4,259,638.120	448.672	0.005	0.001	0.005	−0.013
621,375.933	4,259,646.226	454.775	−0.009	0.004	0.009	0.032
621,416.258	4,259,667.686	463.661	0.007	−0.011	0.013	0.030
621,419.022	4,259,658.232	464.618	0.001	0.008	0.008	0.046
621,345.185	4,259,659.272	454.267	0.002	0.018	0.006	0.024
621,321.298	4,259,660.311	452.106	−0.010	−0.026	0.028	0.036

In addition, to increase the level of detail in the fortification walls and thus avoid the occlusions due to the effects of terrain relief (i.e., areas occluded or without information in the model generated by aerial photogrammetry), a combination of terrestrial photogrammetry and terrestrial laser scanner (TLS) was employed for improving the final 3D hybrid model. As a result, a total of 36 terrestrial oblique images and 13 TLS point clouds were acquired in order to avoid areas without information, guaranteeing a subcentimeter resolution.

4.2. Workflow

The application of the multi-data source and multi-sensor fusion workflow was tested in the study area of "Tolmo de Minateda," which includes a total of 9 ha.

Firstly, the aerial images were processed by the automated photogrammetric approach and the cameras were self-calibrated according to Section 3.2.2. As a result of this process, the raw reconstructed point cloud is obtained which contains 4,271,354 points, while the TLS integrated point cloud reaches up to 1,314,136 points. Secondly, the geo-referencing of the 3D model was solved by the employment of 28 control points homogeneously distributed across the site (but with higher density in the interest area), while ten were used as checkpoints. Finally, the final multi-resolution 3D model after triangulation is obtained (Figure 8), encompassing the whole study area with a spatial resolution of 3 cm. A total of 10,542,505 triangles were obtained.

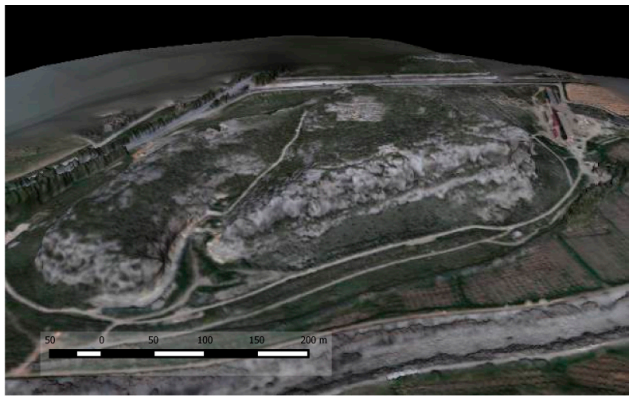

(**a**)

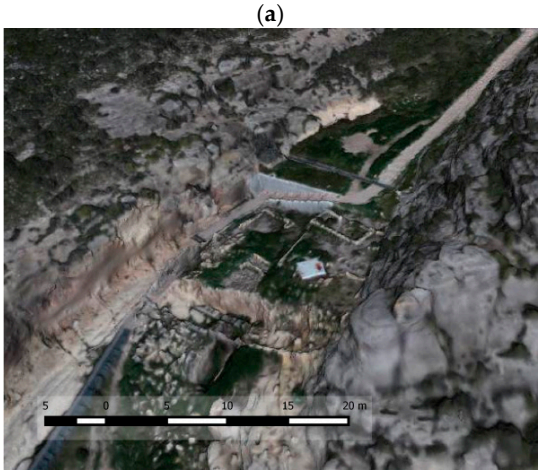

(**b**)

Figure 8. Multi-resolution 3D model of the archaeological settlement (**a**). Detailed 3D model of "El Reguerón" (**b**).

For the detailed area which integrates different data sources (i.e., terrestrial laser scanner and photogrammetry), a spatial filtering of 0.5 cm was applied to avoid areas with excessive point density caused by the different overlaps.

By this multi-resolution approach, the final inspection of the archaeological site could be adapted to any area, as illustrated with "El Reguerón", where the subcentimete resolution achieved for the walls and construction (Figure 9b) was integrated with the rest of the archaeological site (Figure 9a). This multi-resolution capability opens a range of possibilities for a spatial analysis, settlement interpretation, pattern recognition, and the establishing of relationships among the elements (sites, artefacts locations, etc.).

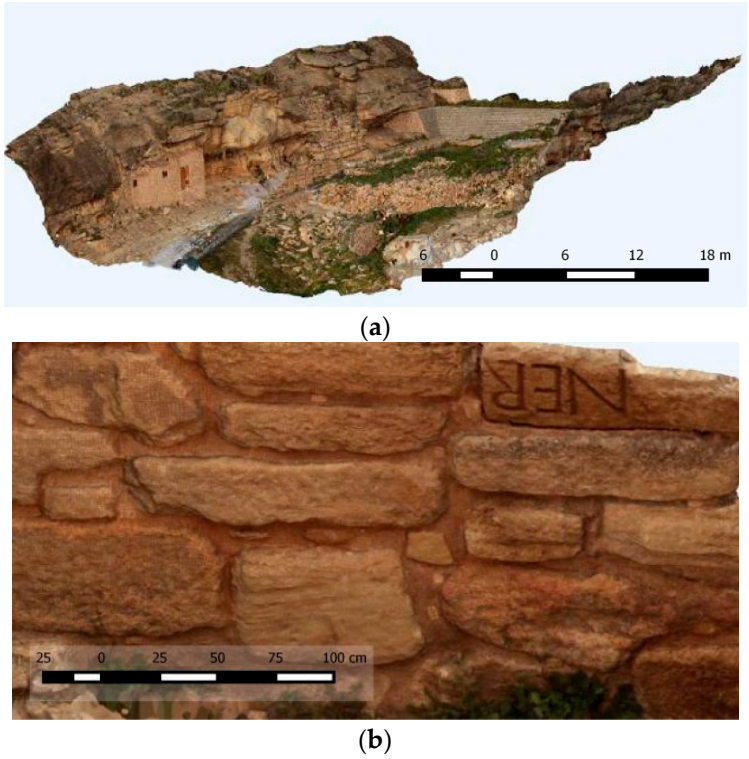

Figure 9. Multi-resolution model of "El Reguerón" area (**a**) and detail for the wall (**b**).

In order to validate the final integration of the different data sources, a series of checkpoints were used. The different error components are shown in Table 4. The average vertical error (2.6 cm) was higher than the horizontal error (1.4 cm), as was expected for the GNSS technique. An average precision of 3 cm for the 3D vector error was obtained, which is statistical compatible with the expected a priori error of 3.1 cm composed by the model and GNSS check point errors.

To manage more efficiently the available information of the archaeological settlement, true orthoimages were generated as derived products (Figure 10), since they combined the photorealistic texture with the metric properties in an easy-to-use document for non-experts.

However, to allow a more complete interpretation and to make use of the potential of the generated 3D product, an integration with a 3DGIS tool, GeoWeb3D, was performed. In particular, the 3D geometry provided by the multi-sensor approach has been integrated with 2D archaeological archives such as sketches, pictures, part details, etc., thus enhancing the subsequent analysis and providing problem solving and decision-making capabilities. Figure 11 shows the integration of different historical events in the reconstructed 3D model.

The integration of 2D information and 3D models allows us to extract intangible information that improves the analysis capabilities of the archaeological settlement. For instance, Figure 11 integrates an archaeological sketch of defensive constructions (2012) with the generated hybrid 3D model (2015). It should be noted that the high accuracy and proportion of the sketch is a perfect coincidence of the main homologous entities. However, some detached blocks belonging to the wall of the 3D model do not appear in the sketch. Analysing the position of blocks in the 3D model, it seems that they were spread along the natural drainage bed of the Tolmo, possibly suggesting that a runoff flow took place from the upper part of the Tolmo, providing this current block distribution.

(**a**) (**b**)

Figure 10. True orthoimages of the whole settlement (**a**) and defensive area "El Reguerón" (**b**).

(**a**)

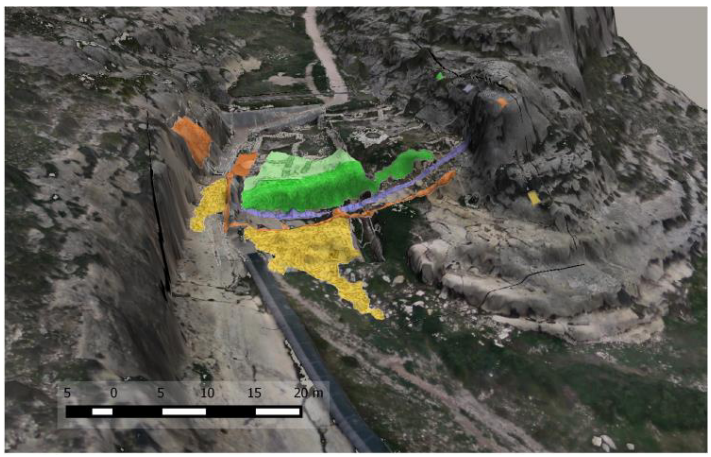

(**b**)

Figure 11. Archaeological sketch (**a**) overlapped with the 3D model (**b**).

Next, with the aim of showing the potential of analysing in situ the archaeological settlement, "El Reguerón" was tested using a mobile device (smartphone). The simplification and optimisation level was fixed considering different aspects: (i) the amount of 2D information which should be integrated; (ii) the minimum size of the interest elements and (iii) the level of reduction. A minimum resolution of 10 cm was established for the "El Reguerón" area.

Looking to the smallest and most emblematic elements of "El Reguerón," it can be confirmed that these correspond to the blocks of the wall, which are bigger than the minimum resolution, meaning that they should be correctly represented. Subsequently, an iterative optimization process of the mesh was performed maintaining relevant information and stopping when the threshold of resolution (10 cm) was surpassed. As we can see in Table 5, the simplified and optimised models maintain the initial resolution (10 cm), with a level of reduction of 75% in comparison with the simplified model (without optimisation).

The simplification and optimisation procedures have removed 31,039,445 points of the 33,856,298 initial points. However, in order to assess the final error of the simplification and optimisation strategy, we have compared the simplified and optimised model with the original point cloud, obtaining an average error of 0.2 mm and a standard deviation of $\pm$22 mm.

As we can see in Figure 12, higher discrepancies are located in peripheral areas due to the presence of vegetation with an irregular typology. Conversely, the walled area exhibits minimum discrepancies always less than $\pm$5 mm.

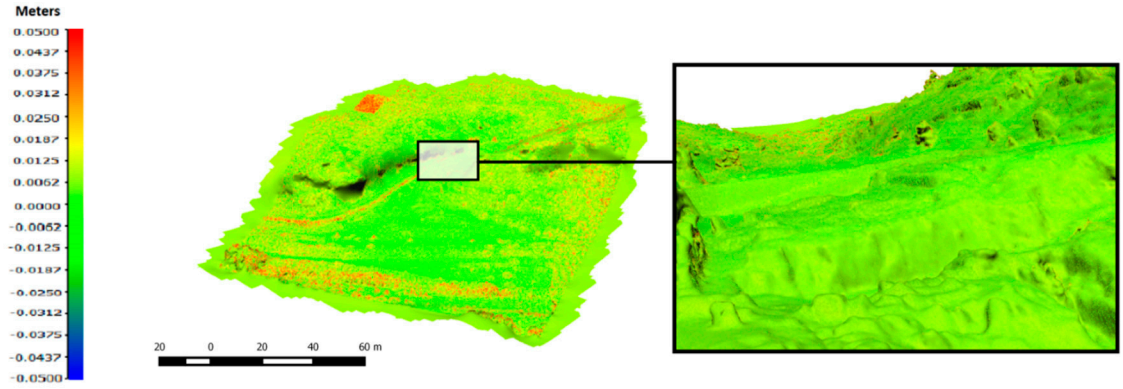

Figure 12. Analysis of discrepancies between the simplified-optimised 3D model and the original point cloud (**Left**) and a detailed comparison over the walled area (**Right**).

Finally, results were presented through the Web based on the Open Source library Cesium. A specific template based on HTML language was prepared to show the 3D models and additional information using external geospatial services such as WMS, MapServer, Google Earth or Bing, among others. Thanks to the flexibility and portability of the mobile devices, it was possible for the archaeologist to interact directly with the platform at the field: recording data and adding new information with corresponding attributes and descriptions. An example is outlined in Figure 13, where the application is loaded in a smartphone BQ Aquaris E4.5 using Android 4.4.2 and Google Chrome 45. Results were incorporated to the archaeological information system and the spatial data infrastructure of the archaeological cultural heritage of Castilla La Mancha (ideARQ + SIA) [50].

Additionally, the optimal value of points and triangles for the proper management of 3D models in smartphones was examined. For this aim, three levels of simplification were analysed using three, two and one million(s) triangles, respectively. Afterwards, loading and operation times together with RAM were monitored in order to see the best simplification level for a conventional smartphone. Table 6 outlines the results obtained.

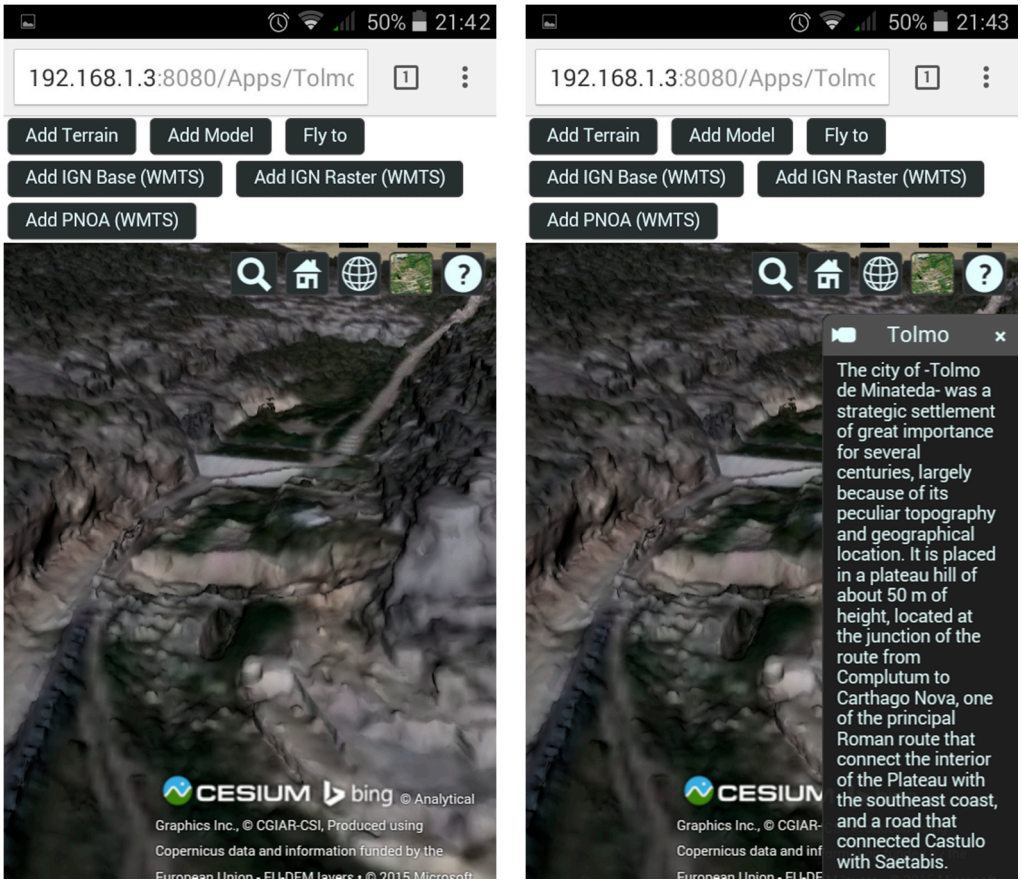

Figure 13. "El Regueron" 3D model and its additional information loaded in a smartphone (Base model from: © Analytical Graphics, Inc., © CGIAR-CSI, Produced using Copernicus data and information funded by the European Union—EU-DEM layers, © Commonwealth of Australia (Geoscience Australia) 2012) [19].

Table 6. Times and resources required with lighter models using mobile devices.

Model	Number of Points	Number of Triangles	
3M	1,408,636	2,816,156	
	Load	Operation	RAM consumption
	10 s	2–4 s	2.39 GB
2M	986,150	1,971,309	
	Load	Operation	RAM consumption
	8 s	1–3 s	2.24 GB
1M	493,198	985,653	
	Load	Operation	RAM consumption
	3 s	Instantaneous	1.79 GB

As we can see, with less than one million triangles, very good loading and operation times (instantaneous) are obtained, as well as an affordable RAM consumption for the majority of smartphones. Therefore, for optimal user experience and navigation for each visualization level (defined in terms of spatial resolution; see Section 3.2.5), the maximum display area is cropped accordingly to this empirical number of triangles.

5. Conclusions

This paper presents a methodology based on a combination of multiple sensors, platforms and techniques, which has been tested in a complex archaeological site. As is shown in the experimental results, the automation provided by the photogrammetric and laser techniques, along with the versatility of the aerial platforms (paratrike and Unmanned Aerial Vehicle UAV), provide the suitability of this methodology for complex archaeological sites.

The potential of ultralight aerial platforms (paratrike) is highlighted, due to its payload and flight autonomy, which overpasses the UAVs capabilities. Regarding the usual archaeological surveys, one of the main differential factors in this work has been the integration of aerial images at different resolutions, terrestrial images and terrestrial laser scans.

The generation of high resolution products based on photogrammetry requires high computational costs. To this end, the presented algorithms, such as Affine Scale Invariant Feature Transform ASIFT, have been developed to take advantage of Graphical Processing Unit GPU capabilities, reduce time operations and consequently improve workflow efficiency.

The management of the final models through a 3DGIS tool opens new analysis capabilities for the archaeologist (e.g., analysis though time, archaeological investigations, integration of historical and geometric models).

Finally, it has been demonstrated that through the simplification and optimization strategies, complex hybrid 3D modes which enclose 2D information can be flexibly shown through the Web and even embedded in smartphones. As a result, we can interact directly with hybrid 3D models using mobile devices, allowing the recording, storage and analysis of data in situ. The implemented methodology to optimize the visualization and interaction of geomatics products has proven to be effective. However, it lacks a fully complete user interaction, since the final navigation is constrained by the definition of the visualization level. To overcome this limitation, a future work line is aimed to a more efficient visualization management by the 3DGIS tool, avoiding the definition of level of visualization by the final user.

The technical case outlined in this paper could be of great interest for different stakeholders:

- *Researchers* for the interpretation, spatial and temporal analysis of the archeological settlement thanks to the integration capabilities and portability of the system.
- *Managers* through the monitoring of the archaeological settlement through time, the diffusion of the site using videos, documents, etc.
- *Students* who could exploit the didactical possibilities of the 3D inspection, interaction and superposition of thematic information.
- *General public* allowing a flexible and enjoyable accessibility to the archaeological settlement which complements and provides added value to a visit to an historical site.

The data acquisition and processing methodologies from Geomatic science broaden the possibilities of sensors, configurations and/or combination as future perspectives. Concretely, the resolution of the external orientation of the images directly, just using the integrated Global Navigation Satellites System GNSS/IMU Inertial Measurement Unit of the aerial platform, would allow us to speed up the field work and processing time. Furthermore, in order to obtain realistic textured models and orthoimages, the use of techniques such BRDF (Bidirectional Reflectance Distribution Function) to improve the radiometric parameters will be studied.

Acknowledgments: This research has been developed in the framework of the research project "*Infraestructura de datos espaciales de patrimonio arqueológico de Castilla-La Mancha*" (POII-2014-004-P) of the 2014-2017 Scientific Research Projects cofounded by the European Regional Development Fund. The authors would like to thank the Ministry of Education, Culture and Sport of Castilla-La Mancha, especially to the Directorate-General for Universities, Research and Innovation, the Directorate-General for Cultural and the Museum of Albacete. We also specially thank Lorenzo Abad Casal (University of Alicante), Sonia Gutiérrez Lloret (University of Alicante), Rubí Sanz Gamo (Museum of Albacete) and Blanca Gamo Parras (Museum of Albacete) for their support during the course of this study.

Author Contributions: All authors conceived, designed and performed the experimental campaign and the implemented methodology. José Alberto Torres processed and analysed the results. All authors wrote the manuscript.

Conflicts of Interest: The authors declare no conflict of interest.

Abbreviations

AGI	Analytical Graphics, Inc.
ASIFT	Affine Scale Invariant Feature Transform
BRDF	Bidirectional Reflectance Distribution Function
CCRS	Compound Coordinate Reference System
CRS	Coordinate Reference System
DSM	Digital Surface Model
DTM	Digital Terrain Model
ETRS89	European Terrestrial Reference System 1989
EPSG	European Petroleum Survey Group
GIS	Geographical Information System
GNSS	Global Navigation Satellites System
GPS	Global Positioning System
GPU	Graphical Processing Unit
GSD	Ground Sample Distance
HTML	HyperText Markup Language
ICP	Iterative Closest Point
IMU	Inertial Measurement Unit
LSM	Least Squares Matching
MI	Mutual Information
MUSAS	MUltiSpectral Airborne Sensors
ORSA	Optimized Random Sampling Algorithm
RAM	Random Access Memory
RANSAC	Random Sample Consensus
RTK	Real-Time Kinematic
SGM	Semi-Global Matching
SIFT	Scale Invariant Feature Transform
TLS	Terrestrial Laser Scanner
UAV	Unmanned Aerial Vehicle
UTM	Universal Transverse Mercator
VRML	Virtual Reality Modeling Language
WMS	Web Map Service

Appendix: 3D Web Visualization

The management of a 3D textured model is a key part of any spatial data infrastructure. However, it requires an efficient visualization system to visualize the geometric and semantic information. In spite of the mesh simplification and optimization process mentioned in Section 3.2.5, it is possible to optimize the visualization of 3D models in terms of WebGL framework Cesium. Some authors [52] propose an approach based on a custom geometry loader implemented in the Cesium APIs. By this approach any 3D element is rendered and handled by the Cesium rendering code. However, these authors remark some drawbacks in terms of memory and performance. Another alternative is the employment of the GL Transmission Format (glTF) proposed in [53] which allows directly loading the data to the WebGL buffers. This format aims to be a standard for data exchange and rendering. Although this glTF format is able to deliver an arbitrary number of mesh data buffers within a single file, it completely lacks any mechanism for progressive data transmission. Trying to overcome this limitation, new file formats are being developed [54]. The basic idea would be to improve the data streaming by means of a Level of Detail (LoD) visualization in order to reduce the number of WebGL draw calls.

Following this line, the implemented solution is based on the optimization of visualization levels. For each user call, a specific 3D sub-model is loaded accordingly to the user position, view orientation and zoom level. This is a trade-off between the visualized area and the model resolution, keeping an optimal number of mesh triangles for an easy navigation in terms of loading time and user experience.

The main drawback is that the final user navigation has to be constrained into a set of positions to avoid the movement outside the active visualization level. The generation of the 3D sub-models for visualization purposes implies a spatial resolution simplification, where the visualization areas are extracted according to the optimal number of triangles mentioned above. The 3D sub-models are created in a discrete number of levels, where the minimum allowed resolution change is established at 5%.

References

1. Gomez-Lahoz, J.; Gonzalez-Aguilera, D. Recovering traditions in the digital era: The use of blimps for modelling the archaeological cultural heritage. *J. Archaeol. Sci.* **2009**, *36*, 100–109. [CrossRef]
2. Bevan, A.; Li, X.; Martinón-Torres, M.; Green, S.; Xia, Y.; Zhao, K.; Zhao, Z.; Ma, S.; Cao, W.; Rehren, T. Computer vision, archaeological classification and China's Terracotta Warriors. *J. Archaeol. Sci.* **2014**, *49*, 249–254. [CrossRef]
3. González-Aguilera, D.; Muñoz-Nieto, Á.; Rodríguez-Gonzálvez, P.; Menéndez, M. New tools for rock art modelling: Automated sensor integration in Pindal Cave. *J. Archaeol. Sci.* **2011**, *38*, 120–128. [CrossRef]
4. Hakonen, A.; Kuusela, J.-M.; Okkonen, J. Assessing the application of laser scanning and 3D inspection in the study of prehistoric cairn sites: The case study of Tahkokangas, Northern Finland. *J. Archaeol. Sci.* **2015**, *2*, 227–234. [CrossRef]
5. Themistocleous, K.; Ioannides, M.; Agapiou, A.; Hadjimitsis, D.G. The methodology of documenting cultural heritage sites using photogrammetry, UAV and 3D printing techniques: The case study of Asinou Church in Cyprus. In Proceedings of the Third International Conference on Remote Sensing and Geoinformation of Environment, Cyprus, Nicosia, 16 March 2015; pp. 16–19.
6. Lai, L.; Sordini, M.; Campana, S.; Usai, L.; Condò, F. 4D recording and analysis: The case study of Nuraghe Oes (Giave, Sardinia). *Digit. Appl. Archaeol. Cult. Herit.* **2015**, *2*, 233–239. [CrossRef]
7. Torres, J.A.; Hernandez-Lopez, D.; Gonzalez-Aguilera, D.; Moreno Hidalgo, M.A. A hybrid measurement approach for archaeological site modelling and monitoring: The case study of Mas D'is, Penàguila. *J. Archaeol. Sci.* **2014**, *50*, 475–483. [CrossRef]
8. Achille, C.; Adami, A.; Chiarini, S.; Cremonesi, S.; Fassi, F.; Fregonese, L.; Taffurelli, L. UAV-based photogrammetry and integrated technologies for architectural applications—Methodological strategies for the after-quake survey of vertical structures in Mantua (Italy). *Sensors* **2015**, *15*, 15520–15539. [CrossRef] [PubMed]
9. Ortega-Terol, D.; Moreno, M.A.; Hernández-López, D.; Rodríguez-Gonzálvez, P. Survey and classification of Large Woody Debris (LWD) in streams using generated low-cost geomatic products. *Remote Sens.* **2014**, *6*, 11770–11790. [CrossRef]
10. Hailey, T. The powered parachute as an archaeological reconnaissance vehicle. *Archaeol. Prospect.* **2005**, *12*, 69–78. [CrossRef]
11. Herrero-Huerta, M.; Hernández-López, D.; Rodriguez-Gonzalvez, P.; González-Aguilera, D.; González-Piqueras, J. Vicarious radiometric calibration of a multispectral sensor from an aerial trike applied to precision agriculture. *Comput. Electron. Agric.* **2014**, *108*, 28–38. [CrossRef]
12. Trimble Indoor Mobile Mapping Solution, TIMMS. Available online: http://www.applanix.com/solutions/land/timms.html (accesed on 15 February 2016).
13. Viametris, Indoor Mobile Mapping System. Available online: http://viametris.fr/Produits_IMMS.php (accesses on 15 February 2016).
14. Canter, P.; Stott, A.; Rich, S.; Querry, J. Creating georeferenced indoor maps, images and 3D models: Indoor mapping for high accuracy and productivity. *J. Chart. Instit. Civ. Eng. Surv.* **2010**, *1*, 20–22.
15. Rivero-Juárez, J.; Martínez-García, E.A.; Torres-Mendez, A.; Mohan, R.E. 3D heterogeneous multi-sensor global registration. *Procedia Eng.* **2013**, *64*, 1552–1561. [CrossRef]
16. Nilosek, D.; Sun, S.; Salvaggio, C. Geo-Accurate model extraction from three-dimensional image-derived point clouds. In Proceedings of the Algorithms and Technologies for Multispectral, Hyperspectral, and Ultraspectral Imagery XVIII, Baltimore, MD, USA, 23 Aril 2012.

17. Geoweb3d—3D GIS Visualization. Available online: http://www.geoweb3d.com/ (accessed on 15 February 2016).
18. WebGL Virtual Globe and Map Engine. Available online: http://cesiumjs.org/ (accessed on 15 February 2016).
19. AGI—Software to Model, Analyze and Visualize Space, Defense and Intelligence Systems. Available online: http://www.agi.com/ (accessed on 15 February 2016).
20. Le, H.S. An approach to construct SGIS-3D: A three dimensional WebGIS system based on DEM, GeoVRML and spatial analysis operations. In Proceedings of the 2nd IADIS International Conference Web Virtual Reality and Three-Dimensional Worlds, Freiburg, Germany, 27–29 July 2010; pp. 317–326.
21. Von Schwerin, J.; Richards-Rissetto, H.; Remondino, F.; Agugiaro, G.; Girardi, G. The MayaArch3D project: A 3D WebGIS for analyzing ancient architecture and landscapes. *Lit. Linguist. Comput.* **2013**, *28*, 736–753. [CrossRef]
22. Auer, M.; Agugiaro, G.; Billen, N.; Loos, L.; Zipf, A. Web-based visualization and query of semantically segmented multiresolution 3D models in the field of cultural heritage. *Proc. ISPRS* **2014**, *II-5*, 33–39. [CrossRef]
23. Takasu, T. RTKLIB: Open source program package for RTK-GPS. In Proceedings of the Free and Open Source Software for Geospatial (FOSS4G), Tokyo, Japan, 1–2 November 2009.
24. Hernandez-Lopez, D.; Felipe-Garcia, B.; Gonzalez-Aguilera, D.; Arias-Perez, B. An automatic approach to UAV flight planning and control for photogrammetric applications: A test case in the Asturias region (Spain). *Photogramm. Eng. Remote Sens.* **2013**, *79*, 87–98. [CrossRef]
25. 3D Measurement Technology from FARO. Available online: http://www.faro.com/ (accessed on 15 February 2016).
26. Besl, P.; McKay, N. A method for registration of 3-D Shapes. *IEEE Trans. Pattern Anal. Mach. Intell.* **1992**, *14*, 239–256. [CrossRef]
27. Fernández-Hernandez, J.; González-Aguilera, D.; Rodríguez-Gonzálvez, P.; Mancera-Taboada, J. Image-based modelling from Unmanned Aerial Vehicle (UAV) photogrammetry: An effective, low-cost tool for archaeological applications. *Archaeometry* **2015**, *57*, 128–145. [CrossRef]
28. Morel, J.M.; Yu, G. ASIFT: A new framework for fully affine invariant image comparison. *SIAM J. Imaging Sci.* **2009**, *2*, 438–469. [CrossRef]
29. Gruen, A. Adaptive least squares correlation: A powerful image matching technique. *S. Afr. J. Photogramm. Remote Sens. Cartogr.* **1985**, *14*, 175–187.
30. Moisan, L.; Stival, B. A probabilistic criterion to detect rigid point matches between two images and estimate the fundamental matrix. *Int. J. Comput. Vis.* **2004**, *57*, 201–218. [CrossRef]
31. Fischler, M.A.; Bolles, R.C. Random sample consensus: A paradigm for model fitting with applications to image analysis and automated cartography. *Commun. ACM* **1981**, *24*, 381–395. [CrossRef]
32. Rieke-Zapp, D.H.; Nearing, M.A. Digital close range photogrammetry for measurement of soil erosion. *Photogramm. Rec.* **2005**, *20*, 69–87. [CrossRef]
33. Hartley, R.; Zisserman, A. *Multiple View Geometry in Computer Vision*; Cambridge University Press: New York, NY, USA, 2003.
34. Kraus, K.; Jansa, J.; Kager, H. *Advanced Methods and Applications Volume 2. Fundamentals and Standard Processes Volume 1*; Institute for Photogrammetry Vienna University of Technology: Bonn, Germany, 1997.
35. Snavely, N.; Seitz, S.M.; Szeliski, R. Modeling the world from Internet photo collections. *Int. J. Comput. Vis.* **2008**, *80*, 189–210. [CrossRef]
36. Deseilligny, M.P.; Clery, I. Apero, an open source bundle adjustment software for automatic calibration and orientation of set of images. *ISPRS Int. Arch. Photogramm. Remote Sens. Spat. Inf. Sci.* **2011**, *38*, 269–277.
37. Kukelova, Z.; Pajdla, T. A minimal solution to the autocalibration of radial distortion. In Proceedings of the IEEE Conference on Computer Vision and Pattern Recognition, Minneapolis, MN, USA, 17–22 June 2007.
38. Sturm, P.; Ramalingam, S.; Tardif, J.P.; Gasparini, S.; Barreto, J. Camera models and fundamental concepts used in geometric computer vision. *Found. Trends® Comput. Graph. Vis.* **2011**, *6*, 1–183. [CrossRef]
39. Hirschmuller, H. Stereo processing by semiglobal matching and mutual information. *IEEE Trans. Pattern Anal. Mach. Intell.* **2008**, *30*, 328–341. [CrossRef] [PubMed]
40. Micmac Website. Available online: http://www.tapenade.gamsau.archi.fr/TAPEnADe/Tools.html (accessed on 15 February 2016).

41. Rothermel, M.; Wenzel, K.; Fritsch, D.; Haala, N. SURE: Photogrammetric surface reconstruction from imagery. In Proceedings of the LC3D Workshop, Berlin, Germany, 4–5 December 2012; pp. 1–9.
42. Bourke, P. An algorithm for interpolating irregularly-spaced data with applications in terrain modelling. In Proceedings of the Pan Pacific Computer Conference, Beijing, China, 1 January 1989.
43. Rodríguez-Gonzálvez, P.; Nocerino, E.; Menna, F.; Minto, S.; Remondino, F. 3D surveying & modeling of underground passages in WWI fortifications. *Int. Arch. Photogramm. Remote Sens. Spat. Inf. Sci.* **2015**. [CrossRef]
44. Kazhdan, M.; Bolitho, M.; Hoppe, H. Poisson surface reconstruction. In Proceedings of the 4th Eurographics Symposium on Geometry, Sardinia, Italy, 26–28 June 2006; pp. 61–70.
45. Attene, M. A lightweight approach to repairing digitalized polygon meshes. *Vis. Comput.* **2010**, *26*, 1393–1406. [CrossRef]
46. Varnuška, M.; Parus, J.; Kolingerová, I. Simple holes triangulation in surface reconstruction. In Proceedings of the ALGORITMY 2005, Vysoke Tatry, Podbanske, 13–18 March 2005.
47. Garland, M.; Heckbert, P. Surface simplification using quadric error metrics. In Proceedings of the Special Interest Group on Computer Graphics and Interactive Techniques (SIGGRAPH), Los Angeles, CA, USA, 3 August 1997; pp. 209–216.
48. Minto, S.; Remondino, F. Online access and sharing of reality-based 3D models. *Sci. Res. Inf. Technol.* **2014**, *4*, 17–28.
49. Lorensen, W.E.; Cline, H.E. Marching cubes: A high resolution 3D surface construction algorithm. *ACM Siggraph Comput. Graph.* **1987**, *21*, 163–169. [CrossRef]
50. Abad Casal, L.; Lloret, S.G.; Parras, B.G.; Guillen, P.C. El Tolmo de Minateda (Hellín, Albacete, España): Un proyecto de investigación y puesta en valor del patrimonio. *Debates Arqueol. Mediev.* **2012**, *2*, 351–381.
51. IdeARQ + SIA. Available online: http://161.67.130.146/test/potree/puntos_fot_tolmo_2015/examples/puntos_fot_tolmo_2015.html (accessed on 15 February 2016).
52. Prandi, F.; Devigili, F.; Soave, M.; Di Staso, U.; De Amicis, R. 3D web visualization of huge CityGML models. *Proc. ISPRS* **2015**, *40*, 601–603. [CrossRef]
53. Robinet, F.; Cozzi, P. Gltf—The Runtime Asset Format for WebGL, OpenGL ES, and OpenGL. Available online: https://github.com/KhronosGroup/glTF/blob/master/README.md (accessed on 30 May 2016).
54. Limper, M.; Thöner, M.; Behr, J.; Fellner, D.W. SRC-a streamable format for generalized web-based 3D data transmission. In Proceedings of the 19th International ACM Conference on 3D Web Technologies, Vancouver, BC, Canada, 8–10 August 2014; pp. 35–43.

3.3 Combinación de características geométricas y radiométricas en la evaluación de pinturas rupestres.

Frente a las habituales técnicas de clasificación de imágenes basadas únicamente en la respuesta espectral captada por diversos sensores como cámaras fotográficas convencionales o multiespectrales, en este artículo se presenta una metodología de clasificación no supervisada basada en la combinación de información radiométrica y geométrica.

El análisis de pinturas rupestres requiere de técnicas no invasivas, por lo que para la captura de datos geométricos y radiométricos se emplearon cámaras convencionales RGB, cámaras multiespectrales y sistemas láser escáner terrestres. El empleo de estos sensores junto con técnicas láser, de visión computacional y de clasificación no supervisada de imágenes, ha permitido llevar a cabo un análisis tanto a nivel local como global de las pinturas rupestres de El Abrigo Grande de Minateda, en el municipio de Hellín (Albacete, España).

La metodología propuesta en este artículo consiste en la realización de la clasificación no supervisada de tres pinturas representativas del yacimiento, procediendo posteriormente a la depuración de los resultados mediante el análisis geométrico de las imágenes. De esta forma, las grietas y huecos cuya respuesta espectral es similar tanto en bandas RGB como en el Infrarrojo cercano, y que, en consecuencia, suelen generar errores de clasificación, son eliminados mediante el análisis geométrico, atendiendo a su forma, rugosidad y profundidad. Respecto al análisis de la forma se ha tenido en cuenta la característica de circularidad presente en los huecos frente a las formas más alargadas características de las grietas. Finalmente,

empleando como verdad terreno la clasificación supervisada de las pinturas, efectuada por personal experto, mediante técnicas tradicionales (Análisis de Componentes Principales-PCA), se ha mostrado, cualitativa y cuantitativamente, como la metodología de trabajo aquí propuesta permite obtener resultados similares requiriendo considerablemente menos intervención manual.

Adicionalmente, se ha generado el modelo 3D del abrigo mediante fotogrametría y láser escáner terrestre, permitiendo así el análisis de las pinturas también en un ámbito global. De esta manera se ha podido observar la relación de las pinturas con el soporte base y se ha comprobado como los productos geomáticos son una herramienta idónea para el investigador a la hora de analizar diferentes aspectos como la iluminación o la posición espacial de las pinturas respecto del abrigo, altura respecto al suelo, dimensiones, etc.

De las labores de investigación acometidas se concluye la ventaja que presenta la incorporación de información geométrica en los procesos de clasificación de imágenes en el ámbito del análisis de pinturas rupestres, aumentando su interés el hecho del bajo coste asociado, al extraerse de los mismos sensores tanto la información geométrica como radiométrica.

Contents lists available at ScienceDirect

Digital Applications in Archaeology and Cultural Heritage

journal homepage: www.elsevier.com

Combining geometrical and radiometrical features in the evaluation of rock art paintings

Jose Alberto Torres-Martínez[a], Luis Javier Sánchez-Aparicio[a,*], David Hernández-López[b], Diego González-Aguilera[a]

[a] Department of Land and Cartographic Engineering. University of Salamanca, High Polytechnic School of Avila, Hornos Caleros, 50, 05003 Avila, Spain
[b] Regional Development Institute-IDR, University of Castilla-La Mancha, 02071 Albacete, Spain

ARTICLE INFO

Keywords:
Rock art
Terrestrial Laser Scanner
Close-range Photogrammetry
Multispectral camera
Radiometric classification
Geometrical features

ABSTRACT

Rock art painting is one of the most ancient manifestation of Cultural Heritage. Its fragility demands the use of non-destructive methods for the evaluation of engraved or painted signs contained in caves or shelters. However, most of existing approaches involve the exploitation of radiometric information coming from digital images captured by RGB cameras, showing several drawbacks such as: (i) lack of scale; (ii) lack of flexibility and (iii) high user interaction, among others. In order to provide added value to these approaches, this paper describes a methodology able to combine radiometrical and geometrical features captured by different geomatic sensors (multispectral cameras and terrestrial laser scanner), allowing not only the extraction of the painted signs presented, but also evaluating different aspects of great importance in the understanding of rock art (e.g. the presence of topographic accidents that could influence on the painted signs traces or its visibility under different illumination conditions).

1. Introduction

Nowadays, Cultural Heritage is considered a keystone of the modern society (Herbert, 1995), becoming its preservation a hot topic for the Scientific Community (Del Pozo-Aguilera et al., 2016; Rodríguez-Gonzálvez et al., 2015). From the digitalization of architectural monuments (Sánchez-Aparicio et al., 2014) and prehistoric caves (Azema et al., 2013; Fritz et al., 2016; Puchol et al., 2013, Rodríguez-Gonzálvez et al., 2012), to the aerial surveying of archeological settlements (Fernández-Hernandez et al., 2015, Gomez-Lahoz and González-Aguilera, 2009), geomatics sensors has been widely tested as a tool for Cultural heritage conservation, either alone or in combination (Aguilera et al., 2006; Torres-Martínez et al., 2016).

Inside the wide diversity of monuments, sculptures, paintings, etc. that make up our Cultural Legacy, the rock art paintings or engravings are one of the most ancient manifestations of the humanity. These works, which date from at least 40,000 years, were made on rock surfaces (Bourdier et al., 2015; Robert et al., 2016), suffering a constant degradation by agents such as the water or the atmosphere. The use of non-contact techniques allow us to evaluate not only the paintings or engravings presented (Burens et al., 2011; Defrasne, 2014; Pinçon et al., 2010), but also aspects such as the presence of non-accesible areas or the influence of the topographic accidents in the painted or engraved traces (Lejeune, 1985; López-Montalvo and Sanz, 2005; Robert, 2016, Sauvet et al., 1998). These considerations place the geomatic sensors, such as the Terrestrial Laser Scanner (TLS) or the digital cameras, as the most suitable solutions for the recording of these art manifestations (Seidl et al., 2015; Zeppelzauer et al., 2015).

Regarding TLS, its characteristics can offer a wide range of advantages such as the non-contact nature, the fast data acquisition or the non-light conditions required to capture the data. As a result, large and complex sites can be recorded in 3D in a short period of time. Additional to these geometrical measurements, TLS systems can also record intensity values related with the wavelength used. On the other hand, RGB and multispectrals sensors allow the capture of a variety of different wavelengths and also enable for the 3D reconstruction of complex sites using approaches such as Structure from Motion (SfM), a technique that has proven to be an appropriate solution in archaeologial

* Corresponding author.
Email addresses: josealberto@usal.es (J.A. Torres-Martínez); luisj@usal.es (L.J. Sánchez-Aparicio); david.hernandez@uclm.es (D. Hernández-López); daguilera@usal.es (D. González-Aguilera)

http://dx.doi.org/10.1016/j.daach.2017.04.001
Received 5 December 2016; Received in revised form 25 March 2017; Accepted 18 April 2017
Available online xxx

works (Cefalu et al., 2013; Lerma et al., 2013) since it combines the advantages of the computer vision (automation and flexibility) and photogrammetry (accuracy and reliability) and whose accuracy and resolution can compete with those obtained by the TLS systems (Rodríguez-Gonzálvez et al., 2014).

However, common strategies for the evaluation of the paintings presented in the rock art are limited to the use of decorrelation strategies (e.g. Decorrelation Strech-DS or principal component analysis-PCA) of images captured by RGB sensors (Cerrillo-Cuenca and Sepúlveda, 2015; Domingo et al., 2015) that only use the single radiometric response captured by the sensors. Although the use of orthoimages and unsupervised pixel-based classifications can provide a suitable solution (Rogerio-Candelera, 2015), the geometrical and radiometrical features of both products are not exploited or combined together to support the final solution. For instance, voids or topographic accidents can generate shadows that distort the multispectral classification results, requiring the use of additional strategies able to filter these problems.

A complete study of the paintings presented on a rock art shelter demands not only the evaluation of the painted or engraved signs, but also to record these signs through accurate 3D virtual models able to reproduce hypotetic situations such as: to simulate different illumination conditions or to analyse spatial geometrical relations (e.g. the relation between the depth an the areas painted) (Domingo et al., 2013).

According to remarked above, this paper presents a methodology for combining geometrical and radiometrical features in the evaluation of rock art paintings presented in a shelter using two different scales: (i) *a local scale*, looking over all those properties needed for a complete understanding of the traces presented for each motif; and (ii) *a global scale,* to evaluate the whole shelter and its spatial relationship with the existing motifs. To validate this approach, a phase-shift laser scanner (Faro Focus 120), a full frame reflex camera (Canon 5D) and a multispectral camera (Mini MCA 6) were applied in the evaluation of the painted sings presented in the Minateda Great shelter (Albacete, Spain), one of the most important Levantine Rock art shelters (Breuil, 1920; Mas et al., 2013).

This paper has been organized in the following way: after this introduction, Section 2 presents the sensors and methods used during the evaluation of the rock-shelter; Section 3 shows the results of the proposed methodology and finally in Section 4 depicts the main conclusions.

2. Materials and methods

In this section the three geomatics sensors used in this work together with the approach developed are described.

2.1. Materials

2.1.1. Terrestrial laser scanner sensor: Faro Focus 120

Considering the complexity of the shelter as well as its difficult accessibility the TLS Faro Focus 120 (Table 1) was used.

Table 1
Faro Focus 120 technical specifications.

Physical principle	Phase shift
Field of view (degrees)	360 H x 320 V
Measurement range (m)	0.6 − 120
Accuracy nominal value at 25 m (mm)	2
Beam divergence (mrad)	0.19
Capture rate (points/sec)	122,000 / 976,000
Spatial resolution at 10 m (mm)	6
Wavelength (nm)	905 / near infrared
Radiometric resolution (bits)	11- bits

Due to the size of the shelter (19.59×3.65 m) evaluated, several TLS stations were considered, each one placed on an arbitrary local coordinate system. The registration of these stations into a common local coordinate system was performed using a coarse to fine strategy defined in Sánchez-Aparicio et al. (2014). As a result of this registration an accurate 3D representation of the shelter, in the near infrared band, was obtained.

2.1.2. Digital camera sensors: Canon 5D and Mini MCA-6

Two passive sensors were used and evaluated: a full frame RGB reflex digital camera (Canon 5D Mk II) and a multispectral digital camera (Mini MCA-6).

Equipped with a Canon EF 20 mm wide-angle lens, Canon 5D Mk II is a high resolution full frame reflex camera (Table 2) capable of capturing visible information in the following wavelengths: (i) Red-650 nm; (ii) Green-532 nm; and (iii) Blue-473 nm.

Regarding the multispectral sensor, a lightweight Multiple Camera Array (Mini MCA-6) was used. This sensor includes a total of 6 individual CMOS sensors with filters for the visible and near infrared spectrum (NIR) (Table 3), allowing the acquisition of a wide range of wavelengths: (i) Green-530 nm; (ii) Red1–672 nm; (iii) Red2–700 nm; (iv) NIR1–742 nm; (v) NIR2–778 nm; and (vi) NIR3–801 nm.

2.2. Methodology

In the present study case a standard SfM procedure, implemented in the photogrammetric software GRAPHOS (González-Aguilera et al., 2016), was applied for the photogrammetric 3D model generation, comprising the following stages: (i) automatic extraction and key-point matching; (ii) hierarchical orientation of images; and (iii) dense point cloud generation.

As a result, a dense and accurate point cloud can be obtained from the multiple images acquired where each pixel in the image renders a 3D point of the object.

Given the high density of points provided by both approaches (laser scanning and SfM) the orthogonal projection of these points provides the generation of digital images with metric values (orthoimages), corrected from geometrical distortions and perspective effects. Based on these orthoimages pixel-based classification strategies were applied through the use of statistical methods (e.g. Maximum Likelihood or Fuzzy k-means algorithms), which deal with multispectral bands to ex-

Table 2
Canon 5D Mk II technical specifications.

Sensor type	CMOS
Sensor size (mm)	36 × 24
Image size (pixels)	5616 × 3744
Geometric resolution (Mp)	21.1
Pixel size (μm)	6.4
Focal length (mm)	20
Radiometric resolution	14 bits
Channels	Red, Green, Blue

Table 3
Mini MCA-6 technical specifications.

Sensor type	CMOS
Sensor size (mm)	6.7 × 5.3
Image size (pixels)	1280 × 1024
Geometric resolution (Mp)	1.3
Pixel size (μm)	5.2
Focal length (mm)	9.6
Radiometric resolution	10 bits

tract informational classes from the orthoimages generated, allowing more flexibility and less user interaction than decorrelation methods.

Although pixel-based approaches provide more flexibility and less user interaction than decorrelation methods, they can be influenced by the presence of geometrical accidents such as voids, elevation or cracks, causing the creation of local shadows and thus disturbing the final classification results. Geometrical accidents can be related with local changes in the curvature of the rock surface or even with roughness changes. According with these assumptions and considering the flexibility provided by the pixel-based methods, the Gaussian curvature (Magid et al., 2007) as well as the roughness of the point cloud were considered to support the pixel-based classification. Regarding the roughness, several local PCA analysis were carried out with the aim of extracting the direction of minimum dispersion (first Eigen-vector) which corresponds with the normal of the points considered (Rodríguez-Martín et al., 2016). Later the roughness is estimated evaluating the distance between the plane, defined with the centroid of the point cloud and the first Eigen vector, and each point considered.

It is worth mentioning, that the classification of pixels according with their radiometrical and geometrical response is not the only requirement to evaluate the rock art paintings. Geometrical components, such as the distribution of motifs along the shelter, the spatial relation between motifs, the influence of the topographic accidents in the traces of motifs, or the relation between the shelter depth and the motifs distribution are aspects that have been analyzed. More precisely, the evaluation of the digital depth model and its contour lines associated were used to analyse the motifs traces and its relationship with the main contour lines. In addition, the digital depth model and its 3D model were used to analyse the spatial distribution of motifs along the shelter and also to simulate virtual viewpoints of the shelter and the motifs with different lightning conditions.

A graphical summarize of the whole process is shown in Fig. 1.

3. Experimental results

3.1. Minateda rock-shelter

Located in the Archeological Park of Tolmo de Minateda near the city of Hellín, within the province of Albacete (Spain), Minateda Great Shelter is placed on a strategic area between the West and East part of the Iberian Peninsula (Montés, 2010) (Fig. 2). This localization gives the shelter a blending of different artistic tendencies. Showing more than 400 motifs painted on a Miocenic biocalcerinite formation, with a total length of 20 m and 8 m of height. Inside this space, several narrative natural scenes are presented, as well as motifs of hunting and battles (Breuil, 1920), establishing the Minateda Great Shelter as one of the most important Spanish Levantive rock-art shelter (Mas et al., 2013).

3.2. Multispectral point clouds

According with the sensors used, two point clouds were generated: (a) Laser scanning point cloud and (b) Multispectral photogrammetric point cloud.

Regarding the laser scanning, eight laser stations were required and aligned using a coarse-to fine, comprising the following stages: (i) pair-wise registration through the Iterative Closest Point (ICP) algorithm (Besl and McKay, 1992) and (ii) a global registration by means of the Generalized Procrustes Analysis (GPA) (Toldo et al., 2010), using the ICP registration as initial approximation. As a result, a complete 3D point cloud of the rock-shelter in the near infrared (905 nm) with a total of 82,244,854 points and a registration error of 0.003±0.001 m, was obtained.

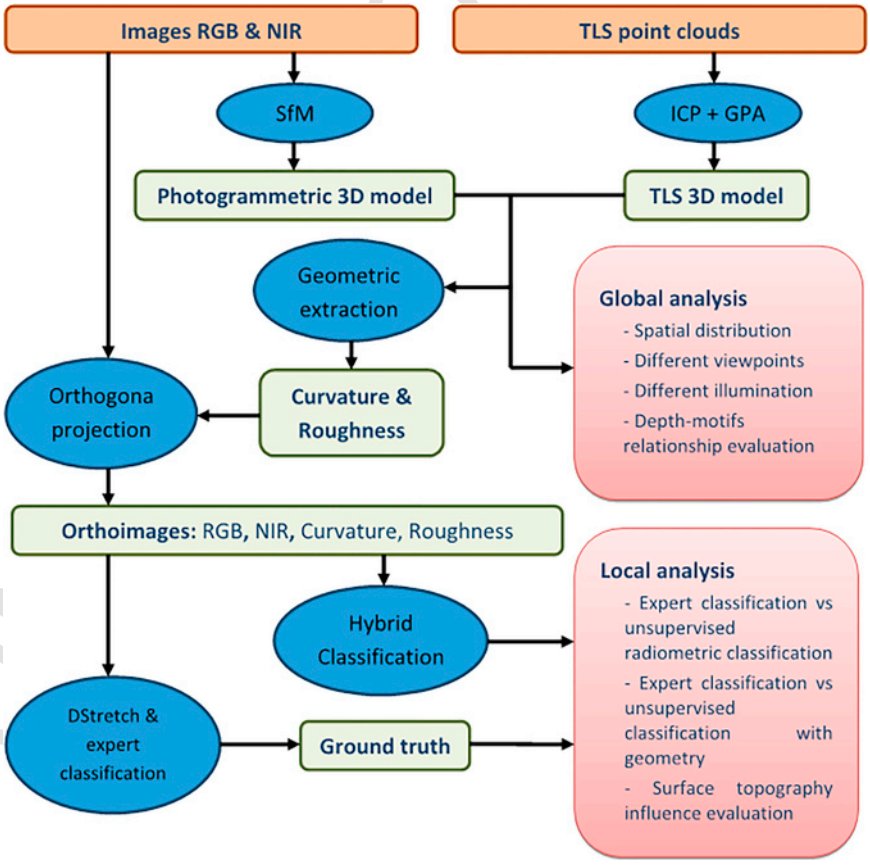

Fig. 1. Workflow for the proposed methodology.

Fig. 2. Case study area: Great shelter of Minateda (Spain).

Regarding the photogrammetric point clouds, one of the main milestones of the photogrammetric technique is its flexibility to cope with different spectral bands captured with different sensors. However, deal with different sensors requires taking into account the following considerations:

- Type of sensor. Meanwhile the Canon 5D presents a unique Bayer sensor, the Mini MCA-6 camera shows six different CMOS sensors with specific filters and lenses. Each MCA camera station is composed by 6 images with different intrinsic (principal distance, principal point and lens distortion) and extrinsic (location and orientation) parameters. According with Kraus (2007), the baseline between stations is a critical factor in the final accuracy of the photogrammetric point cloud. Therefore, introduce in the photogrammetric adjustment the different channels of the multispectral camera would provide an unsuitable base to ratio value. With the aim of optimizing this problem, only the fifth channel (lower-center cone) of the multispectral camera was considered for the photogrammetric reconstruction, registering the rest of the channels against this one. To this end, the following workflow was applied: (i) Geometrical calibration of the images; (ii) Key-point extraction and matching and (iii) Affine transformation. As a result, several multiband images were obtained, corrected from geometrical distortions and registered in relation with the fifth channel, throwing a mean registration error of 0.79±0.52 pixels.
- Photogrammetric network design. Guarantee quality in the 3D photogrammetric models requires of planning a good photogrammetric stations distribution (i.e. network). In particular, two different groups of images were considered: (i) parallel images and (ii) convergent images. 215 images were acquired with the Canon 5D, whereas 90 images were taken with the Mini MCA-6. Regarding the MCA-6 sensor, the images acquired were focused on the painted area of the shelter.
- Multimodal matching. Since the approach developed requires the use of algorithms able to extract and matching keypoints at different spectrums (i.e. images coming from different wavelengths), a modification of the usual features extraction method (Lowe, 1999), was applied. More precisely, the keypoint detector and descriptor MSD (Tombari and Di Stefano, 2014) and SURF (Bay et al., 2008) were applied, respectively, using a robust matching strategy implemented in the software GRAPHOS.

Finally, multispectral and RGB images captured by MCA-6 and Canon 5D, respectively, were used as input in the SfM workflow using GRAPHOS software. Regarding MCA images, null values were considered for the distortion parameters and the principal point (these values remain fixed during the SfM approach).

During the first phase (orientation) a sparse point cloud composed by 101,122 keypoints was obtained. Concerning the scaling of the point cloud, 7 control points and 5 check points were used from the laser scanning point cloud using artificial targets (Fig. 3) (Table 4).

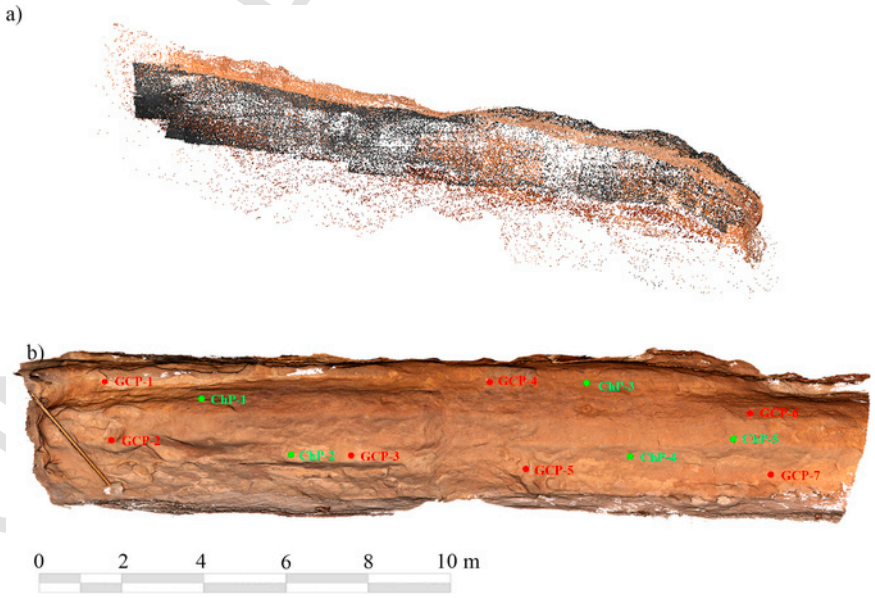

Fig. 3. Results obtained during the SfM approach: (a) Sparse point cloud obtained during the orientation; and (b) 3D dense point cloud and distribution of the control points (in red colour) and check points (in green colour). (For interpretation of the references to color in this figure legend, the reader is referred to the web version of this article.)

Table 4
RMSE and errors obtained during the photogrammetric reconstruction.

Point name	*X* error (mm)	*Y* error (mm)	*Z* error (mm)
ChP−1	−1.43	−0.19	1.53
ChP−2	5.99	−2.15	0.29
ChP−3	−4.43	−1.19	−0.96
ChP−4	0.51	−0.00	−0.63
ChP−5	0.18	−0.19	1.53
RMSE	3.40	1.96	1.09

Finally, a dense matching was carried out by means of the MicMac algorithm (Pierrot-Deseilligny et al., 2015) obtaining as a result a dense and photorealistic point cloud of the rock-shelter, whose quality (0.003±0.001 m) and density (74,457,717 points) is similar to the one provided by the TLS point cloud (82,244,854 points) (Fig. 4) (Fig. 5).

3.3. Unsupervised pixel-based classification for the extraction of motifs

Due to the large number of bands as well as the complexity and extension of the rock-shelter, three test areas (A, B, C) were used for the evaluation of the best band combination. These areas were considered according to the geometrical accidents presented on it. For the test area

Fig. 4. Graphical comparison between point clouds: (a) coming from TLS; and (b) coming from digital camera.

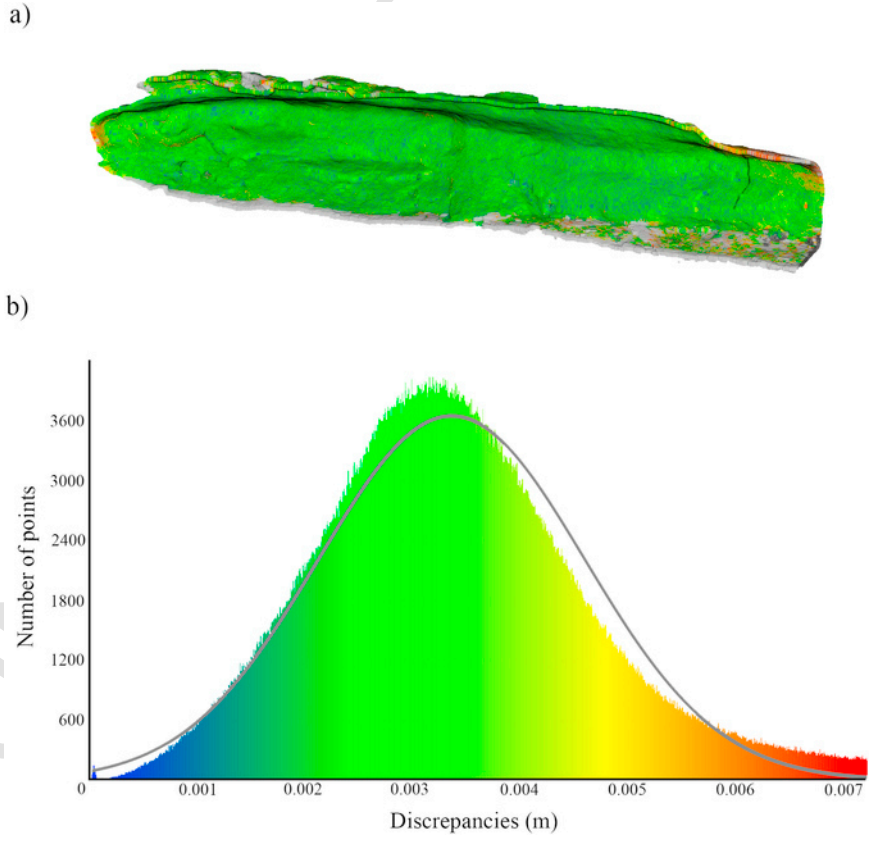

Fig. 5. Geometrical discrepancies between the laser and photogrammetric point cloud: (a) Comparison between 3D models (laser vs. photogrammetry); and (b) histogram of errors distribution.

A is possible to observe the presence of voids inside and near the motifs; for the test area B the voids are near the motif; and for the test area C no voids are near or inside the motif (Fig. 6).

Obtained the different radiometric bands (a total of 9 images with a 2 mm of GSD), a pixel-based classification was performed using the multispectral orthoimages as input data (Fig. 7). Since each sensor encloses its own resolution, the multispectral orthoimages were homogenized to a 2 mm resolution. The non-supervised Fuzzy-k-means algorithm was used following the next combination of bands: (i) 1st band from laser scanner (LS band); (ii) 2nd 3rd and 4th bands from Canon 5D (5D band); and (iii) 5th, 6th, 7th, 8th, 9th and 10th bands from Mini MCA-6 (MCA-6 band).

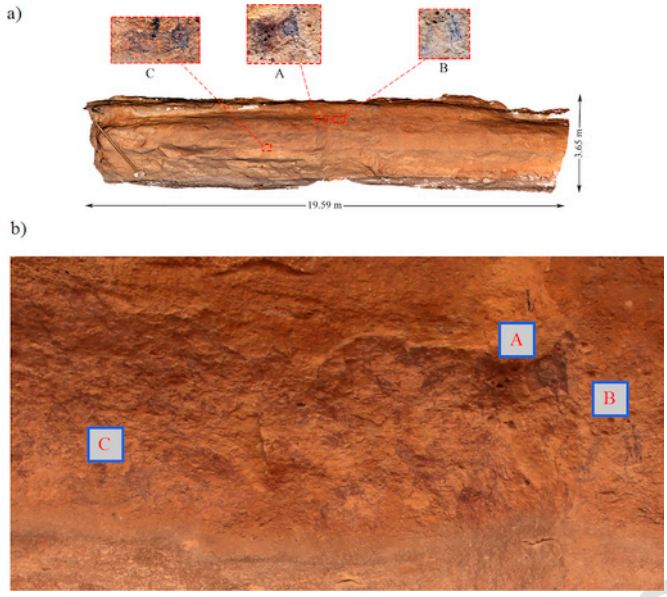

Fig. 6. Test areas (A, B, C) used during the evaluation of bands. (a) Distribution within the shelter; (b) Detail of the test area.

During the first phase of the radiometric analysis, which considers only the radiometric response captured by the different sensors, two informational classes were evaluated: Motif and Background. Complementary to this, the results obtained using decorrelation of RGB channels by means of the Decorrelation Stretch algorithm (Le Quellec et al., 2015) supported by a manual classification of an expert were considered as ground truth. This algorithm transforms the initial colour values through the Kafhumen-Loève theorem, reducing the correlation between the RGB channels of the camera and remarking the differences between the radiometric information captured by the spectral bands. Decorrelated the RGB channels, a manual classification of the results, by an expert, was carried out (Fig. 8).

According with the results obtained (Table 5) (Fig. 8), it is possible to observe that, topographic accidents such as voids are classified in the same class than the motif class, being more evident in the passive bands (5D and MCA-6) (Fig. 8). This comes to reinforce the need to use additional layers able to detect and classify the voids as well as other geometrical accidents.

Geometrically, rock areas affected by the presence of cracks or voids are characterized by local changes of curvature and/or roughness. Considering this assumption, a hybrid classification, combining the radiometry and the geometry of the areas evaluated was carried out. To this end, the geometrical operators defined in Section 2.2, Gaussian curvature and roughness, were used.

According with this new consideration, a total of three informational classes were taken into account: Motif; Background and Geometrical accidents. Previously to the hybrid classification, a sensitivity analysis was performed testing the influence of the kernel size used to generate this geometrical information.

The results of the sensitivity analysis suggest that the best kernel size for the roughness and Gaussian curvature is 0.05 m. Extracted the geometrical information of the test areas, a projection of these values on to the orthoimages was performed, obtaining as a result two addi-

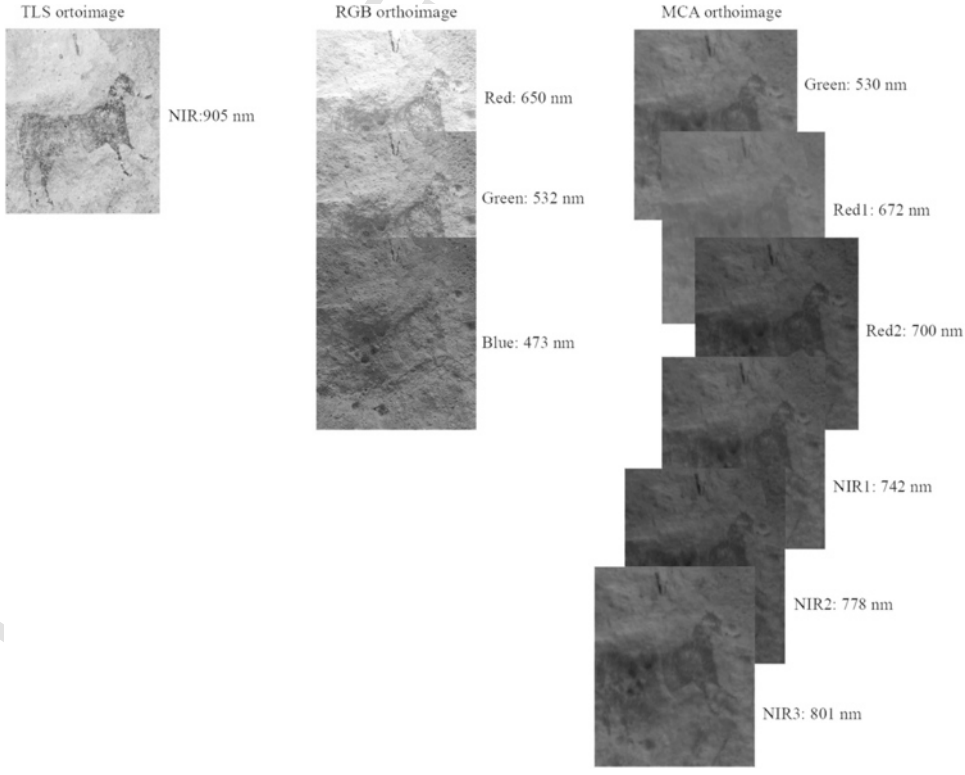

Fig. 7. Graphical representation of the different multispectral orthoimages generated.

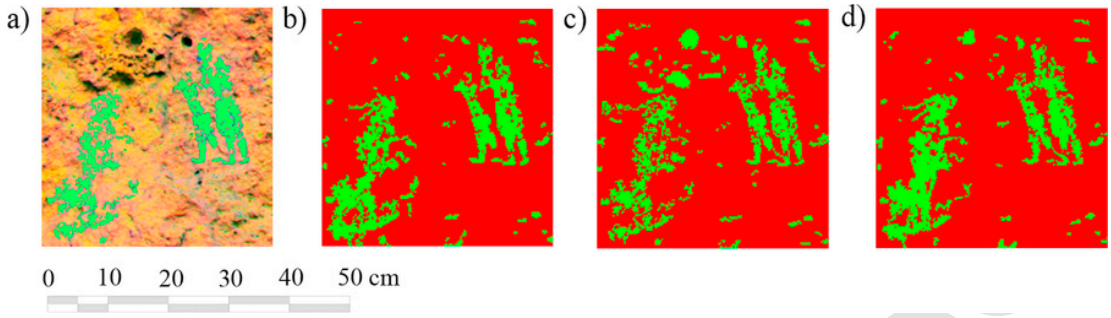

Fig. 8. Results obtained during the first phase for the test area B: (a) Decorrelation; (b) LS band; (c) 5D band and (d) MCA-6 band. Red pixels correspond with the background informational class and green pixels with the motif informational class. (For interpretation of the references to color in this figure legend, the reader is referred to the web version of this article.)

Table 5
Percentage of pixels belonging to the motif informational class.

Method	Sensor	A (%)	B (%)	C (%)
Decorrelation (Ground Truth)	Canon 5D	15.60	10.64	19.28
Unsupervised classification	Laser Scanner	17.89	15.59	20.40
	Canon 5D	17.88	15.37	19.37
	Mini MCA − 6	18.07	15.77	18.98

tional layers registered in the same coordinate system than the rest of the bands. These additional bands enclose the geometrical information of the motifs and its surroundings (Fig. 9) (Table 6) (Table 7).

Finally and extracted the three thematic classes, a minimum user interaction was required with the aim of classifying all those connected groups presented in the geometrical accidents class to the motif or background classes (Table 8).

With the aim of evaluating the performance of the results obtained during the different classifications carried out, two quality analysis were used: (i) quantitative analysis to evaluate the number of pixels classified as motif; and (ii) qualitative analysis, observing the similarity between the motif traces extracted with the decorrelation strategy and those extracted with the unsupervised classifications.

On this basis, it is possible to observe an overall improvement of the results obtained during the unsupervised classification adding geometrical layers (Table 9) (Fig. 10). In particular, for test areas A and B, important quantitative and qualitative improvements were observed. For test area C, no improvement was observed on the quantitative results, meanwhile an improvement from the qualitative point of view was obtained. Regarding the geometrical bands used (roughness and curvature), both bands show a similar performance, being slightly better in the roughness case.

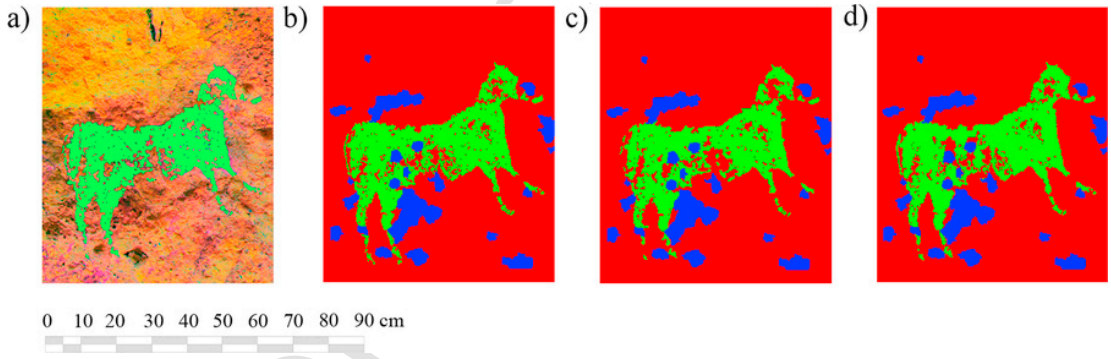

Fig. 9. Multispectral classification combining radiometrical and the roughness band in test area A: (a) Decorrelation; (b) LS band; (c) 5D band; and (d) MCA-6 band. Red colour represents the background, green colour the motif; and blue colour the geometrical alterations on the rock surface. (For interpretation of the references to color in this figure legend, the reader is referred to the web version of this article.)

Table 6
Percentage of pixels belonging to each informational classes (combining radiometric and roughness bands).

Class	Test area	Decorrelation	LS	5D	MCA-6
Background	A	–	76.93	77.93	76.89
	B	–	79.73	82.49	79.80
	C	–	78.88	79.71	80.08
Motif	A	15.60	15.75	14.74	15.78
	B	10.64	13.49	10.73	13.42
	C	19.28	19.99	19.16	18.79
Geometrical accidents (Roughness band)	A	–	7.33	7.33	7.33
	B	–	6.78	6.78	6.78
	C	–	1.13	1.13	1.13

Table 7
Percentage of pixels belonging to each informational classes (combining radiometric and curvature bands).

Class	Test area	Decorrelation	LS	5D	MCA-6
Background	A	–	81.58	82.50	81.63
	B	–	82.65	85.49	82.67
	C	–	77.87	78.53	79.01
Motif	A	15.60	15.84	14.92	15.79
	B	10.64	13.68	10.84	13.66
	C	19.28	19.97	19.31	18.83
Geometrical accidents (Curvature bands)	A	–	2.58	2.58	2.58
	B	–	3.67	3.67	3.67
	C	–	2.16	2.16	2.16

Table 8
Percentage of pixels belonging to Motif class after considering the geometrical bands (Roughness and Curvature).

Method	Sensor	Geometrical Layer	A (%)	B (%)	C (%)
Decorrelation	Canon 5D	–	15.60	10.64	19.28
Unsupervised classification	Laser Scanner	Roughness	16.45	11.78	19.99
		Curvature	16.49	11.84	19.97
	Canon 5D	Roughness	15.54	10.84	19.16
		Curvature	15.30	10.88	19.31
	Mini MCA − 6	Roughness	16.30	11.77	18.79
		Curvature	16.43	11.83	18.82

Table 9
Quantitative evaluation of the results obtained during the radiometric classification (initial stage) and its improvement with the geometrical layers (refined stage).

		Motif error (%)		
Sensor	Test area	Initial Stage	Refined Stage Roughness	Refined Stage Curvature
Laser Scanner	A	14.68	5.40	5.83
	B	44.20	12.69	13.23
	C	3.10	1.97	2.10
Canon 5D	A	14.60	0.23	0.73
	B	42.14	0.22	0.25
	C	5.50	5.35	6.06
Mini MCA − 6	A	15.79	5.31	5.61
	B	45.85	13.34	13.14
	C	6.94	7.70	7.87

3.4. Spatial analysis of the Minateda´s rock-shelter

The identification of painted signs using the different bands that compose the orthoimages is not the only requirement for a complete documentation of the art presented in rock-shelters. Especially in Levantine rock-art where the representation of complex narrative scenes is presented (Walker, 1971).

Geometrical aspects such as the influence of accidents on the rock surface, the diagnosis of the rock shelter (Jordá Cerdá, 2009; Ripoll, 1963), the viewpoint from where the rock-art was conceived or the identification of potential compositions and scenes are aspects to be considered. These aspects can be analyzed through the evaluation of the geometrical features presented in the point cloud at different scales: motif scale and rock-shelter scale.

3.4.1. Analysis of geometric aspects at motif scale

Trying to find a relationship between the detailed rock surface reconstructed and the selection of the areas where the motifs were painted, it could be observed a relationship between the topographic accidents presented and the direction of some of the traces, as well as the morphology of the motifs painted.

Considering the results provided by the pixel-based classification, as well as the geometrical information provided by the digital depth models, we can to relate the traces presented in the motif with the topographic accidents presented in the rock surface. Particularly, the following steps were implemented: (i) traces extraction based on Canny operator (Canny, 1986); (ii) contours lines creation and segmentation with an interval of 5 mm; and (iii) distance evaluation between the motif trace and each contour curve using a threshold of 2 cm. As a result, and after the traces and contour lines extraction, all those edge pixels with a separation higher than 2 cm from the contour line were rejected. Finally, all those groups of connected pixels with less than 50 pixels (about 10 cm) were excluded since they can be considered as non-representative (Fig. 11).

It is possible to observe that part of the horse anatomy (test area A) is influenced by the rock-surface (Fig. 12).

3.4.2. Analysis of geometric aspects at shelter scale

On the other hand, a global analysis of the compositions presented, such as the geometrical disposition of the scene narrated or the relation between the depth of the shelter and the motifs presented on it, are important aspects to understand the rock art presented on the shelter. According with these needs, the following steps were applied: (i) point cloud decimation; (ii) PCA alignment of the point cloud; (iii) depth, roughness and curvature evaluation; (iv) mesh creation; (v) projection of the results obtained during the radiometric and geometric classification; and (vi) evaluation at global level.

Due to the large amount of data captured (82,244,854 points for the laser scanning and 74,457,717 points for the photogrammetry), a previous decimation of the point cloud was required. To this end a density filter, with a threshold value of 0.01 m, was applied to pass from

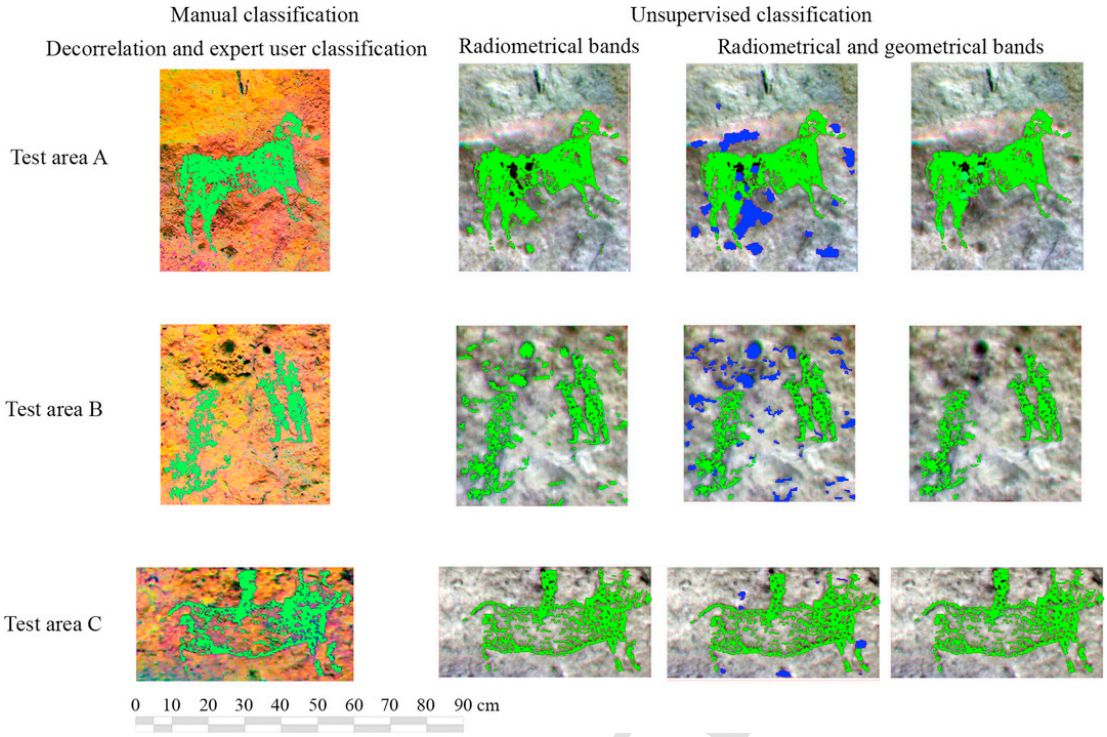

Fig. 10. Qualitative analysis of the results obtained along the different radiometric analysis carried out with Mini MCA-6 multispectral camera (false colour made with bands 10th-5th-7th).

the raw point cloud to an optimized one, composed by 9,226,243 points in the case of the laser scanning point cloud and 11,286,665 points for the photogrammetric one, representing around the 10% of the original point clouds.

The simplified point clouds obtained by the photogrammetric or laser scanning were referencing in a local coordinate system considering the *X* axis aligned with respect to the longitudinal axis of the rock-shelter, enabling an evaluation between the depth of the shelter and the motifs presented. More precisely, a PCA analysis of the point cloud was carried out, obtaining the direction of maximum dispersion (third Eigen-vector), which corresponds with the longitudinal axis of the shelter. Later, a depth analysis of the shelter was carried out considering a vertical plane along the longitudinal axis of the rock shelter as comparison plane (Fig. 13b).

Since meshes are considered as an ideal product to visualize and consult information derived from geomatic sensors, the simplified and aligned point clouds are converted into meshesusing the Poisson surface reconstruction algorithm (Kazhdan et al., 2006). As a result, a 3D mesh of the rock shelter was obtained with 1,286,637 triangles in the case of the Laser Scanner model and 861,581 triangles for the photogrammetric one. Finally, the information extracted during the radiometric (Fig. 13a) and geometric analysis (Fig. 13b) was mapped over the mesh, allowing the analysis of the possible relationships between the different layers considered: motifs and depth layers.

Due to the large number of motifs presented and since the main focus of the present paper is to highlight the potentialities offered by the proposed method, only a partial mapping of the motifs presented in the shelter was performed. It should be noted that motifs mapped are close to the most protected part of the shelter (Fig. 13b) with an average height of 3.20 m with respect to the rock shelter base. Values higher than the average stature of a Neolithic man (1.65 m) (Ehler and Vancata, 2009). However, the topography presented on the rock-shelter, with a concavity in its central part (Fig. 13b), could be used to paint at this height, since the mean distance between the concavity of the rock shelter and the paintings is 1.20 m. Note also that this area corresponds to a full illuminated area at night, considering a bonfire placed on its central part (Fig. 14a).

As exposed Domingo et al. (2013), one of the main limitations that present traditional two-dimensional techniques for the analysis of rock-art paintings is the difficulty for obtaining different viewpoints and analyses the motifs painted on the shelter, especially in those large and complex caves or shelters. This limitation can be solved with the use of the proposed method, being possible to evaluate the shelter from different viewpoints (Fig. 14b).

4. Conclusions

In this paper a new approach based on the combination of radiometrical and geometrical features for the evaluation of rock art paintings has been presented. The density, accuracy and the radiometric values of the point clouds captured by geomatic sensors such as laser scanner systems, RGB and multispectral cameras can be used to evaluate the motifs presented on a scene at local and global level.

Our approach requires less user interaction in comparison with common practices (Decorrelation Stretch or PCA analysis), being possible to work not only with multispectral data, but also with the geometry of the evaluated areas and allowing the extraction of voids or cracks. Regarding the geometric layers, roughness and Gaussian curvature, both prove to be efficient strategies improving the results obtained during the pixel-based classification: from an average accuracy of 84.98% (test area A), 55.94% (test area B) and 94.82% (test area C) to 96.15%, 91.15% and 94.83%, respectively. With respect to the sensor used, the best results were observed in those classifications that use the Canon 5D bands, probably due to the similarity between the channels used during the Decorrelation Stretch and the pixel-based classification, but also because the analog-to-digital conversion is performed in 14 bits per colour, a substantial increase from the 11 bits of the laser Faro Focus. In addition, the on-chip RGB colour filter uses a standard Bayer pattern over the sensor elements which prevents the false colour and the presence of noise.

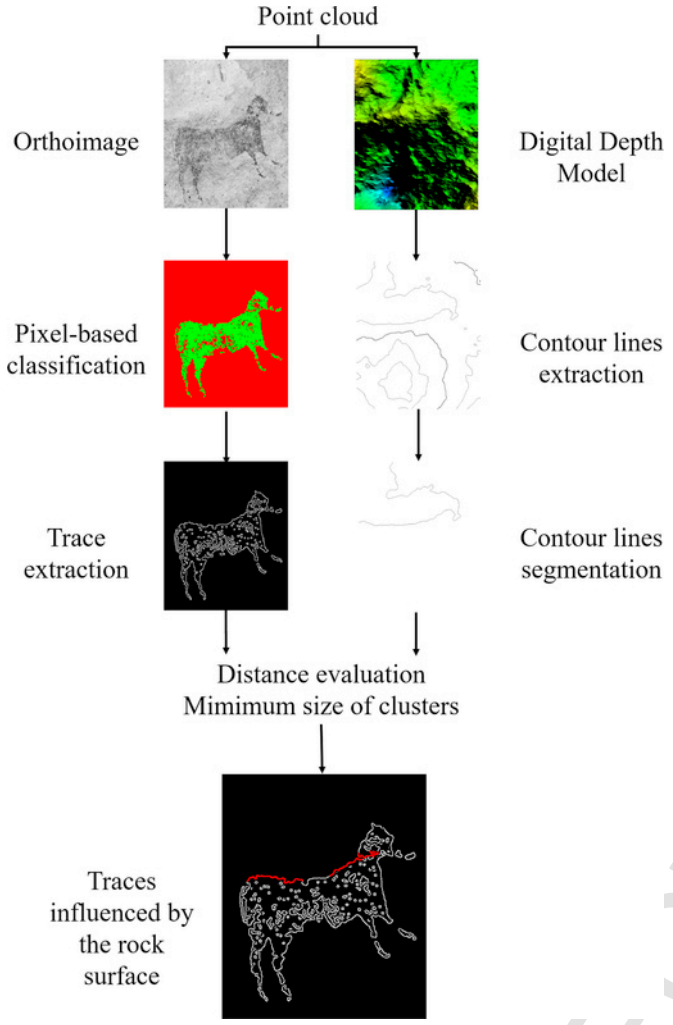

Fig. 11. Schematic representation of the analysis of geometric aspects at motif scale and applied to test area A.

Additionally to these geometrical strategies, the present article presents a method able to relate the topographic accidents presented on the rock surface with the quality of the traces is presented, increasing the wide variety of useful information that can be extracted through the proposed method, such as the relation between the rock shelter depth and the location of motifs. All this information can be visualized and consulted easily through the use of a multilayer mesh model.

Inside this wide variety of features (radiometric and geometric) that can be extracted by the proposed method, further investigations could be focused on the dissemination through 3D printed models or the analysis through time by means of 3DGIS tools, as well as the evaluation of other pathological processes such as the presence of biological organisms.

Acknowledgements

This paper has been developed in the framework of the research project "Infraestructura de datos espaciales de patrimonio arqueológico de Castilla-La Mancha" (POII-2014-004-P) of the 2014–2017 Scientific Research Projects cofounded by the European Regional Development Fund.

The authors would like to thank the Ministry of Education, Culture and Sport of Castilla-La Mancha. Especially to the Directorate-General for Universities, Research and Innovation, the Directorate-General for Cultural and the Museum of Albacete. Authors would also like to thank Lorenzo Abad Casal (University of Alicante), Sonia Gutiérrez Lloret (University of Alicante), Rubí Sanz Gamo (Museum of Albacete) and Blanca Gamo Parras (Museum of Albacete) for their valuable support during the course of this study.

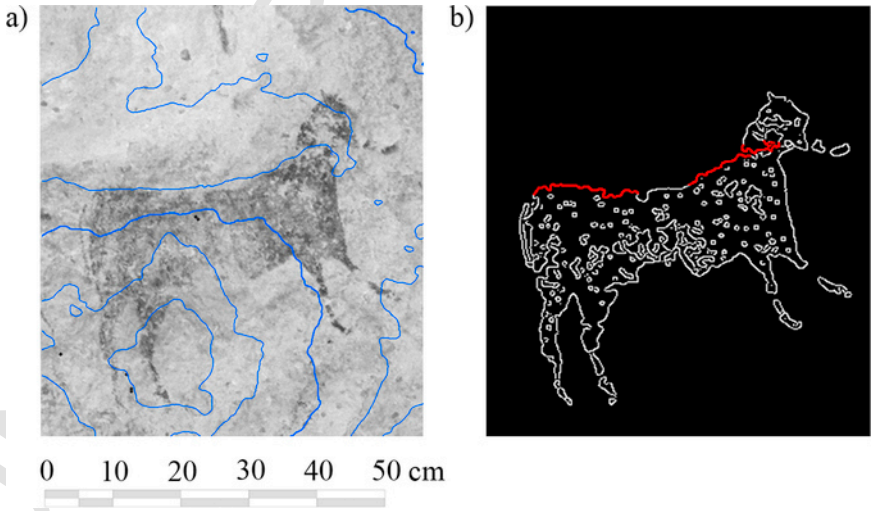

Fig. 12. Results obtained in test area A during the evaluation of the influence of topographic accidents in the horse anatomy.

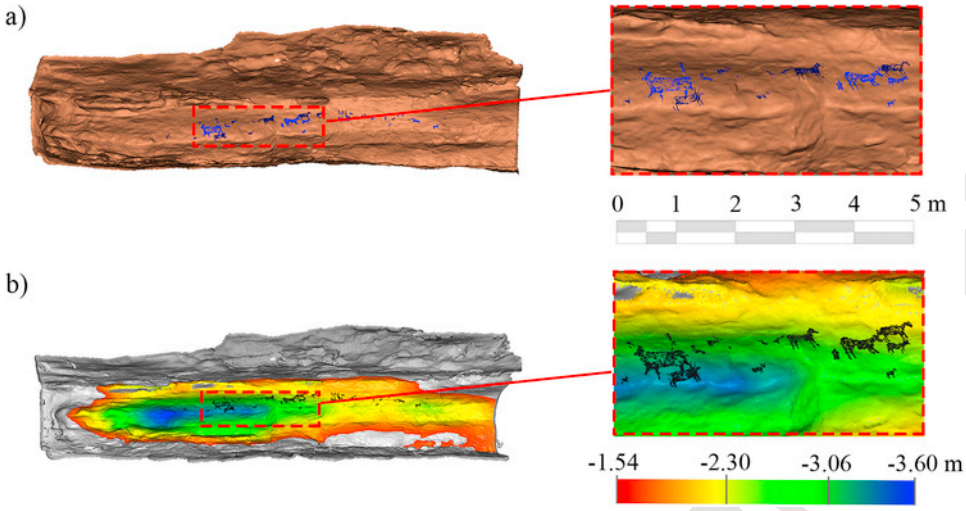

Fig. 13. Mapping of the information obtained during the radiometric and geometric analysis: (a) Partial reconstruction of the motifs presented in the rock-shelter; (b) Visualization of the relationship between the depth and the motifs presented in the rock shelter.

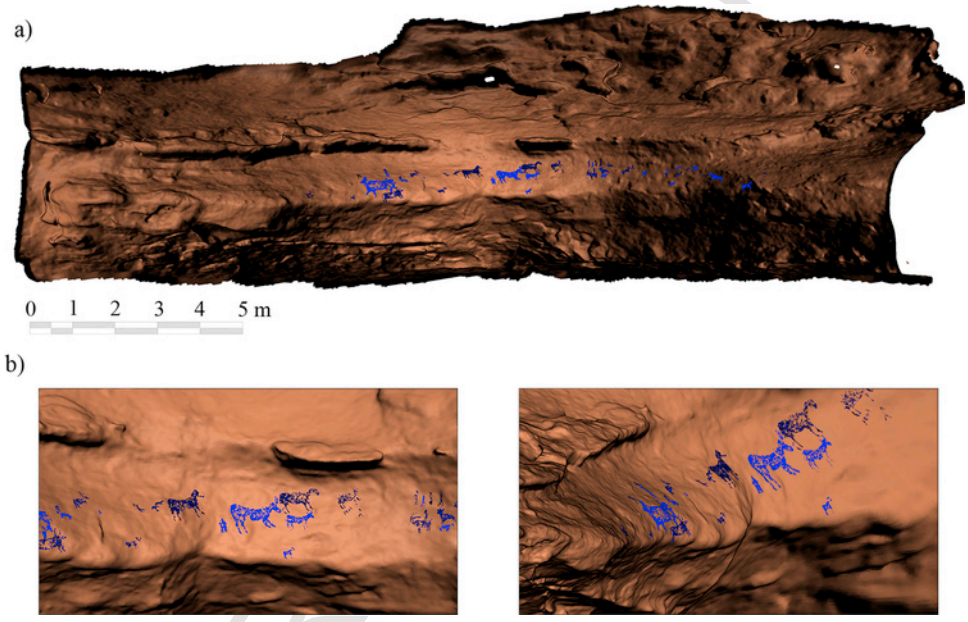

Fig. 14. Different simulations carried out with the model obtained: (a) Simulation of the rock shelter during the night and with a bonfire on the middle; (b) Perspective views from different points during the simulated scene.

References

Aguilera, D., Lahoz, J., Finat, J., Martinez, J., Fernandez, J., San Josem, J., 2006. Terrestrial laser Canning and low-cost aerial photogrammetry in the archeological modeling of a Jewish tanneries, ISPRS Commission V Symposium Image Engineering and Vision Metrology, Dresden. Citeseer, p. 27.

Azema, M., Gely, B., Bourrillon, R., Lhomme, D., 2013. La grotte ornée paléolithique de Baume Latrone (Gard, France): la 3D remonte le temps…. Palethnologie n°5, 244–246.

Bay, H., Ess, A., Tuytelaars, T., Van Gool, L., 2008. Speeded-up robust features (SURF). Comput. Vision. Image Underst. 110, 346–359.

Besl, P.J., McKay, N.D., 1992. Method for registration of 3-D shapes, Robotics-DL tentative. Int. Soc. Opt. Photonics 586–606.

Bourdier, C., Fuentes, O., Pinçon, G., 2015. Contribution of 3D technologies to the analysis of form in late palaeolithic rock carvings: the case of the Roc-aux-Sorciers rock-shelter (Angles-sur-l'Anglin, France). Digit. Appl. Archaeol. Cult. Herit. 2, 140–154.

Breuil, H., 1920. Les peintures rupestres de la péninsule Ibérique: Les roches peintes de Minateda (Albacete). XI. Masson et Cie.

Burens, A., Grussenmeyer, P., Guillemin, S., Carozza, L., Bourrillon, R., Petrognani, S., 2011. Numérisation 3D de la grotte des Fraux (Saint-Martin-de-Fressengeas, Dordogne, France): approche multiscalaire. In: Jaillet, S., Ployon, E., Villemin, T. (Eds.), Images et modèles 3D en milieux naturels.. Edytem, université de Savoie, Chambery, pp. 183–190 (Collection Edytem, no 12).

Canny, J., 1986. A computational approach to edge detection. IEEE Trans. Pattern Anal. Mach. Intell. 679–698.

Cefalu, A., Abdel-Wahab, M., Peter, M., Wenzel, K., Fritsch, D., 2013. Image based 3D reconstruction in Cultural heritage preservation. ICINCO 1, 201–205.

Cerrillo-Cuenca, E., Sepúlveda, M., 2015. An assessment of methods for the digital enhancement of rock paintings: the rock art from the precordillera of Arica (Chile) as a case study. J. Archaeol. Sci. 55, 197–208.

Defrasne, C., 2014. Digital image enhancement for recording rupestrian engravings: applications to an alpine rockshelter. J. Archaeol. Sci. 50, 31–38.

Del Pozo-Aguilera, S., Herrero-Pascual, J., Felipe-García, B., Hernández-López, D., Rodríguez-Gonzálvez, P., González-Aguilera, D., 2016. Multispectral Radiometric Analysis of Façades to Detect Pathologies from Active and Passive Remote Sensing. Remote Sens. 8, 80.

Domingo, I., Villaverde, V., López-Montalvo, E., Lerma, J.L., Cabrelles, M., 2013. Latest developments in rock art recording: towards an integral documentation of Levantine rock art sites combining 2D and 3D recording techniques. J. Archaeol. Sci. 40, 1879–1889.

Domingo I. Carrión B. Blanco S. Lerma J.L. 2015. Evaluating conventional and advanced visible image enhancement solutions to produce digital tracings at el Carche rock art shelter Digit. Appl. Archaeol. Cult. Herit. 2 79–88

Ehler, E., Vancata, V., 2009. Neolithic transition in Europe: evolutionary anthropology study. Anthropologie 47, 185.

Fernández-Hernandez, J., González-Aguilera, D., Rodríguez-González, P., Mancera-Taboada, J., 2015. Image-Based Modelling from Unmanned Aerial Vehicle (UAV) Photogrammetry: an Effective, Low-Cost Tool for Archaeological Applications. Archaeometry 57, 128–145.

Fritz, C., Willis, M.D., Tosello, G., 2016. Reconstructing Paleolithic cave art: the example of Marsoulas cave (France). J. Archaeol. Sci.: Rep.

Gomez-Lahoz, J., Gonzalez-Aguilera, D., 2009. Recovering traditions in the digital era: the use of blimps for modelling the archaeological cultural heritage. J. Archaeol. Sci. 36, 100–109.

González-Aguilera, D., López-Fernández, L., Rodriguez-Gonzalvez, P., Guerrero, D., Hernandez-Lopez, D., Remondino, F., Menna, F., Nocerino, E., Toschi, I., Ballabeni, A., Gaiani, M., 2016. DEVELOPMENT OF AN all-purpose free PHOTOGRAMMETRIC tool. Int. Arch. Photogramm. Remote Sens. Spat. Inf. Sci. XLI-B6, 31–38.

Herbert, D.T., 1995. Heritage, tourism and society. Mansell Publishing.

Jordá Cerdá, F., 2009. Formas de vida económica en el arte rupestre levantino.

Kazhdan, M., Bolitho, M., Hoppe, H., 2006. Poisson surface reconstruction, In: Proceedings of the fourth Eurographics symposium on Geometry processing.

Kraus, K., 2007. Photogrammetry: geometry from images and laser scans. Walter de Gruyter.

Le Quellec, J.-L., Duquesnoy, F., Defrasne, C., 2015. Digital image enhancement with DStretch: is complexity always necessary for efficiency?. Digit. Appl. Archaeol. Cult. Herit.

Lejeune, M., 1985. La paroi des grottes, premier "mur" support artistique et document archéologique. Le mur dans l′art et l′archéologie. Art. Et. Fact., n°2. Liège 15–24.

Lerma, J.L., Navarro, S., Cabrelles, M., Seguí, A.E., Hernández, D., 2013. Automatic orientation and 3D modelling from markerless rock art imagery. ISPRS J. Photogramm. Remote Sens. 76, 64–75.

López-Montalvo, E., Sanz, I.D., 2005. Nuevas tecnologías y restitución bidimensional de los paneles levantinos: primeros resultados y valoración crítica del método, Actas del III Congreso del Neolítico en la Península Ibérica: Santander, 5 a 8 de octubre de 2003. Serv. De. Publ. 719–728.

Lowe, D.G., 1999. Object recognition from local scale-invariant features, Computer vision, 1999. In: Proceedings of the seventh IEEE international conference on. Ieee, pp. 1150–1157.

Magid, E., Soldea, O., Rivlin, E., 2007. A comparison of Gaussian and mean curvature estimation methods on triangular meshes of range image data. Comput. Vision. Image Underst. 107, 139–159.

Mas, M., Jorge, A., Gavilán, B., Solís, M., Parra, E., Pérez, P.-P., 2013. Minateda rock shelters (Albacete) and post-palaeolithic art of the Mediterranean Basin in Spain: pigments, surfaces and patinas. J. Archaeol. Sci. 40, 4635–4647.

Pierrot-Deseilligny, M., Rupnik, E., Girod, L., Belvaux, J., Maillet, G., Deveau, M., Choqueux, G., 2015. MicMac, Apero, Pastis and Other Beverages in a Nutshell. ENSG, IGN, Champs-Sur-Marne, France.

Pinçon G., Bourdier C., Fuentes O., Abgrall A., 2010. De la manipulation des images 3D. In: In Situ [En ligne], 13.

Puchol, O.G., McClure, S.B., Senabre, J.B., Villa, F.C., Porcelli, V., 2013. Increasing contextual information by merging existing archaeological data with state of the art laser scanning in the prehistoric funerary deposit of Pastora Cave, Eastern Spain. J. Archaeol. Sci. 40, 1593–1601.

Ripoll, E., 1963. Pinturas rupestres de la Gasulla (Castellón). Monografías de Arte Rupestre. Arte Levantino 2.

Robert E., 2016. Le rôle du support dans la construction des images au sein l′art paléolithique européen, in Groenen (M., dir.), Styles, techniques and graphic expression in rock art, Actes de la session du 17ème congrès mondial de l′UISPP, British Archaeological Reports, pp. 174–195.

Robert, E., Petrognani, S., Lesvignes, E., 2016. Applications of digital photography in the study of Paleolithic cave art. J. Archaeol. Sci.: Rep.

Rodríguez-González, P., Garcia-Gago, J., Gomez-Lahoz, J., González-Aguilera, D., 2014. Confronting passive and active. Sens. Non-Gaussian Stat. Sens. 14, 13759.

Rodríguez-González, P., Nocerino, E., Menna, F., Minto, S., Remondino, F., 2015. 3D SURVEYING & modeling OF underground passages IN WWI FORTIFICATIONS. Int. Arch. Photogramm. Remote Sens 17–24.

Rodríguez-González, P., Mancera-Taboada, J., González-Aguilera, D., Muñoz-Nieto, , Armesto, J., 2012. A hybrid approach to create an archaeological visualization system for a Palaeolithic cave. Archaeometry 54, 565–580.

Rodríguez-Martín M. Rodríguez-González P. Lagüela S. González-Aguilera D. 2016. Macro-photogrammetry as a tool for the accurate measurement of three-dimensional misalignment in welding Autom. Constr. 71 189–197

Rogerio-Candelera, , 2015. Digital image analysis based study, recording, and protection of painted rock art. Some Iberian experiences. Digit. Appl. Archaeol. Cult. Herit. 2, 68–78.

Sánchez-Aparicio, L.J., Riveiro, B., Gonzalez-Aguilera, D., Ramos, L.F., 2014. The combination of geomatic approaches and operational modal analysis to improve calibration of finite element models: a case of study in Saint Torcato Church (Guimarães, Portugal). Constr. Build. Mater. 70, 118–129.

Sauvet G., Tosello G., 1998. Le mythe paléolithique de la caverne, in Sacco F., Sauvet G. dir., Le propre de l′homme, Psychanalyse et préhistoire, Paris, Delachaux et Niestlé, coll. Champs psychanalytiques, pp. 55–90.

Seidl, M., Wieser, E., Alexander, C., 2015. Automated classification of petroglyphs. Digit. Appl. Archaeol. Cult. Herit. 2, 196–212.

Toldo, R., Beinat, A., Crosilla, F., 2010. Global registration of multiple point clouds embedding the Generalized Procrustes Analysis into an ICP framework, 3DPVT 2010 Conference.

Tombari, F., Di Stefano, L., 2014. Interest Points via Maximal Self-Dissimilarities, Asian Conference on Computer Vision. Springer, pp. 586–600.

Torres-Martínez, J.A., Seddaiu, M., Rodríguez-González, P., Hernández-López, D., González-Aguilera, D., 2016. A multi-data source and multi-sensor approach for the 3D reconstruction and web visualization of a complex Archaelogical site: the case study of "Tolmo De Minateda". Remote Sens. 8, 550.

Walker, M., 1971. Spanish levantine rock art. Man 553–589.

Zeppelzauer, M., Poier, G., Seidl, M., Reinbacher, C., Breiteneder, C., Bischof, H., Schulter, S., 2015. Interactive segmentation of rock-art in high-resolution 3D reconstructions, 2015 digital heritage. IEEE 37–44.

4. CONCLUSIONES Y PERSPECTIVAS FUTURAS

4.1 CONCLUSIONES

Las investigaciones realizadas durante el desarrollo de esta Tesis Doctoral han permitido acometer satisfactoriamente los objetivos planteados inicialmente y realizar una aportación al desarrollo de las áreas de conocimiento en que se ha apoyado. Esta aportación ha sido materializada mediante la publicación en revistas de impacto especializadas de las metodologías y resultados obtenidos fruto de estas investigaciones. A continuación se comentan más detalladamente las conclusiones derivadas de estas investigaciones, así como las líneas de trabajo futuras que quedan abiertas como continuación de los trabajos aquí realizados.

Geotecnologías como la fotogrametría terrestre, la fotogrametría aérea y el láser escáner terrestre han sido empleadas en esta Tesis Doctoral, demostrando ser una solución rápida y precisa para la generación de modelos tridimensionales fotorrealísticos y ortofotografías verdaderas de alta resolución. Se ha probado además su adecuación para la documentación y monitorización de yacimientos arqueológicos, siendo aplicadas en diferentes escenarios e instantes. Se ha demostrado que cada una de las geotencologías empleadas presenta una serie de ventajas y de inconvenientes, siendo la solución idónea la combinación de todas ellas. Para ello, se ha visto que la base fundamental consiste en la correcta selección y materialización de un sistema de referencia común, por lo que se

hace imprescindible una minuciosa planificación de los trabajos de señalización y determinación del marco de referencia, teniendo en cuenta las particularidades de cada técnica, así como del instrumental a emplear.

Respecto al empleo de fotogrametría aérea, se ha demostrado que las plataformas aéreas como los vehículos aéreos no tripulados (UAVs) y aeronaves ligeras, como los paramotores, son complementarias pudiendo ser combinadas con la finalidad de obtener modelos tridimensionales multi-resolución adaptados a las necesidades de cada área de estudio. De esta manera, son aprovechadas las ventajas que presenta el paramotor, como son la capacidad de carga o la mayor velocidad y autonomía, y las ventajas que presentan los UAV, como son la capacidad de realizar tomas estáticas y oblicuas, el acceso a sitios remotos y la posibilidad de capturar imágenes de gran detalle a corta distancia.

El empleo de las plataformas aéreas mencionadas, junto con las técnicas terrestres fotogramétricas y de láser escáner, ha permitido no solo la optimización de la determinación geométrica, al obtener modelos multi-resolución, sino también una mejora en la captura de la información radiométrica, al emplear de forma óptima la metodología correspondiente a cada caso, esto es, la información aérea para la determinación y texturizado de planos horizontales y la información terrestre para el caso de planos verticales. Además, se ha mostrado como, junto con estas mejoras obtenidas en los procesos de captura de la información y generación de los productos geomáticos, también es posible mejorar los procesos de análisis y monitorización de yacimientos arqueológicos, haciendo para ello uso de las nuevas herramientas GIS3D. Como se ha visto, estas modernas herramientas abren al usuario un abanico de posibilidades como los análisis multi-

temporales o la integración de información 2D/3D (e.g. superposición de cartografía histórica sobre el modelo 3D).

Sin embargo, la obtención de productos geomáticos de alta resolución conlleva un elevado coste computacional, lo que ha llevado a emplear en este trabajo algoritmos que permiten obtener altos rendimientos mediante el empleo de la Unidad Gráfica de Proceso (GPU), reduciendo de esta forma los tiempos de computación y mejorando por tanto la eficiencia en el flujo de trabajo. Además, se ha mostrado como el empleo de técnicas de simplificación y optimización de nubes de puntos, y el uso del estándar WebGL, posibilita obtener modelos tridimensionales ligeros que son capaces de ser publicados mediante servicios Web-GIS. Este aspecto supone un valor añadido al hacer posible la interactuación con los productos geomáticos desde dispositivos móviles como los smartphones, permitiendo de este modo que el usuario pueda consultar, editar y analizar la información sobre el propio terreno.

Por último, se ha visto también como los productos geomáticos de alta precisión estudiados son una herramienta idónea para la evaluación de abrigos rupestres. Concretamente, se ha mostrado como mediante una aproximación combinada de información geométrica y radiométrica se incrementa la capacidad de análisis. Se ha demostrado que la incorporación de información geométrica mejora los resultados obtenidos mediante los métodos de clasificación no supervisados, siendo estos habitualmente de carácter únicamente radiométrico. El método expuesto ha sido aplicado para el caso de pinturas rupestres y el abrigo rocoso en que se encuentran, representando no solo una mejora de los resultados, sino también del proceso, suponiendo un aumento del automatismo. Por otra parte, la

incorporación de diferentes sensores activos y pasivos ha permitido evaluar las pinturas en un amplio espectro pudiendo de esta forma aprovechar la información captada en diferentes longitudes de onda. Finalmente, se ha mostrado también como gracias al análisis combinado y al empleo del modelo 3D es posible estudiar las pinturas en su conjunto, permitiendo evaluar información relevante como: la ubicación espacial de las pinturas en el abrigo, la influencia de la roca en los trazados o las condiciones de iluminación para el dibujante.

4.2 PERSPECTIVAS FUTURAS

Las técnicas y materiales empleados durante esta Tesis Doctoral han permitido llevar a cabo las investigaciones que dan respuesta a las cuestiones que se han ido planteado antes y durante su realización. Sin embargo, como consecuencia del avance técnico y metodológico se han planteado nuevas cuestiones que quedan abiertas para futuras investigaciones.

Respecto a las áreas tratadas en esta Tesis Doctoral se plantean como futuros trabajos:

- Mejorar los procedimientos de orientación externa directa, tanto en UAVs como en paramotor, haciendo uso de los datos procedentes de sistemas Global Navigation Satellite System/ Inertial Measurement Unit

(GNSS/IMU) con la finalidad de acelerar los trabajos de campo y el tiempo de procesado, con la consecuente reducción de costes asociados.

- Investigación de la adecuación de otras plataformas aéreas como autogiros para el desarrollo de los trabajos fotogramétricos, así como la incorporación de más sensores a bordo, como cámaras térmicas y sensores láser del tipo LiDAR.

- Estudiar la incorporación de técnicas como el Bidirectional Reflectance Distribution Function (BRDF) para la mejora de las texturas fotorrealísticas de modelos y ortofotografías.

- Mejorar las herramientas de interacción en la difusión de productos geomáticos vía Web-GIS para permitir una carga dinámica automática de diferentes niveles de resolución en función del nivel de zoom.

- Estudiar la adaptabilidad de los métodos combinados geométricos y radiométricos para el análisis de pinturas y grabados rupestres en diferentes condiciones y lugares.

- Investigar el potencial de nuevas herramientas como los sistemas móviles LiDAR de tipo mochila (back-pack mapping) o las cámaras hiperespectrales en el ámbito arqueológico.

REFERENCIAS BIBLIOGRÁFICAS

Aber, J. S., R. Sobieski, D. A. Distler, & M. C. Nowak. (1999). Kite Aerial Photography for Environmental Site Investigations in Kansas. *Transactions of the Kansas Academy of Science,* 102(1–2): 57–67.

Achille, C., Adami, A., Chiarini, S., Cremonesi, S., Fassi, F., Fregonese, L., & Taffurelli, L. (2015) UAV-based photogrammetry and integrated technologies for architectural applications- Methodological strategies for the after-quake survey of vertical structures in Mantua (Italy). *Sensors*, 15, 15520–15539.

Anderson, R. C. (2001). Kite Aerial Photography for Archaeology: An Assessment and Short Guide. *British School at Athens Studies,* 8: 167–180

Aguilera, D., Lahoz, J., Finat, J., Martinez, J., Fernandez, J., & San Josem, J. (2006). Terrestrial laser Canning and low-cost aerial photogrammetry in the archeological modeling of a Jewish tanneries. Paper presented at the *ISPRS Commission V Symposium "Image Engineering and Vision Metrology",* Dresden.

Block, I. (1988). Photography: 'Shooting' the Past from on High. *Archaeology,* 41(3): 58–59.

Casula, G, Fais, S., & Ligas, P. (2009). Experimental Application of 3-D Terrestrial Laser Scanner and Acoustic Techniques in assessing the quality

of stones used in monumental structures. *Int. Journ. of Microstructure and Materials Properties*, 4(1), 45–56.

Ceraudo, G. (2013). Aerial Photography in Archaeology, in C. Corsi, B. Slapšak and F. Vermeulen, eds., *Good practice in Archaeological Diagnostics: Non-invasive Survey of Complex Archaeological sites*. Cham, Switzerland: Springer, 11–30.

Cowley, D. C., & Stichelbaut, B. (2012). Historic aerial photographic archives for European archaeology: Applications, potential and issues. *European Journal of Archaeology*, 15(2).

Cosso, T., Ferrando, I., & Orlando, A. (2014). Surveying and mapping a cave using 3D laser scanner: The open challenge with free and open source software. *ISPRS - International Archives of the Photogrammetry, Remote Sensing and Spatial Information Sciences*, XL-5, 181–186.

Defrasne, C. (2014). Digital image enhancement for recording rupestrian engravings: applications to an alpine rockshelter. *Journal of Archaeological Science, 50*, 31-38.

Domingo, I., Villaverde, V., López-Montalvo, E., Lerma, J. L., & Cabrelles, M. (2013). Latest developments in rock art recording: towards an integral documentation of Levantine rock art sites combining 2D and 3D recording techniques. *Journal of Archaeological Science, 40*(4), 1879-1889.

Doneus, M., I. Miholjek, G. Mandlburger, N. Doneus, G. J. J. Verhoeven, C. Briese, & M. Pregesbauer. (2015). Airborne Laser Bathymetry for Documentation of Submerged Archaeological Sites in Shallow Water, in F. Menna, E. Nocerino, S. Del Pizzo, F. Bruno and F. Remondino, eds., *The*

International Archives of the Photogrammetry, Remote Sensing and Spatial Information Sciences. *Volume XL-5/W5, 2015 Underwater 3D Recording and Modeling*. 16th–17th April 2015, Piano di Sorrento, Italy. Piano di Sorrento: CIPA, 99–107.

Fussell, A. (1982). Terrestrial photogrammetry in Archaeology. *World Archaeology,* 14(2): 157-172.

González-Aguilera, D., Muñoz-Nieto, A., Rodriguez Gonzalvez, P., & Menéndez, M., (2011a). New tools for rock art modelling: automated sensor integration in Pindal Cave. *J. Archaeol. Sci*., 38 (1), 120e128.

González-Aguilera, D., Rodríguez-Gonz_alvez, P., Armesto, J., & Arias, P., (2011b). Trimble GX200 and Riegl LMS-Z390i sensor self-calibration. *Opt. Express,* 19 (3), 2676e2693.

Hailey, T. (2005). The powered parachute as an archaeological reconnaissance vehicle. *Archaeol. Prospect*, 12, 69–78.

Hakonen, A., Kuusela, J.-M., & Okkonen, J. (2015). Assessing the application of laser scanning and 3D inspection in the study of prehistoric cairn sites: The case study of Tahkokangas, Northern Finland. *J. Archaeol. Sci*., 2, 227–234.

Herrero-Huerta, M., Hernández-López, D., Rodriguez-Gonzalvez, P., González-Aguilera, D., & González-Piqueras, J. (2014). Vicarious

radiometric calibration of a multispectral sensor from an aerial trike applied to precision agriculture. *Comput. Electron. Agric*., 108, 28–38.

Kazhdan, M., Bolitho, M., & Hoppe, H. (2006). Poisson surface reconstruction. In *Proceedings of the 4th Eurographics Symposium on Geometry*, Sardinia, Italy, pp. 61–70.

Kuznetsova I., Kuznetsova D., & Rakova X. (2015). The use of surface laser scanning for creation of three dimentional digital model of monument. *Procedia Engin*., 100, 1625–1633.

Lai, L., Sordini, M., Campana, S., Usai, L., & Condò, F. (2015). 4D recording and analysis: The case study of Nuraghe Oes (Giave, Sardinia). *Digit. Appl. Archaeol. Cult. Herit*., 2, 233–239.

Landeschi, G., Dell'Unto, N., Lundqvist, K., Ferdani, D., Campanaro, D. & Leander Touati, A. (2016). 3D-GIS as a platform for visual analysis: Investigating a Pompeian house. *Journal of Archaeological Science*, 65, pp.103-113.

Le, H.S. (2010) An approach to construct SGIS-3D: A three dimensional WebGIS system based on DEM, GeoVRML and spatial analysis operations. In *Proceedings of the 2nd IADIS International Conference Web Virtual Reality and Three-Dimensional Worlds*, Freiburg, Germany, pp. 317–326.

Le Quellec, J.-L., Duquesnoy F. & Defrasne C., (2015). Digital image enhancement with DStretch: Is complexity always necessary for efficiency?, *Digital Applications in Archaeology and Cultural Heritage*, 2, 55-67.

Lerma, J.L., Navarro, S., Cabrelles, M., & Vllaverde, V. (2010). Terrestrial laser scanning and close range photogrametry for 3D archaeological documentation: The upper palaeolithic cave of Parpalló as a case study. *Archeol. Sci.*, *37*, 499–507.

Lejeune, M., (1985). La paroi des grottes, premier "mur" support artistique et document archéologique. Le mur dans l'art et l'archéologie. *Art et Fact*, n°2. Liège, pp.15-24.

Lindgren, S., & Galeazzi F. (2013). 3D Laser Scanning in Cave Environment: the Case of Las Cuevas, Belize. Acquisition of the Cave System and Excavation Area. In: Addison, A. C., Guidi, De Luca, L., and Pescarin, S. (eds.), *Digital Heritage International Conference, Marseille, France, Volume 1. Proceedings of the Institute of Electronical and Electronics Engineers (IEEE)*: 219-222.

López-Montalvo, E., & Sanz, I. D. (2005). Nuevas tecnologías y restitución bidimensional de los paneles levantinos: primeros resultados y valoración crítica del método. Paper presented at the *Actas del III Congreso del Neolítico en la Península Ibérica*: Santander.

Mills, J., & Andrews, D. (2011). 3D Laser Scanning for Heritage (second edition – First Edition authors: Barber, D., Mills, J.): Advice and guidance

to users on laser scanning in archaeology and architecture. *Swindon: Historic England Publishing*.

Mozas-Calvache, A. T., J. L. Pérez-García, F. J. Cardenal Escarcena, E. Mata-Castro, & J. Delgado-García. (2012). Method for Photogrammetric Surveying of Archaeological Sites with Light Aerial Platforms. *Journal of Archaeological Science,* 39: 521–530.

Oltean, I.A., & Hanson, W.S. (2007). Reconstructing the Archaeological Landscape of Southern Dobrogea: Integrating Imagery. In: M. Ehlers & U. Michel, eds. *Remote Sensing for Environmental Monitoring, GIS Applications, and Geology VII. Proceedings of SPIE Vol. 6749, no. 674906*. Florence: Society of Photo-Optical Instrumentation Engineers.

Ortega-Terol, D., Moreno, M.A., Hernández-López, D., & Rodríguez-Gonzálvez, P. (2014). Survey and classification of Large Woody Debris (LWD) in streams using generated low-cost geomatic products. *Remote Sens*., 6, 11770–11790.

Remondino, F., Barazzetti, L., Nex, F., Scaioni, M. & Sarazzi, D., (2011). UAV photogrammetry for mapping and 3d modeling– current status and future perspectives. *International Archives of the Photogrammetry, Remote Sensing and Spatial Information Sciences*, 38(1), p.C22.

Remondino, F. (2012). Worth a thousand words - Photogrammetry for archaeological 3D surveying. In *Interpreting Archaeological Topography – 3D Data, Visualisation and Observation*, R. Opitz and D. Cowley (Eds), pp.115-122. ISBN: 978-1-84217-516-3, Oxbow Books, Oxford, UK.

Robert E., (2016). Le rôle du support dans la construction des images au sein l'art paléolithique européen, in Groenen (M., dir.). *Styles, techniques and graphic expression in rock art, Actes de la session du 17ème congrès mondial de l'UISPP*, British Archaeological Reports, pp. 174-195.

Rodríguez-Gonzálvez, P., Jiménez Fernández-Palacios, B., Muñoz-Nieto, Á.L., Arias-Sanchez, P., & Gonzalez-Aguilera, D. (2017). Mobile LiDAR System: New Possibilities for the Documentation and Dissemination of Large Cultural Heritage Sites. *Remote Sens.*, *9*, 189.

Rodríguez-Gonzálvez, P., Nocerino, E., Menna, F., Minto, S., & Remondino, F. (2015). 3D surveying & modeling of underground passages in WWI fortifications. *Int. Arch. Photogramm. Remote Sens. Spat. Inf. Sci.*

Rogerio-Candelera, M. A. (2015). Digital image analysis based study, recording, and protection of painted rock art. Some Iberian experiences. *Digital Applications in Archaeology and Cultural Heritage, 2*(2), 68-78.

Roosevelt, C. H. (2014). Mapping site-level microtopography with Real-Time Kinematic Global Navigation Satellite Systems (RTK GNSS) and Unmanned Aerial Vehicle Photogrammetry (UAVP). *Open Archaeology* (1): 29–53.

Sauvet G. & Tosello G., (1998). Le mythe paléolithique de la caverne, in Sacco F., Sauvet G. dir., Le propre de l'homme, Psychanalyse et préhistoire, Paris, Delachaux et Niestlé, coll. *Champs psychanalytiques*, pp.55-90.

Seidl, M., Wieser, E., & Alexander, C. (2015). Automated classification of petroglyphs. *Digital Applications in Archaeology and Cultural Heritage, 2*(2), 196-212.

Themistocleous, K., Ioannides, M., Agapiou, A., & Hadjimitsis, D.G. (2015). The methodology of documenting cultural heritage sites using photogrammetry, UAV and 3D printing techniques: The case study of Asinou Church in Cyprus. In *Proceedings of the Third International Conference on Remote Sensing and Geoinformation of Environment*, Cyprus, Nicosia, pp. 16–19.

Thomas, H. (2016). Quantitative analysis of two low cost aerial photography platforms: A case study of the Geometric site of Zagora, Greece. *The Journal of Field Archaeology*.

Tucci, G., Cini, D., & Nobile, A. (2011). Effective 3D digitization of archaeological artefacts for interactive virtual museum. *International Archives of the Photogrammetry, Remote Sensing and Spatial Information Sciences* (ISPRS), 38(5/W16), 413–420. http://dx.doi.org/10.5194/isprsarchives-XXXVIII-5-W16-413-2011

Verhoeven, G. (2010). Taking Computer Vision Aloft – Archaeological Three-Dimensional Reconstructions from Aerial Photographs with Photoscan. *Archaeol Prospec*, 18(1): 67–73.

Von Schwerin, J., Richards-Rissetto, H., Remondino, F., Agugiaro, G., & Girardi, G. (2013). The MayaArch3D project: A 3D WebGIS for analyzing ancient architecture and landscapes. *Lit. Linguist. Comput.*, 28, 736–753.

Whittlesey, J. H. (1971). Aerial photo balloon. *Archaeology* 24(2): 174.

Wüst T., S. Nebiker, & R. Landolt, (2004). Applying the 3d GIS DILAS to Archaeology and Cultural Heritage Projects – Requirements and First Results. *The International Archives of the Photogrammetry, Remote Sensing and Spatial Information Sciences*, Vol. 34.

Zeppelzauer, M., Poier, G., Seidl, M., Reinbacher, C., Breiteneder, C., Bischof, H., & Schulter, S. (2015). Interactive segmentation of rock-art in high-resolution 3D reconstructions. In *2015 Digital Heritage*.

ANEXO. FACTOR DE IMPACTO DE LAS PUBLICACIONES

Índices de calidad en publicaciones:

- **SJR Indicator**: Índice de medición de la influencia de una revista científica que tiene en cuenta el número de citas recibidas y la importancia o prestigio de las revistas de las que proceden tales citas. Mide el promedio de influencia científica por artículo en una revista en el año seleccionado mediante los documentos publicados en los tres años anteriores.

- **H Index**: Expresa el número de artículos (h) de la revista que han recibido al menos h citas. Cuantifica tanto la productividad científica de la revista como el impacto científico. Es también aplicable a científicos, países, etc.

- **Total Docs**.: Documentos publicados en el periodo seleccionado. Se consideran todos los tipos de documentos, incluyendo documentos citables y no citables.

- **Total Docs**. **(3years)**: Documentos publicados en los tres años anteriores (el año seleccionado es excluido). Se consideran todos los tipos de documentos, incluyendo documentos citables y no citables.

- **Total References**: Incluye todas las referencias bibliográficas en una revista en el período seleccionado.

- **Total Cites (3 years)**: Número de citas recibidas por una revista en el año seleccionado a los documentos publicados en los tres años anteriores. Se consideran todos los tipos de documentos.

- **Citable Documents**: Número de documentos citables publicados por una revista en los tres años anteriores (se excluyen los documentos

del año seleccionado). Exclusivamente los artículos, las revisiones y los papers de conferencia son considerados.

- **Cites per Document (2 years)**: Citas promedio por documento en un período de 2 años. Se calcula considerando el número de citas recibidas por una revista en el año en curso a los documentos publicados en los dos años anteriores.

- **Cites per Document (3 years)**: Citas promedio por documento en un período de 3 años. Se calcula considerando el número de citas recibidas por una revista en el año en curso a los documentos publicados en los tres años anteriores.

- **Cites per Document (4 years)**: Citas promedio por documento en un período de 4 años. Se calcula considerando el número de citas recibidas por una revista en el año en curso a los documentos publicados en los cuatro años anteriores.

- **REF./DOC.**: Número promedio de referencias por documento en el año seleccionado.

- **Self Cites:** Número de auto-citas de la revista en el año seleccionado a sus propios documentos publicados en los tres años anteriores. Se consideran todos los tipos de documentos.

- **Non-Citable Documents:** Ratio de documentos no citables en el periodo considerado.

- **Uncited Documents:** Número de documentos no citados en los tres años anteriores.

- **% International Collaboration:** Ratio de documentos cuya afiliación incluye direcciones de más de un país.

Artículo 1: A hybrid measurement approach for archaeological site modelling and monitoring: the case study of Mas D'Is, Penàguila.

Revista	**Journal of Archaeological Science**
URL	https://www.journals.elsevier.com/journal-of-archaeological-science/
Editorial	Elsevier
Factor de impacto JCR	2,255
Índice H	82
Quartil	Q1
Ranking	5 (204)


SJR
1.8
1.2
0.6
1999 2001 2003 2005 2007 2009 2011 2013 2015


Total Cites
Self-Cites
4k
2k
0
1999 2001 2003 2005 2007 2009 2011 2013 2015

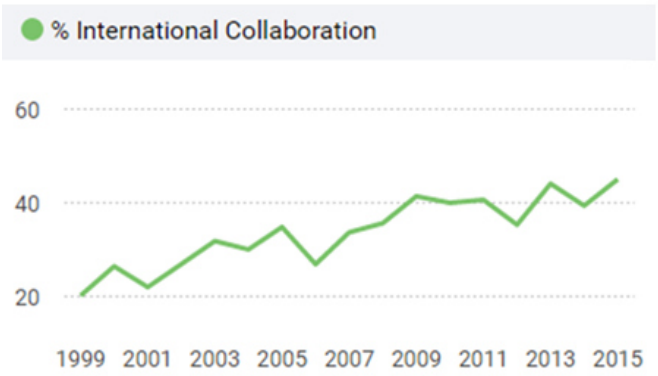
% International Collaboration
60
40
20
1999 2001 2003 2005 2007 2009 2011 2013 2015

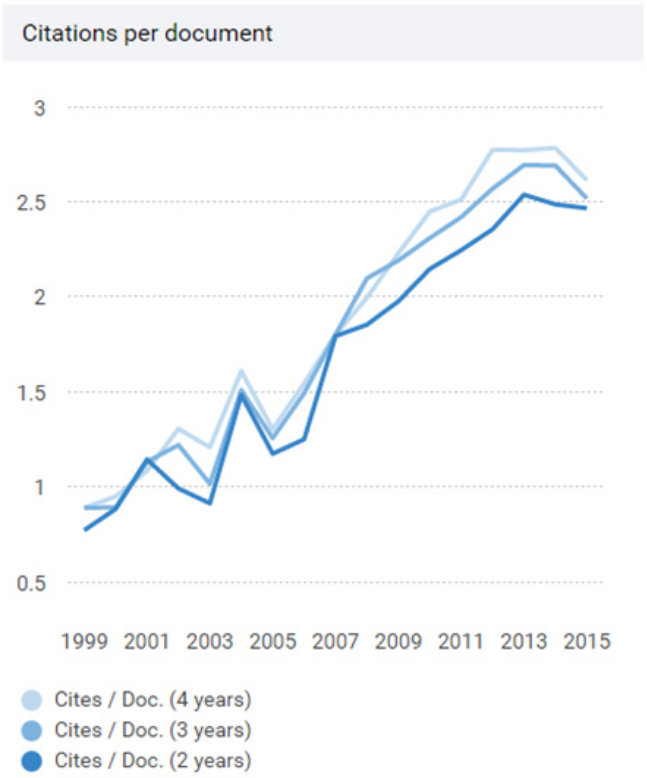
Citations per document
3
2.5
2
1.5
1
0.5
1999 2001 2003 2005 2007 2009 2011 2013 2015
Cites / Doc. (4 years)
Cites / Doc. (3 years)
Cites / Doc. (2 years)

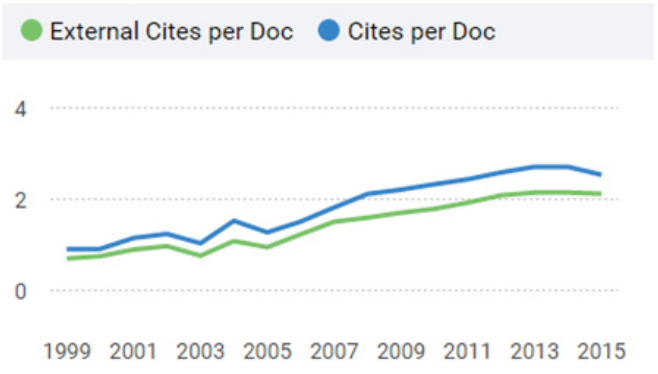
External Cites per Doc
Cites per Doc
4
2
0
1999 2001 2003 2005 2007 2009 2011 2013 2015

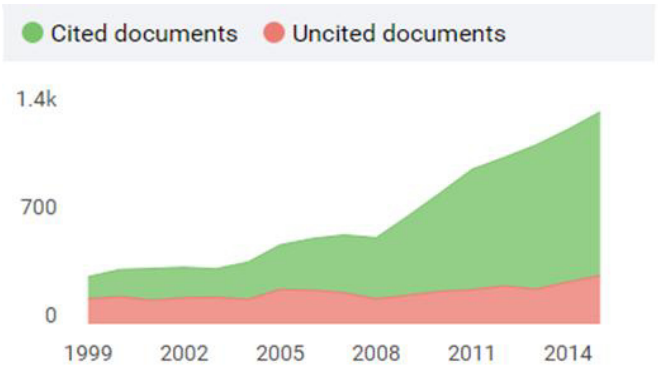
Cited documents
Uncited documents
1.4k
700
0
1999 2002 2005 2008 2011 2014

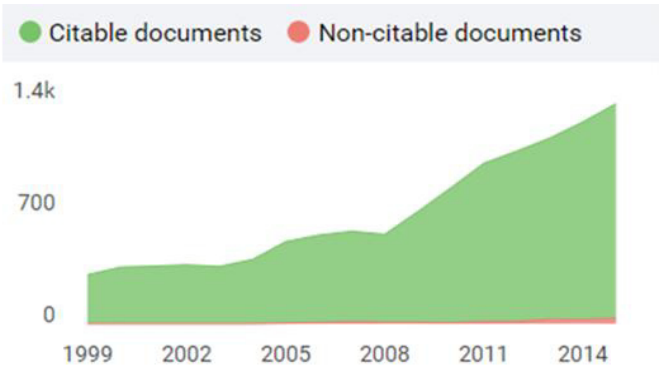
Citable documents
Non-citable documents
1.4k
700
0
1999 2002 2005 2008 2011 2014

Artículo 2: A Multi-Data Source and Multi-Sensor Approach for the 3D Reconstruction and Web Visualization of a Complex Archaelogical Site: The Case Study of "Tolmo De Minateda".

Revista	**Remote Sensing**
URL	http://www.mdpi.com/journal/remotesensing
Editorial	MDPI
Factor de impacto JCR	3,036
Índice H	39
Quartil	Q1
Ranking	10 (170)


SJR
1.8
1.2
0.6
0
2010
2011
2012
2013
2014
2015

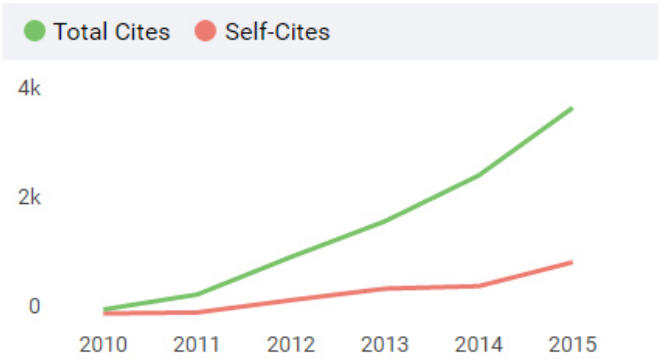
Total Cites
Self-Cites
4k
2k
0
2010
2011
2012
2013
2014
2015


% International Collaboration
50
40
30
20
2010
2011
2012
2013
2014
2015

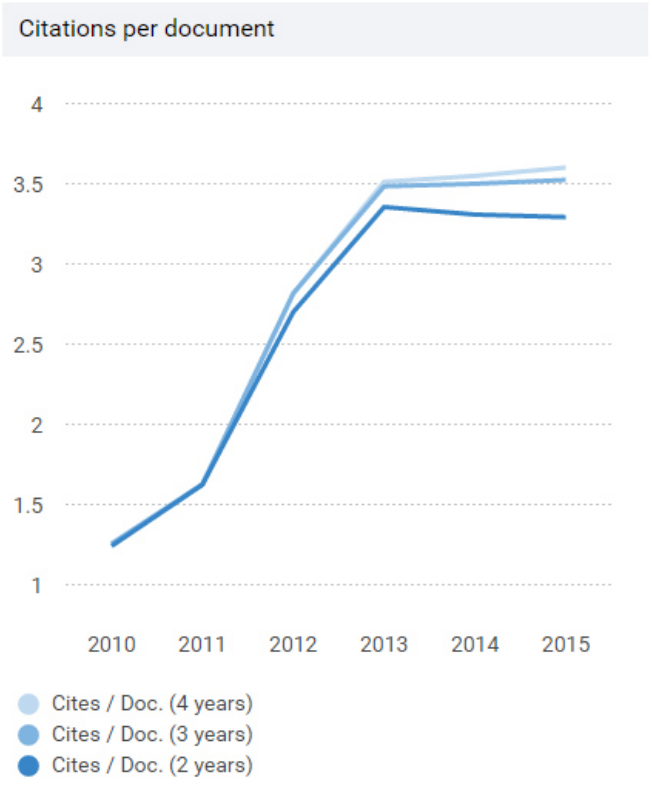
Citations per document
4
3.5
3
2.5
2
1.5
1
2010
2011
2012
2013
2014
2015
Cites / Doc. (4 years)
Cites / Doc. (3 years)
Cites / Doc. (2 years)

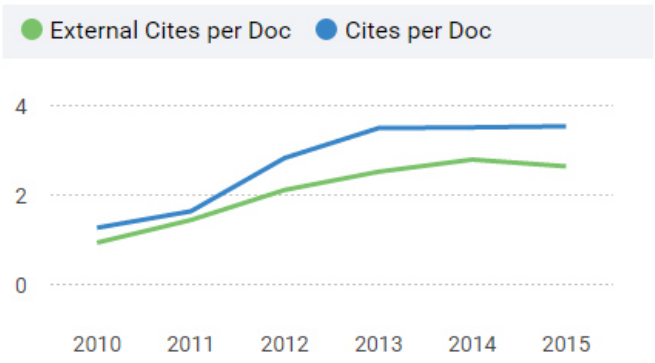
External Cites per Doc
Cites per Doc
4
2
0
2010
2011
2012
2013
2014
2015

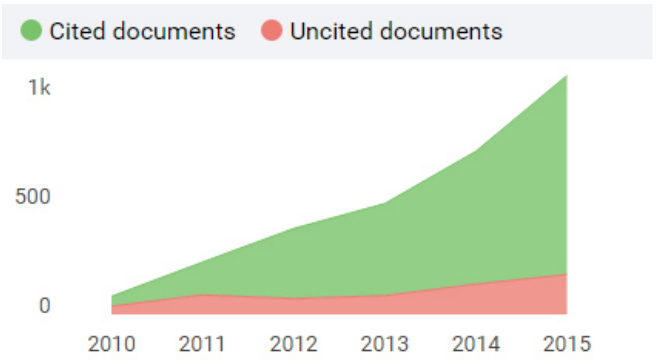
Cited documents
Uncited documents
1k
500
0
2010
2011
2012
2013
2014
2015

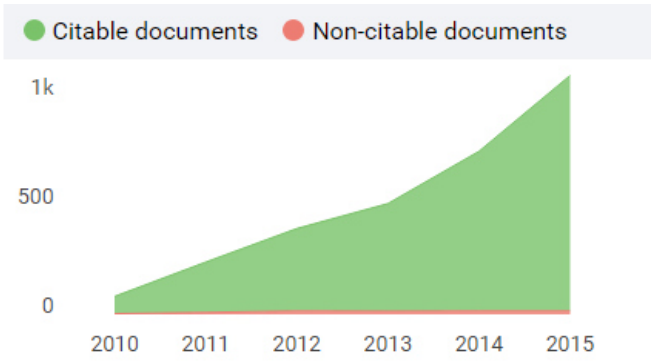
Citable documents
Non-citable documents
1k
500
0
2010
2011
2012
2013
2014
2015

Artículo 3: Combining geometrical and radiometrical features in the evaluation of rock art paintings.

Revista	**Digital Applications in Archaeology and Cultural Heritage**
URL	https://www.journals.elsevier.com/digital-applications-in-archaeology-and-cultural-heritage/
Editorial	Elsevier
CiteScore	0.62
Factor de impacto SJR	0.170
SNIP	0.869
Índice H	2
Quartil	Q2
Ranking	40 (205)

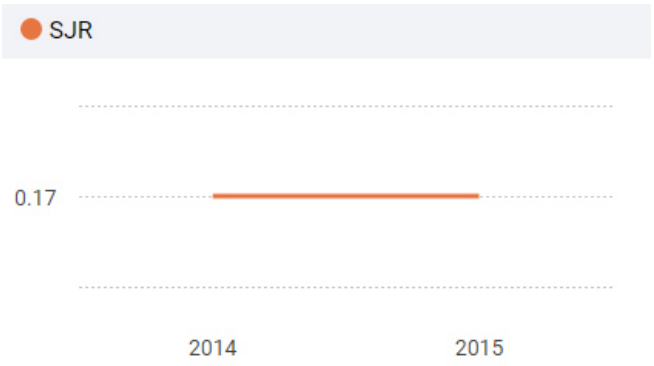
SJR
0.17
2014
2015

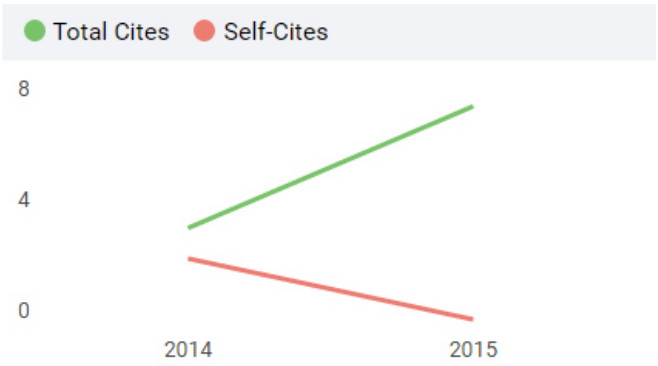
Total Cites
Self-Cites
8
4
0
2014
2015

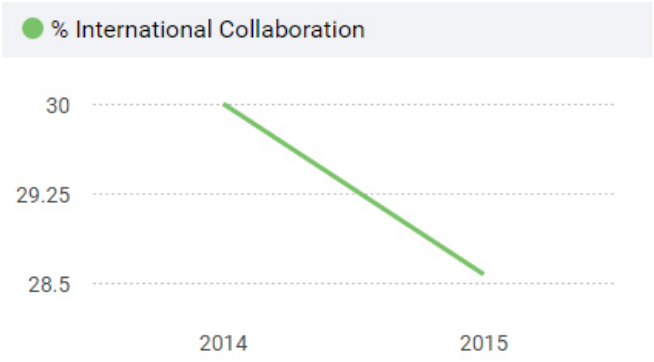
% International Collaboration
30
29.25
28.5
2014
2015

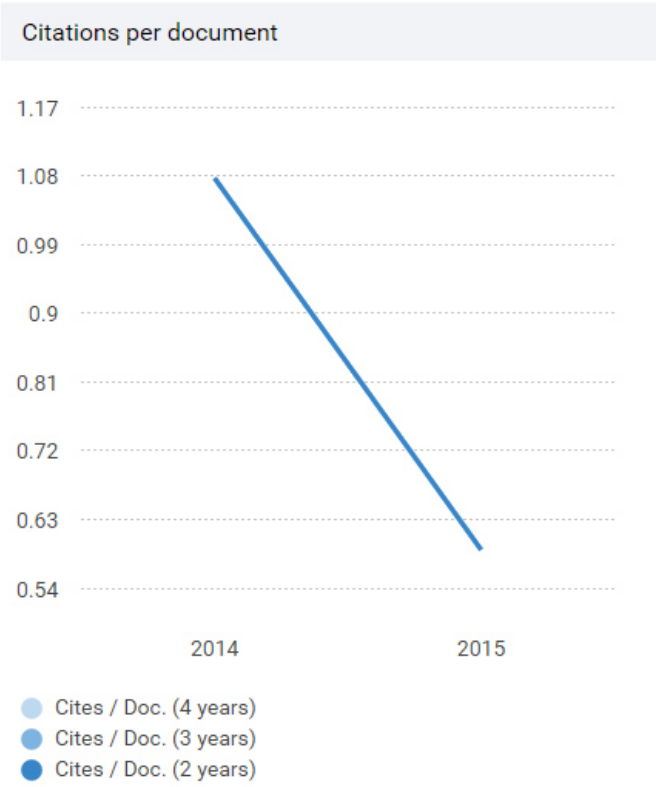
Citations per document
1.17
1.08
0.99
0.9
0.81
0.72
0.63
0.54
2014
2015
Cites / Doc. (4 years)
Cites / Doc. (3 years)
Cites / Doc. (2 years)

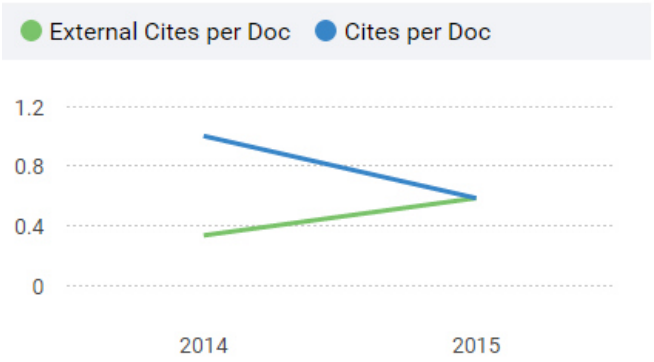
External Cites per Doc
Cites per Doc
1.2
0.8
0.4
0
2014
2015

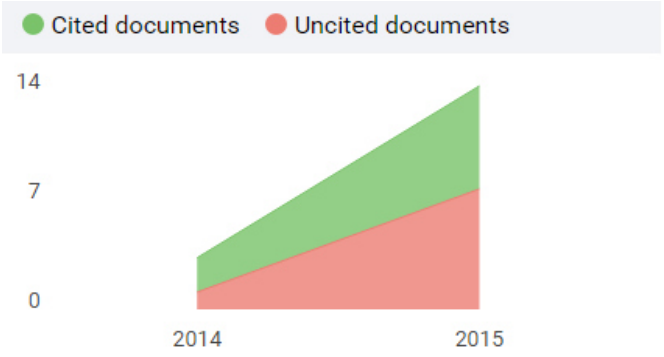
Cited documents
Uncited documents
14
7
0
2014
2015

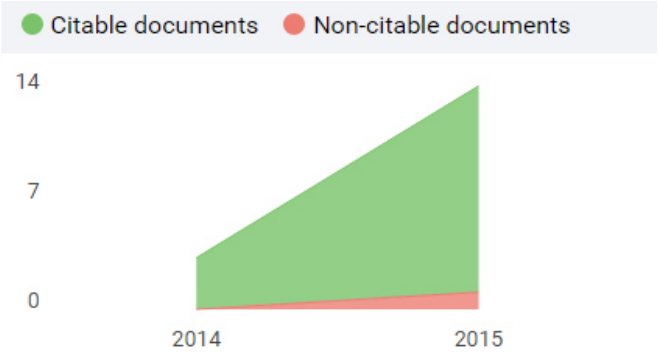
Citable documents
Non-citable documents
14
7
0
2014
2015